NRC Research and/or Technical Assistance Rept

PDR

EGG-SEMI-6022
September 1982

ANALYSIS OF PRIMARY FEED AND BLEED COOLING IN PWR SYSTEMS

D. J. Shimeck
G. R. Berglund
R. A. Dimenna
C. B. Davis
J. P. Adams

U.S. Department of Energy
Idaho Operations Office • Idaho National Engineering Laboratory

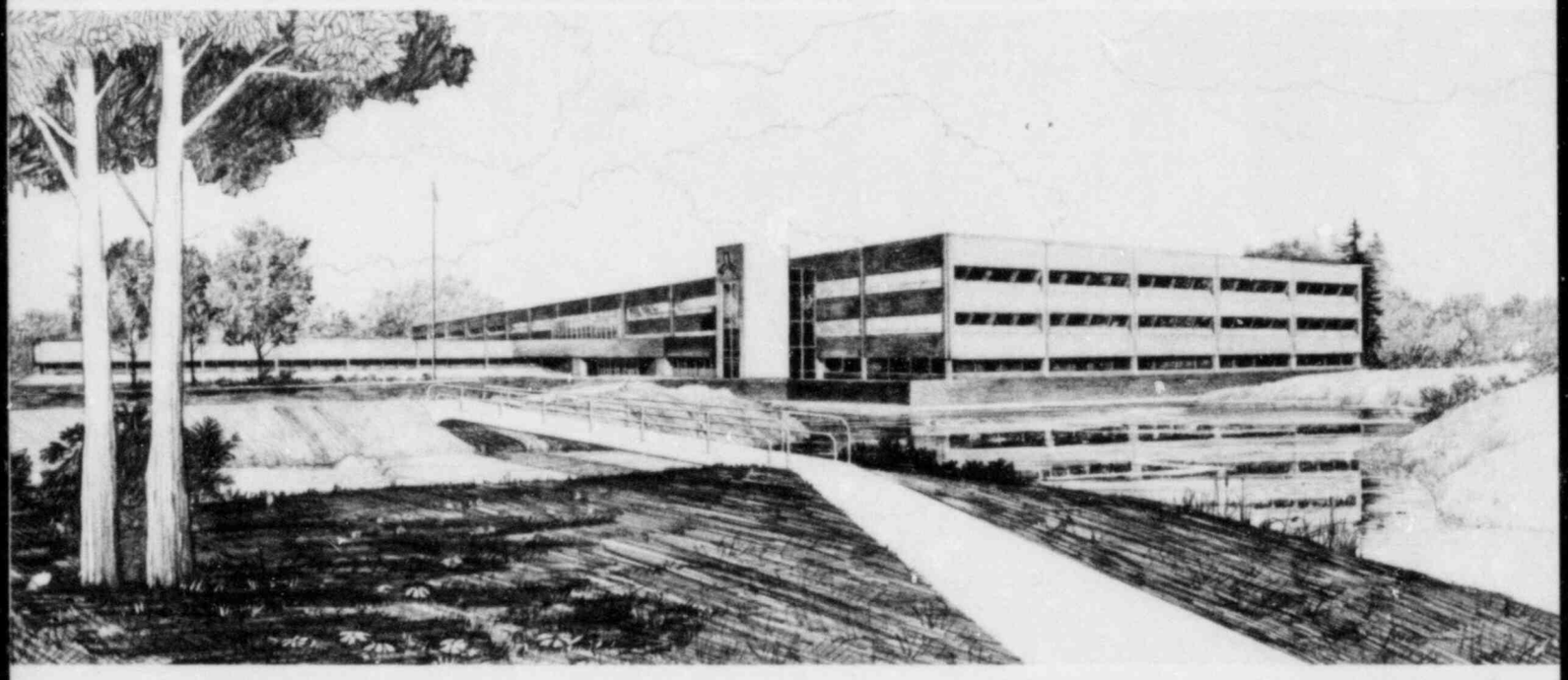

This is an informal report intended for use as a preliminary or working document

8211060553 820930
PDR RES
*
PDR

Prepared for the
U.S. NUCLEAR REGULATORY COMMISSION
under DOE Contract No. DE-AC07-761D01570

EG&G Idaho

EG&G Idaho, Inc.

FORM EG&G-398
(Rev. 11-79)

INTERIM REPORT

Accession No. _____

Report No. EGG-SEMI-6022

Contract Program or Project Title:

Semiscale

Subject of this Document:

Analysis of Primary Feed and Bleed Cooling in PWR Systems

Type of Document:

Topical

Author(s):

D. J. Shimeck
G. R. Berglund
R. A. Dimenna
C. B. Davis
J. P. Adams

Date of Document:

September 1982

Responsible NRC Individual and NRC Office or Division:

R. R. Landry, Reactor Safety Research

This document was prepared primarily for preliminary or internal use. It has not received full review and approval. Since there may be substantive changes, this document should not be considered final.

EG&G Idaho, Inc.
Idaho Falls, Idaho **83415**

Prepared for the
U.S. Nuclear Regulatory Commission
Washington, D.C.
Under DOE Contract No. **DE-AC07-76ID01570**
NRC FIN No. A6038

INTERIM REPORT

ANALYSIS OF PRIMARY FEED AND BLEED COOLING

IN PWR SYSTEMS

Approved: Paul North

P. North, Manager
Water Reactor Research Test Facilities Division

Approved: Gary W. Johnsen

G. W. Johnsen, Manager
WRRTF Experiment Planning and Analysis Branch

ABSTRACT

Primary feed and bleed cooling as it pertains to a pressurized water reactor, describes an operation whereby reactor core cooling is maintained by injecting liquid with pumped emergency core cooling systems and removing the heated/vaporized fluid via the pressurizer power operated relief valve. This report presents a systematic analysis of the capabilities and limitations of primary feed and bleed. First, the system parameters that govern the ultimate capability of feed and bleed are examined along with the inherent assumptions. Data from Semiscale experiments is analyzed. Phenomena that influence the results are identified and analyzed with regard to typicality. Calculations with the RELAP5 computer code are then presented that verify the ability of the code to predict the phenomena observed in Semiscale. Finally, results from RELAP5 are used to predict full-scale plant response during selected feed and bleed scenarios.

FIN. No. A6038
Semiscale Program

SUMMARY

This report presents results from an experimental and analytical study of primary feed and bleed cooling in pressurized water reactor (PWR) type systems. Primary coolant feed and bleed cooling as it pertains to a pressurized water reactor, denotes an operation whereby reactor core cooling is maintained by injecting coolant with pumped emergency core cooling systems and removing the heated/vaporized fluid via the pressurizer power operated relief valve(s) (PORVs). While a number of scenarios may be hypothesized in which feed and bleed cooling might be called for, this study is concerned with conditions in which a complete loss of secondary heat sink occurs. Other assumed conditions include: the reactor has scrammed (decay heat levels), all or some pumped injection systems and the power operated relief valve(s) are operative, the pressurizer heaters are off, and the primary recirculation pumps are tripped. Although limited in scope, the study systematically examines relevant thermal-hydraulic phenomena attendant to feed and bleed. The scope of this study encompasses a simplified analysis of the mass and energy balances associated with feed and bleed, examination of experimental data from the Semiscale and LOFT systems, and RELAP5 computer code analyses of both Semiscale and a full-scale Westinghouse plant.

The parameters that govern the ultimate feasibility of feed and bleed were first examined, and the variables and uncertainties associated with those parameters identified. Examination of primary feed and bleed identifies four key parameters: core decay heat, cooling water injection capacity, PORV energy removal rate, and PORV mass removal rate. Other than core power, the remaining parameters are functions of system pressure. Simple operating maps may be drawn which define a steady-state feed and bleed operating band for selected sets of these four parameters. A lower bound pressure for steady-state operation is defined by an energy balance between the core power and the PORV energy removal rate. An upper bound is defined by a mass balance between the injection capacity and the PORV mass removal rate. Steady-state operation within this band is possible by cycling the PORV to maintain system pressure, and throttling the injection rate to maintain a net mass balance.

Of the above parameters which define a primary feed and bleed operating pressure band, the PORV mass flow rate, and therefore energy removal rate are subject to the most uncertainty since they are strongly influenced by pressurizer coolant conditions. Variations may also occur in the injection capacity (such as assumed failure of injection trains, etc.), and in the core decay heat power, which continually decreases with time. Although limited in their ability to predict transient phenomena, the operating maps provide a method for quickly calculating the influence of variations or uncertainties on the ultimate capability of feed and bleed cooling.

Two primary feed and bleed experiments were conducted in the Semiscale Mod-2A facility to examine the transient thermal-hydraulic behavior associated with feed and bleed and to provide data for computer code assessment. The first of these, Test S-SR-1, experienced excessive uncontrolled primary leakage and was merely used as a data base for examining selected phenomena. The second test used boundary conditions simulating a decay heat level of 2% full power. The high pressure pumped injection capacity was scaled from Zion nuclear plant high pressure injection system flow rates, but disallowed charging pump flow. The PORV relief capacity was approximately representative of PWR-scaled values (actually 20% larger than that of Zion). The aggregate result of the chosen boundary conditions was an operating map with a steady-state band between 7 and 8.2 MPa when saturated steam PORV discharge is assumed.

Results from the experiments showed that when PORV was latched open the pressurizer filled and the PORV discharge appeared to be directly affected by hot leg coolant quality. In the second of the two Semiscale experiments the resulting high mass discharge rate was far in excess of the injection rate and resulted in a rapid system mass depletion. Once sufficient mass inventory had been lost such that the hot leg had voided, the PORV flow closely reflected the predicted saturated steam flow rate. At that point the core was still adequately covered, but a small deficit still existed in the inflow/outflow rates and eventually the core uncovered and heated up. The deficit in the mass balance was small enough that it was within the range of experimental uncertainties, and therefore makes no

direct statement as to the viability of primary feed and bleed. However, the excessive PORV discharge prior to hot leg voiding and the phenomena which caused it are well outside the range of experimental uncertainty. Irrespective of experimental uncertainties, the mass inventory in the Semiscale experiment could not have been maintained with the PORV latched open, until the hot leg voided.

Two factors were identified which directly influence mass flow out the PORV. The first involves differences observed when the PORV was cycled open and shut, versus when it was latched open. Periodic closing of the PORV in Semiscale promoted phase separation and resulted in an average PORV flow rate (when the PORV was open) close to the predicted saturated steam flow rate. Secondly, analysis of Semiscale and LOFT data and analysis of code calculations indicated that the orientation of the surge line connection to the hot leg influences phase separation at the hot leg. Substantial hot leg voiding was necessary to reduce the PORV flow in the Semiscale experiments with a horizontal centerline connection, while minimal voiding was required in a LOFT test with a vertical top connection. Both orientations, and some intermediate angles, are used in current PWR designs.

Posttest calculations were performed with the RELAP5 computer code to predict the Semiscale experimental results. The RELAP5 calculations correctly predicted the filling of the pressurizer and showed excellent quantitative agreement with the two-phase PORV mass discharge rate. The mass loss rate of the system was closely matched. However the calculation used the specified HPIS injection rate (as opposed to the actual rate injected during the test which was lower than specified). The results showed that once the hot leg had been voided the mass depletion trend toward core uncovery may have been arrested in the experiment had the specified injection rate been achieved. Until sufficient mass inventory had been lost to void the hot leg, however, the PORV discharge rate still far exceeded the calculated HPIS injection rate.

The RELAP5 code was next used to perform a calculation for a full-scale plant. The Westinghouse RESAR plant design was selected. A

complete loss of feedwater transient was chosen as a convenient scenario leading to primary feed and bleed cooling. The boundary conditions for this calculation were best estimate and included an ANS decay heat curve and full capacity HPIS and charging pump injection rates. Consistent with the low core power levels at the time feed and bleed was initiated (more than 1 hr after shutdown), and the full injection capability, the injection rate far exceeded the PORV discharge rate and the system was returned to a subcooled condition. This result was consistent with a simple analysis of the operating map for the RESAR plant design, which indicated a wide pressure band within which primary feed and bleed was theoretically possible. Moreover, the RELAP5 analysis of the RESAR plant gained significant credibility by virtue of the success of the Semiscale calculation, which employed the same modeling techniques.

While limited in its overall scope the present study, consisting of both experimental and analytical investigations, has shed considerable light on the subject of primary feed and bleed. A simple analytical approach to determining the feasibility of feed and bleed has been developed and corroborated by experimental data and computer code calculations. The Semiscale experiments have identified the factors influencing PORV discharge, which is the most variable of the boundary conditions influencing feed and bleed. The RELAP5 computer code has been shown capable of predicting the Semiscale experiments, and when applied to a full-scale plant has indicated that primary feed and bleed is a viable cooling mechanism.

Based on the results of this study it seems safe to assume that primary feed and bleed would be a successful recovery procedure in the Westinghouse-type plant designs examined (i.e., RESAR, ZION), assuming undegraded injection capability. Further analysis appears warranted to predict the probable response in Combustion Engineering and Babcock and Wilcox plant designs. In addition, the current NSSS emergency operating procedures relevant to complete loss of secondary heat sink should be reviewed to determine if they adequately reflect an understanding of anticipated plant behavior in light of the results reported herein.

FOREWORD

At the request of the Nuclear Regulatory Commission the Semiscale Program conducted experiments designed to investigate the feasibility of primary coolant system (PCS) feed and bleed as a means of rejecting decay heat in the absence of steam generator heat removal. The results and preliminary analysis of the experiments suggested that a reasonable uncertainty may exist in the ability to effect stable PCS feed and bleed. Since current pressurized water reactor emergency operating guidelines call for primary feed and bleed under certain abnormal conditions, it was considered of some importance that the general subject of feed and bleed be studied in some depth and that the Semiscale results be carefully analyzed so that they might be interpreted in the proper perspective. To this end, the Semiscale Program has conducted an analysis effort involving both experimental results (i.e., Semiscale and LOFT) and full-scale plants. Westinghouse design plants were chosen for the study due to the availability of information and existing computer decks at the INEL. The purpose of this report is to present the results of the analysis of feed and bleed, including the recent Semiscale results.

ACKNOWLEDGMENTS

The authors wish to extend their thanks to L. J. Martinez for his assistance in analyzing the Semiscale data, to G. W. Johnsen for his direction and review, and to J. Berrey and T. Demitropoulos for the preparation of the report.

CONTENTS

FIGURES

TABLES

ANALYSIS OF PRIMARY FEED AND BLEED COOLING IN PWR SYSTEMS

1. INTRODUCTION

Certain transient scenarios may be postulated for pressurized water reactor plants wherein the capability for delivering water to the secondary of the steam generators is lost. Once the remaining water stored in the secondaries is depleted as a result of being boiled off by the decay heat generated in the core, the loss of heat sink will result in pressurization of the primary system. Should this occur, one method that the operator has available to maintain adequate core cooling and to control primary coolant system pressure is to open the power operated relief valve (PORV) on top of the pressurizer and use high pressure pumped emergency core cooling (ECC) injection to maintain inventory. This procedure is commonly referred to as primary feed and bleed. Feed and bleed commences when the PORV(s) are opened (bleed) and high pressure injection begins (feed). The passage of steam out the PORV(s) provides for the rejection of decay heat while the introduction of ECCS coolant provides makeup for the resultant coolant loss.

A number of concerns arise when examining the feasibility of primary feed and bleed. There is the general question as to which parameters ultimately govern the ability of a given plant to maintain a steady-state feed and bleed operation; from what range of initial conditions is it possible to depressurize a system while retaining sufficient mass inventory to keep the core cooled?; what effects do geometry and, in the case of experimental systems scale, induce on integral system behavior? While a multitude of variables and scenarios exist that could lead to this situation, the focus of this present analysis is on primary feed and bleed cooling in a multi-loop pressurized water reactor system typical of a 4-loop Westinghouse design. It will examine the feasibility of achieving a favorable coolant and energy balance under conditions in which:

1. The reactor has scrammed

2. The steam generator secondaries are completely depleted of coolant

3. The high pressure injection system (ECCS) is operative

4. The pressurizer heaters are inactive

5. The pressure-operated relief valve(s) (PORVs) are operative

6. Primary recirculation pumps are off.

The next section of this report will examine the theoretical feasibility of maintaining steady-state feed and bleed cooling by examining the parameters which govern it. The variables and uncertainties that affect feed and bleed operation are identified and briefly discussed. The following section will present an analysis of experiments conducted in the Semiscale Mod-2A experimental facility which involved feed and bleed with scaled PORV and ECC flows. The typicality of the results will then be discussed by reviewing the experimental uncertainties and variables. The last two sections will present results from RELAP5 code predictions of the Semiscale experiments and a best estimate calculation of a scenario involving primary feed and bleed in a full-scale PWR. Finally, conclusions will be summarized from the analysis as a whole.

2. PRINCIPLES OF FEED AND BLEED OPERATION

2.1 Theoretical Feed and Bleed Operation

The objective of primary feed and bleed is to remove core decay heat in the absence of heat transfer in the steam generators while maintaining a favorable coolant inventory. Figure 1 shows the important parameters for determining the feasibility of primary feed and bleed operation and indicates the possibility of a steady-state operating band. The governing parameters which determine this operating band are decay heat level, HPIS flow rate, and PORV flow rate (and enthalpy flow rate). Except for the core decay heat level the remaining parameters are functions of primary system pressure. The lower bound of the operating band represents the minimum pressure at which the PORV can pass enough steam[a] (with the coolant replaced by ambient temperature water) to remove sufficient energy from the system. Steady-state operation below this pressure without additional energy removal paths is not possible. Operation at a pressure above the lower bound may be theoretically accomplished by cycling the PORV open and closed within a desired pressure band.

The upper pressure bound to the steady-state operating band is defined by a balance between the PORV average coolant removal rate and the HPIS coolant injection rate. The average PORV coolant removal rate is simply defined as the core power divided by the difference between inlet and outlet enthalpies:

$$\dot{m}_{AVG} = \dot{Q}_{core}/(h_{out} - h_{in})$$

(This relationship assumes that the coolant removed through the PORV is replaced with ambient temperature water at the same flow rate. Actually a coolant deficit exists at pressures higher than the upper bound and a steady-state condition cannot exist due to a continual loss of system

---

a. It is assumed here that 100% quality steam is discharged through the PORV. The effect of reduced quality is examined later.

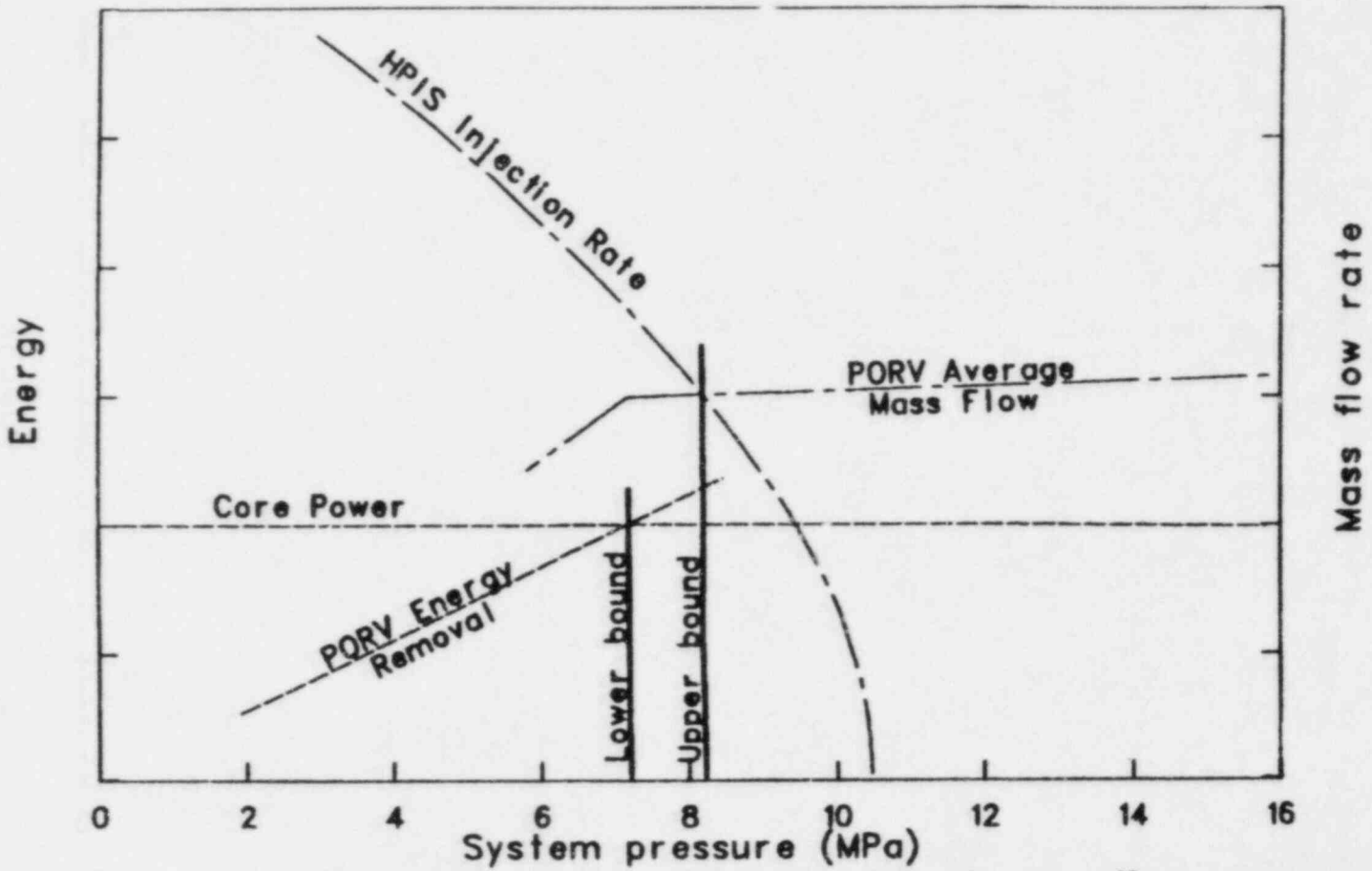

Figure 1. Typical primary feed and bleed operating map. WRRTF 16-8

coolant inventory.) Below the upper bound the system mass inventory can theoretically be maintained within a desired operating range by either throttling the HPIS or cycling it on and off.

A number of studies have been conducted to predict PWR system behavior under feed and bleed operation following loss of secondary heat sink (e.g., References 1 and 2). However, these studies have made use of large thermal-hydraulic computer codes to examine limited numbers of scenarios. The simplified approach presented here, although lacking in its ability to predict the influence of transient phenomena, allows examination of the factors that determine the ultimate capability of feed and bleed for given plant parameters. It presents a starting point for examining the sensitivity of any variations or uncertainties with minimal expenditure of time. Such a study is presented below.

2.2 Uncertainties Associated with Steady-State Operating Pressure Band

In practice the curves discussed above are not well defined due to several uncertainties. Subject to the greatest uncertainty are the PORV mass removal and energy removal curves. The mass flow through the PORV is dependent on the fluid conditions at the top of the pressurizer. If the pressurizer is nearly liquid full the flow through the PORV will be a mixture of liquid and vapor. At a given system pressure this results in greater mass flow than for saturated steam flow through the PORV. The result of having two-phase flow through the PORV is therefore to lower the upper bound pressure.

Uncertainties also arise in the PORV energy removal curve due to two-phase flow. With decreasing quality the energy removal per unit mass decreases while the mass discharge rate increases. Depending upon the quality the energy removal rate at a given pressure may be less than or greater than that for saturated steam. The lower bound of the operating band will vary accordingly.

Another significant variable that affects the width of the operating band is the actual heat load that must be rejected through the PORV. The

energy that must be rejected by the PORV is reduced as core decay heat decreases with time after shutdown and also if additional heat sinks exist. These additional heat sinks may be such things as environmental heat loss or residual water in the steam generator secondaries. The result of additional heat removal paths and/or lower core power is to lower the bottom end of the operating band. Coincident with this is the reduction of PORV average mass flow which raises the upper bound pressure.

Another factor which affects the operating band width is the HPIS injection flow rate. As Figure 1 indicates, the lower the HPIS injection capacity the lower the upper bound of the operating band will be.

The quantitative effects of the uncertainties and/or variances discussed above are illustrated in Figures 2 through 6. For these examples the curves were generated using available data obtained from the Zion I nuclear generating plant,[3,4] a 3411 MW(t) pressurized water reactor. Figure 2 shows a primary feed and bleed map for a 2% decay heat power level. A steady-state operating band is seen to exist between 7.5 and 14 MPa. A decay heat level of 2% of full power is typical of the time period from about 10 min to 20 min after shutdown[a]. Figure 3 is a similar curve, but here no makeup pump injection is assumed; only the HPIS pumps were assumed to be operating. The HPIS pumps are shown to deadhead at about 10.3 MPa. For this case no steady-state operating band exists, since at the minimum pressure where the PORV can remove the energy there is a mass deficit between the PORV coolant removal and the HPIS injection capacity.

Figure 4 shows the primary feed and bleed map for 1-1/2% full power, a decay heat level typical of the period from 1/2 to 1 hr after shutdown, and for only HPIS injection. Comparison to Figure 3 shows that the reduction in core power and corresponding PORV average mass flow both act to establish a steady-state operating band.

---

a. Assuming end-of-life reactor fuel conditions

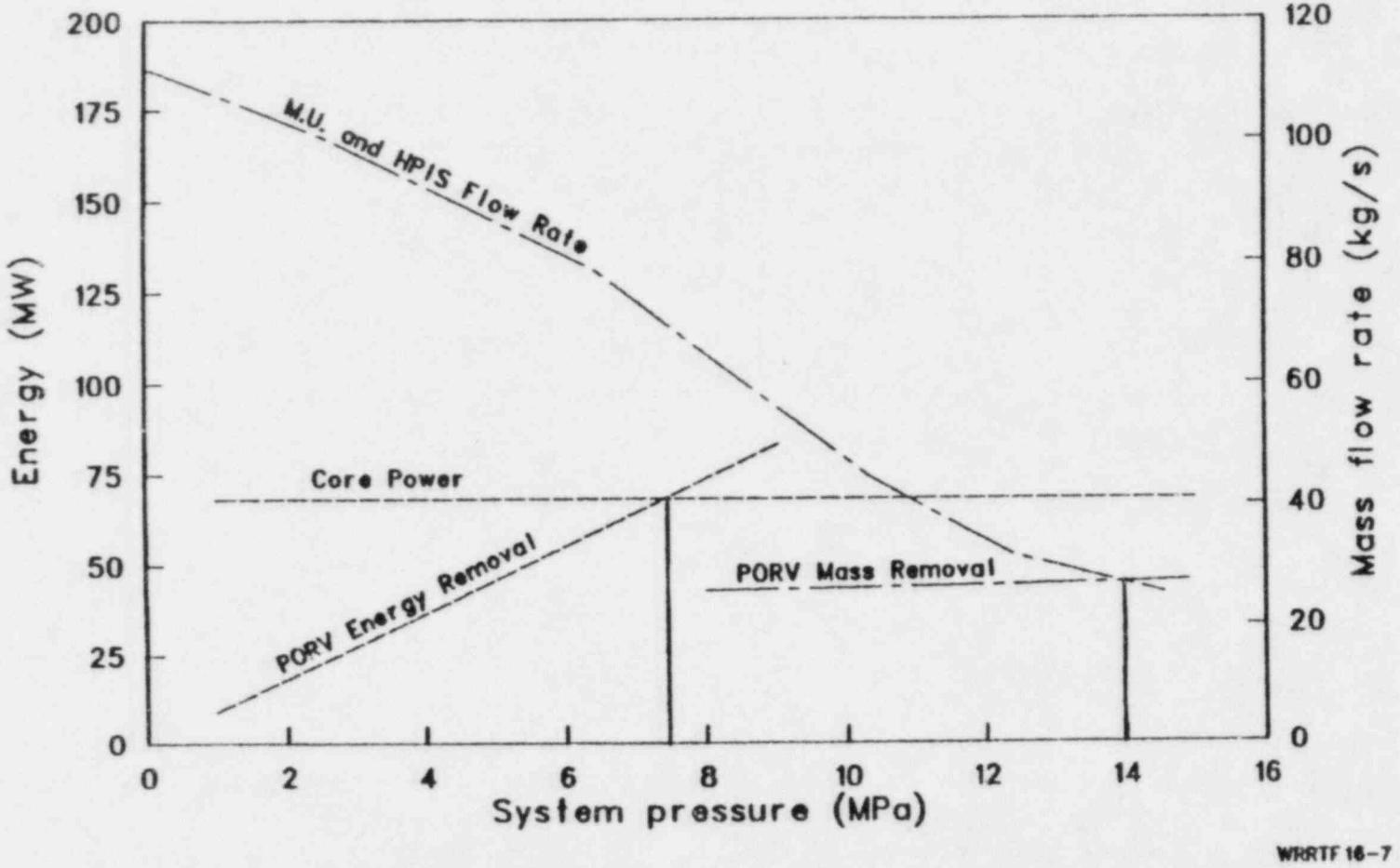

Figure 2. Zion primary feed and bleed operating map for 2% core power.

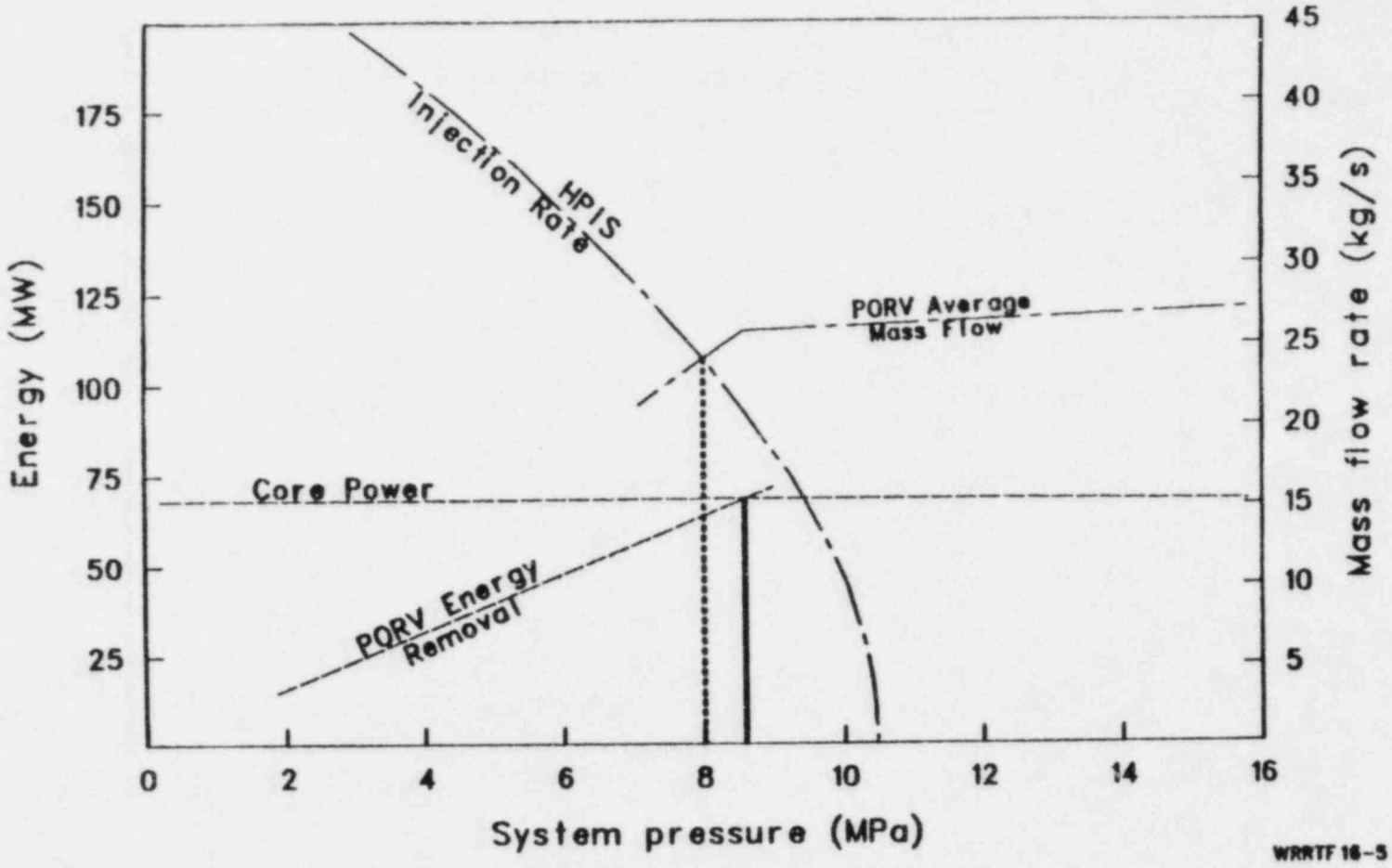

Figure 3. Zion primary feed and bleed operating map for 2% core power without charging pumps

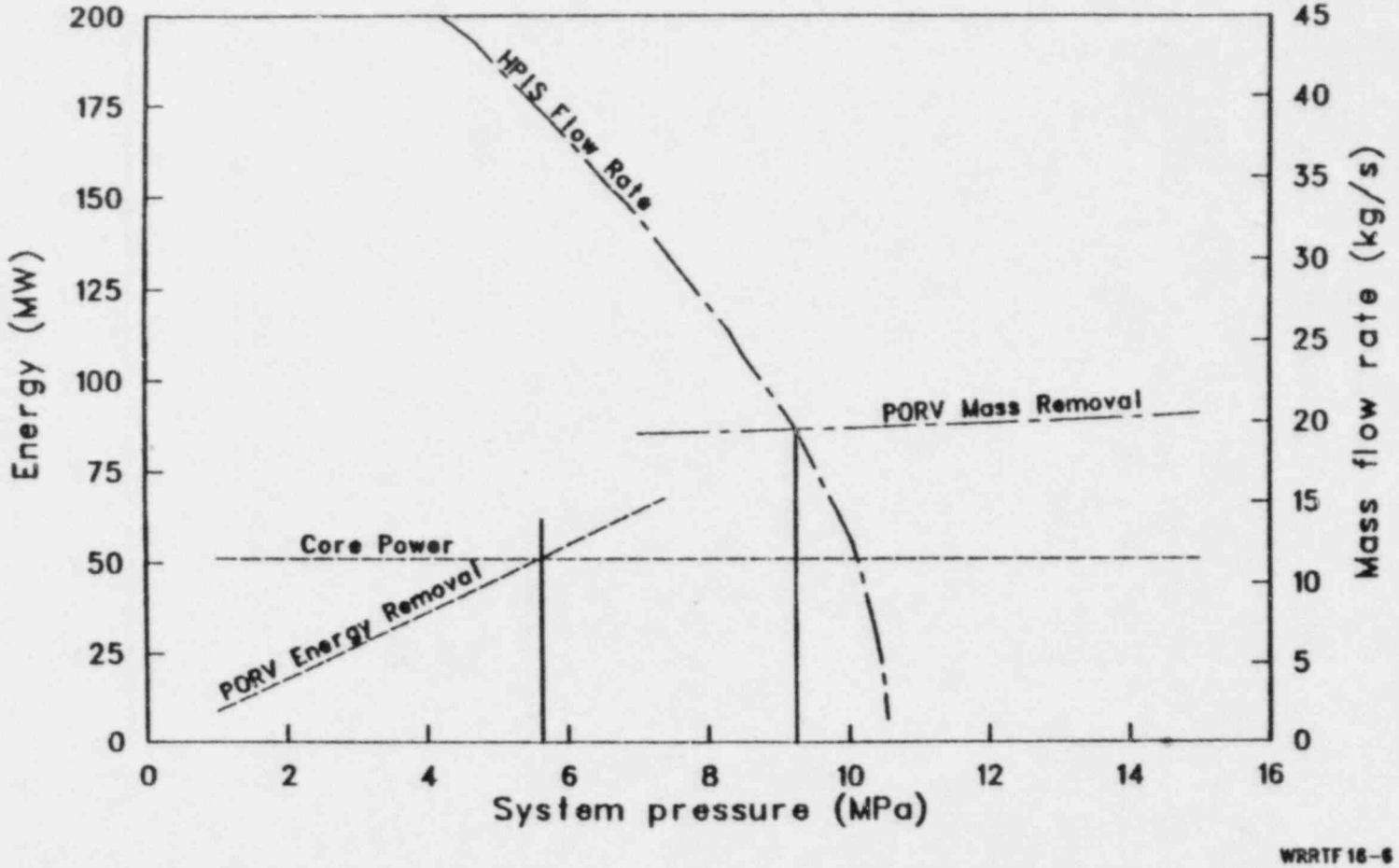

Figure 4. Zion primary feed and bleed operating map for 1.5% core power without charging pumps.

The above curves are based upon the assumption that 100% quality steam exists at the PORV. Figure 5 shows the sensitivity of the PORV energy removal curve to lower qualities as determined with the HEM flow model. Since the energy removal per unit mass decreases while the mass flow rate increases the energy removal rate initially decreases with decreasing quality. However, since the mass flow rate increases substantially with decreasing quality the energy removal rate eventually increases. The effect on the lower operating bound pressure is not large; however, the large increase in PORV mass flow with increased quality rapidly lowers the upper end of the band. As an example, for the conditions used in Figure 4 the operating band does not exist at qualities below approximately 75% (see Figure 6).

The foregoing analysis is useful, in that it provides a basis for examining the feasibility of feed and bleed and for quantitatively assessing the effects of uncertainties or variations in the bounding parameters. However, it does not address transient behavior that may have an important bearing on the ultimate viability of primary feed and bleed. In particular, it should be evident that there exists some uncertainty regarding the ability to safely bring the primary coolant system to within the "feasible" operating pressure band without sustaining unacceptable coolant loss in the process. Factors which bear on this transient process include the primary coolant system state at the initiation of an attempt to feed and bleed, and the nature of the coolant discharged through the PORV(s) in depressurizing the system to within the operating band. These questions can only be addressed through experimentation and the use of computer code analyses.

2.3 Factors Affecting PORV Discharge

Of the factors previously discussed the largest uncertainty affecting the feed and bleed operating band arises from the influence of two-phase PORV flow. The mass flow through the PORV is dependent on upstream fluid conditions at the top of the pressurizer. Several factors contribute to

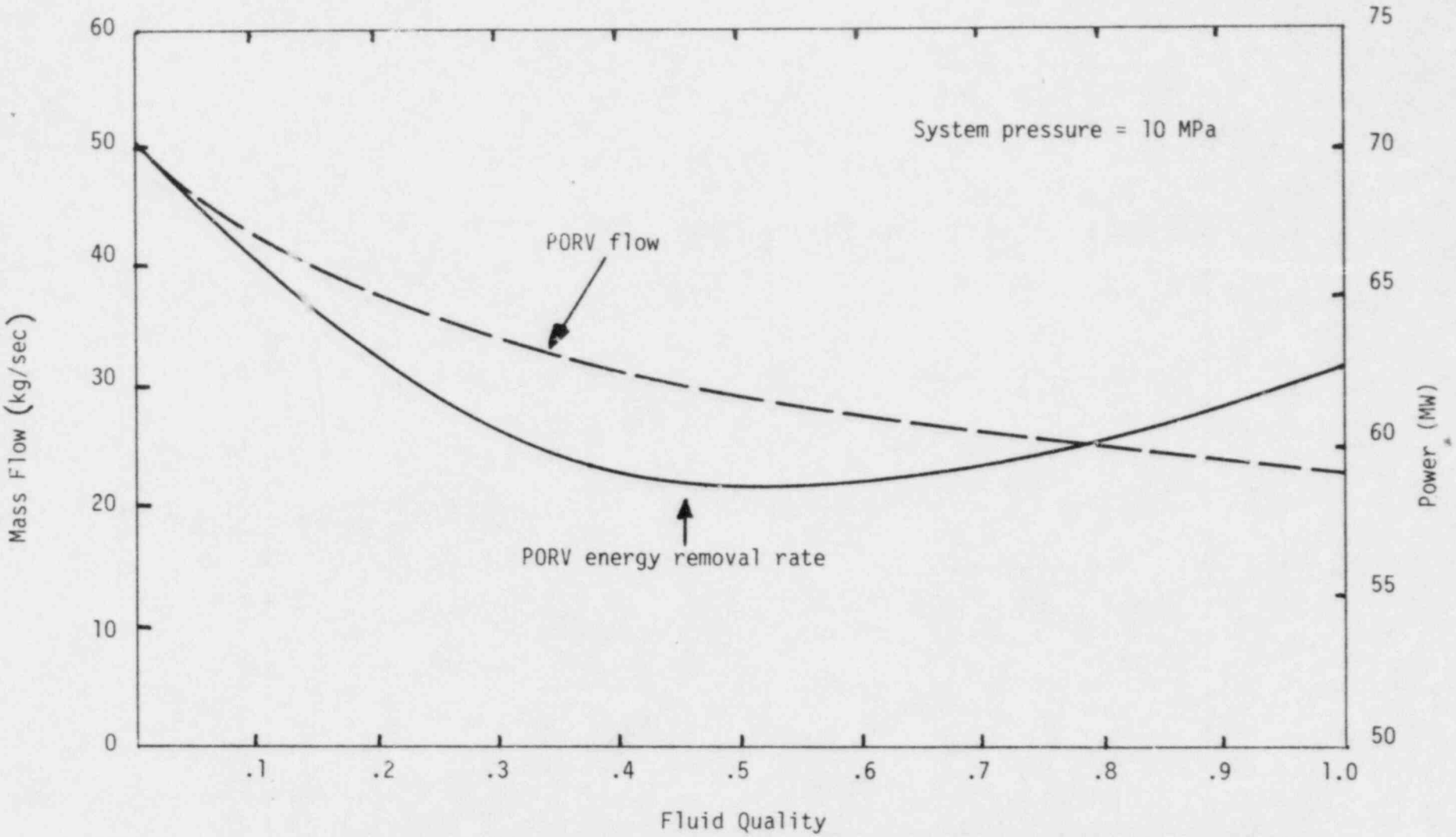

Figure 5. Effect of fluid quality of PORV mass flow and energy removal at 10 MPa.

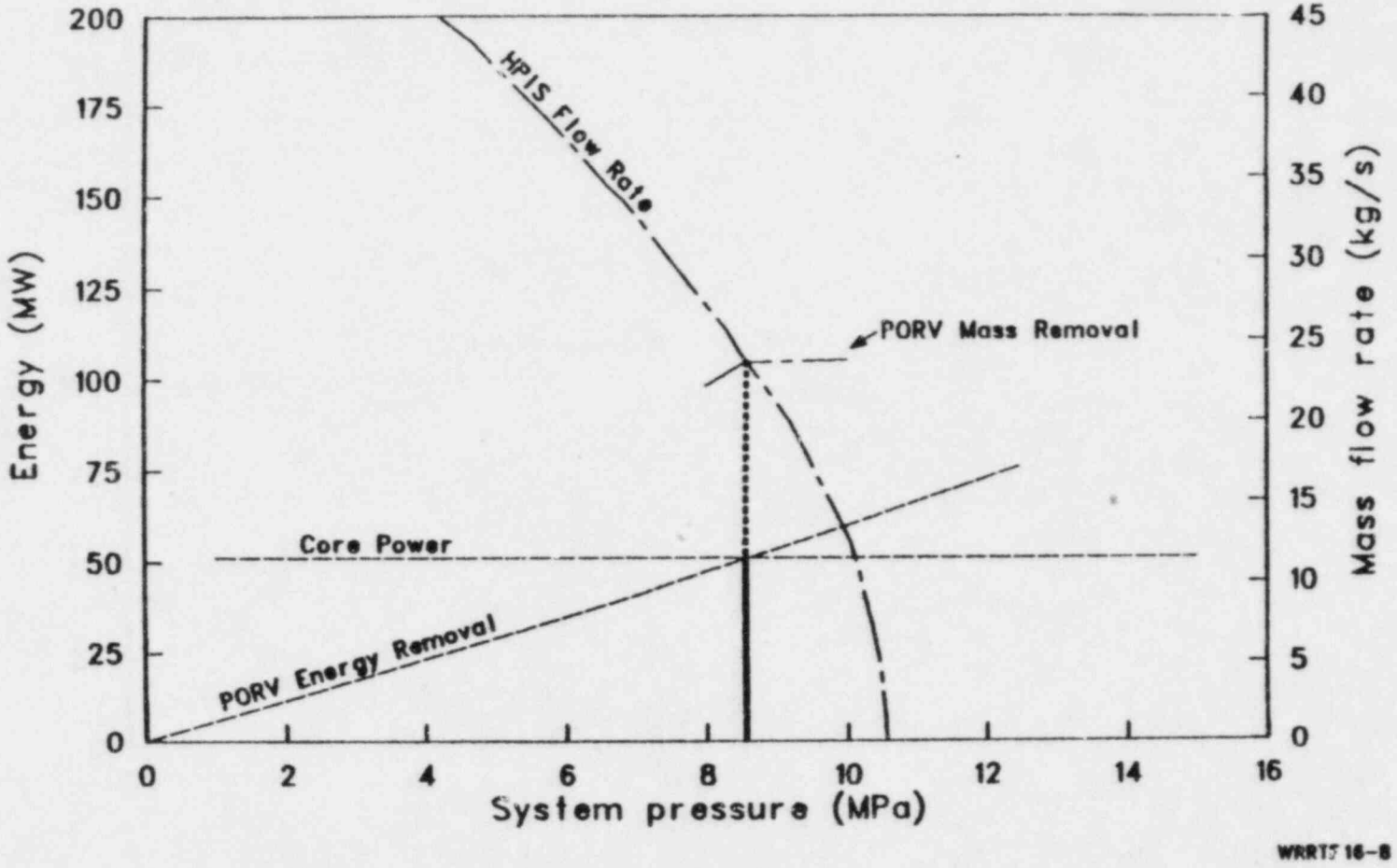

Figure 6. Zion primary feed and bleed operating map for 1.5% core power, no charging flow, and 75% quality PORV upstream conditions.

establishing pressurizer fluid conditions. The ones discussed here are: pressurizer coolant conditions, primary coolant system conditions, pressurizer/surge line geometry, and surge line orientation.

2.3.1 Pressurizer Coolant Conditions and Primary Inventory

If feed and bleed is not initiated soon after losing the secondary heat sink and pressurizer heaters, the primary liquid swell will fill the pressurizer and collapse the steam bubble. Several conditions may form or sustain a vapor bubble at the top of the pressurizer. A vapor bubble can be produced by loss of pressurizer liquid inventory, heating of the fluid to saturation, and/or depressurization. In the present study the pressurizer heaters are assumed to be nonoperational and direct heating is therefore precluded. In a transient depressurization, liquid flashing in the pressurizer will tend to create a high quality region near the top as long as the fluid in the pressurizer is the hottest in the system. However, the liquid swell that accompanies bulk flashing will tend to decrease the quality at the top of the pressurizer. For either a quasi-steady-state situation, or in a transient once the original pressurizer inventory has been replaced with coolant from the hot leg, the PORV fluid conditions are dependent upon the conditions in the hot leg. If the coolant lost through the PORV is replaced by low quality fluid the mass discharge out the PORV will remain fairly high. This will occur until the primary system inventory is reduced enough to cause significant voiding in the hot leg. Once significant hot leg voiding occurs pressurizer/surge line geometry and orientation become important as described below.

2.3.2 Pressurizer/Surge Line Geometry

For a given vapor volume a pressurizer with a large length-to-diameter ratio would have a "tall" void height relative to a pressurizer with a smaller ratio, in addition to also having a smaller cross-section. A steam bubble of greater height would tend to enhance separation from the vapor of liquid droplets created by bubbles breaking through the liquid surface, due to the greater wall surface area and reduced potential for droplets being thrown upward into the high vapor velocity area near the PORV line

entrance.[a] However, since vapor must by necessity pass through the pressurizer liquid from the surge line to the PORV, a large L/D would tend to promote liquid swell and droplet entrainment due to the smaller cross-sectional area.

In any case, the influence of pressurizer geometry is probably overshadowed by the preclusion of counter-current flow in the surge line. Even if a liquid/vapor separation mechanism did exist in the pressurizer, typical surge line velocities are well above flooding limits.[b] Therefore, pressurizer liquid could not drain back to the loop and would continue to be stored in the pressurizer until the PORV discharge quality self-adjusted to accommodate removal of the mass. It therefore appears necessary to have high quality steam supplied from the hot leg in order to have high quality PORV discharge.

2.3.3 Surge Line Orientation

If hot leg voiding does occur, the orientation of the surge line would influence the primary system inventory at which high quality steam entered the pressurizer. Surge line to hot leg connections of various orientations, from horizontal side entrance to vertical top entrance, are used in current PWRs. With the top entrance line, and quiescent hot leg conditions, minimal hot leg voiding is necessary to allow high quality surge line flow. With a side entrance line the hot leg pipe liquid level must drop much lower before high quality flow begins. In either case the surge line flow may still be varied significantly if nonquiescent conditions exist that disrupt stratified flow, such as when primary recirculation pumps are turned on, or a transient depressurization is occurring.

---

a. For typical PWR pressurizer dimensions, the vapor velocity (due to an open PORV) in a vapor filled cross-section is on the order of 1 ft/s which presents little chance of droplet entrainment.

b. Discussed in Section 4.2

2.4 Summary Observations

Based on the foregoing discussion it is concluded that a simplified approach to determining the feasibility of primary feed and bleed in a pressurized water reactor lies in the mapping of energy and mass flows. Moreover, this technique can be used to quantitatively assess the sensitivity of the operating pressure band to variations in the boundary conditions of ECCS flow, PORV flow, and decay heat. The operating map represents an ultimate statement as to whether feed and bleed is possible, and is the starting point for examining specific design features that bear on the operating bounds. It is evident that plausible variations and uncertainties in these parameters can lead to the elimination of a steady-state operating pressure range. Principal among these uncertainties is the coolant discharge through the PORV. The predictability of this single parameter is subject to much greater uncertainty than either decay heat or ECCS flow.

Irrespective of the existence of a theoretically feasible operating pressure band, there remains the question as to whether the reactor system can be safely maneuvered into this pressure range. In this regard it is clear that a dependence must be placed on computer code analyses (with suitable verification) and adequate supporting experimental data. Such analyses and/or experiments should examine the plausible scenarios which lead the operator to commence primary feed and bleed, since the initial condition of the primary coolant system (particularly inventory) will have a significant effect on the outcome.

3. RESULTS FROM SEMISCALE EXPERIMENTS

Experiments were conducted in the Semiscale MOD-2A facility to evaluate system behavior during primary feed and bleed operations. The boundary conditions of HPIS injection rate were scaled from Westinghouse plants with either "high head" (injection capacity up to the safety valve setpoint) or "low head" (pump deadhead at typically 10.3 MPa) HPIS pumps. The PORV discharge capacity was scaled close to the value for a full-size plant, but was slightly larger. This was consistent with the use of core power levels that were on the high end of typical decay heat values, so as to allow more positive observation of system performance with less distortion from environmental heat losses. Consistent with the analysis of Section 2 regarding the ultimate feasiblity of primary feed and bleed cooling, the boundary conditions selected for the Semiscale experiments provided for a steady-state operating band. As described below, the experimental results therefore allowed for examining the influence of the assumptions implicit in those simplified analyses on the true feasilibity of feed and bleed cooling.

3.1 System Configuration

For Semiscale Mod-2A Tests S-SR-1 and 2, the Mod-2A system was configured as shown in Figure 7 The major components of the system were the vessel with electrically heated core and external downcomer, intact and broken loop steam generators, broken loop recirculation pump, and loop piping. The vessel core consists of a 5 x 5 array of internally heated electric rods, 23 of which were powered. The rods are geometrically similar to nuclear rods with a heated length of 3.66 m and an outside diameter of 2.072 cm. The power was distributed such that the center nine rods were powered at 1.25 times the average rod power. The primary system also incorporated the use of external heaters on loop piping and on the pressure vessel to mitigate the effects of heat loss to the environment. A more detailed description of the Mod-2A system may be found in Reference 5.

Since the recirculation pumps were not used during this test, the intact loop recirculation pump was replaced with a section of pipe to

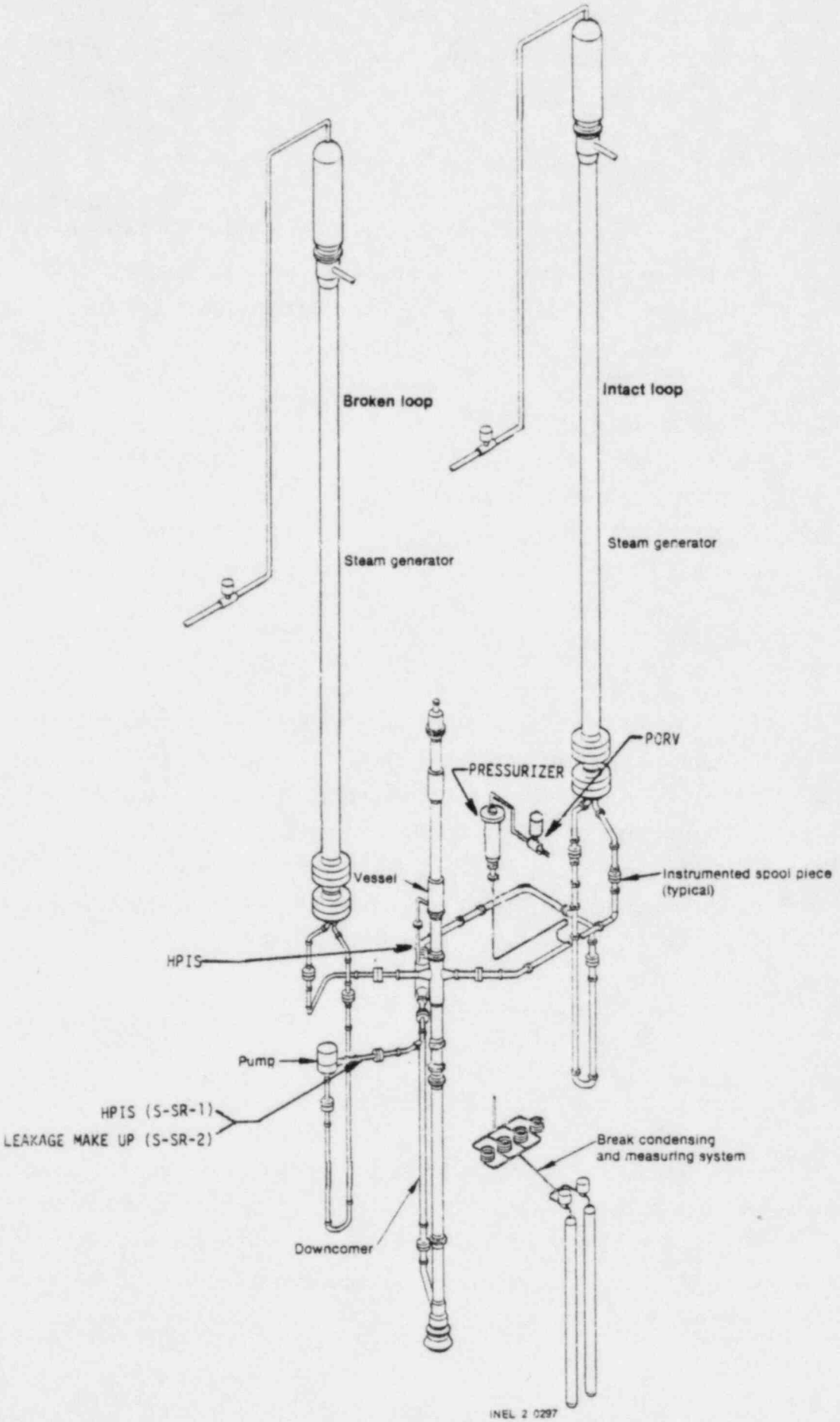

Figure 7. Semiscale system configuration for primary feed and bleed experiments.

preclude a relatively large primary leak. This section of pipe was orificed to represent the scaled hydraulic resistance of a pressurized water reactor primary pump in a locked rotor (stopped) configuration.

Other important configuration details were as follows:

1. The HPIS fluid entered the primary system through both the intact and broken loop cold legs during Test S-SR-1. During Test S-SR-2 all of the HPIS entered through the intact loop cold leg. The broken loop HPIS was used for leakage makeup only.

2. A square edged orifice of 0.1549 cm ID was placed upstream of a remotely controlled valve to simulate two PORVs. The critical flow rate provided by this orifice was typical of the scaled relief rate of PORVs in a full-size PWR. Relative to the published Zion plant PORV capacities the orifice used in the Semiscale experiments had a flow area 20% greater than the correctly scaled value.

3. The outlet line from the pressurizer PORV was connected to the condensing and measurement system. This system was used to condense PORV effluent and measure it so an accurate determination of PORV mass flow rate could be made.

4. For these tests the secondary sides of the intact and broken loop steam generators were drained and isolated.

3.2 Test Procedures and Conditions

3.2.1 Pre-Feed and Bleed Operation Activities

Prior to initiating each experiment the primary was brought to the desired equilibrium temperature (minimal temperature gradients around the primary). The external heaters were powered at the levels indicated in Table 1. Once the desired temperature was obtained the core power was adjusted to maintain steady-state. Thus, the core power compensated for

TABLE 1. EXTERNAL HEATER POWER LEVELS

Location	Power (kW)
Vessel	20
Hot legs	7.1
Cold legs	3.3
I.L. pump suction	8.5
B.L. pump suction	4.2
Total	43.1

the remaining primary environmental heat losses and also heat transfer to the secondary side of the steam generators. Leak rate checks were also made. For Test S-SR-1 the coolant loss was uncompensated. For Test S-SR-2 the leakage was made up by cold water injection into the broken loop cold leg. Results of the leak rate tests are given in Table 2.

3.3 Test Result

Test results are presented in this section for Tests S-SR-1 and 2. Each of these tests was performed with a constant net core power of 40 kW.[a] For Semiscale this represents 2% of full power. This level of heat is representative of decay heat approximately 10 to 20 minutes after a scram and is high enough above Semiscale environmental heat losses to have a measureable effect on system response.

The orifice used to simulate the pressurizer PORVs in a full-size PWR was sized to provide a representative steam relief capacity. The ECC systems of importance for primary feed and bleed are those capable of injecting water at relatively high pressure. The injection rates used for these experiments were typical of the HPI systems in PWRs. As discussed below, two different injection rate versus system pressure curves were used in the tests performed. The aggregate result of the selected boundary conditions on the theoretical primary feed and bleed behavior addressed in Section 2 is discussed for each experiment. An analysis of actual system behavior is then presented.

3.3.1 Test S-SR-1

3.3.1.1 S-SR-1 Predicted Response and Objectives. Test S-SR-1 was performed using a "high head" pumped HPIS injection capacity. The HPIS flow was powered scaled based on HPIS flow information for the North Anna plant.[6] The feed and bleed operating map for Semiscale based on this

---

a. Core power was augmented to compensate for measured environmental heat losses and heat transfer to the secondaries.

TABLE 2. INITIAL TEST CONDITIONS

Parameter	Test S-SR-1	Test S-SR-2 Point 1	Test S-SR-2 Point 2	Test S-SR-2 Point 3
Pressurizer pressure	12.43 MPa	8.16 MPa	6.30 MPa	15.2 MPa
Pressurizer level	80 cm	125 cm	143 cm	108 cm
Core power	78 kW	78 kW	78 kW	78 kW
Net core power (beyond that needed for environmental heat loss)	40 kW	40 kW	40 kW	40 kW
Radial power peaking	1.32	1.33	1.33	1.33
Cold leg fluid temperature				
Intact loop	575 K	520 K	540 K	547 K
Broken loop	551 K	502 K	500 K	517 K
Time of initiation	1300 s	3750 s	8700 s	14,940 s
ECC injection				
HPIS type	high head	low head	low head	low head
Temperature	ambient	ambient	ambient	ambient
Leakage[a]	0.006 kg/s	0.007 kg/s	0.007 kg/s	0.007 kg/s
Environmental heat loss	72 kW	72 kW	72 kW	72 kW

a. Total primary coolant system inventory was approximately 150 kg at typical initial conditions.

scaled HPIS flow capacity and 40 kW core power is shown in Figure 8. Figure 8 indicates that steady-state feed and bleed is theoretically possible between 7.6 and 15.4 MPa assuming 100% quality steam flow through the PORV.

The specific objective of S-SR-1 was to determine the feasibility of operating within the predicted operating band and to examine the thermal-hydraulic effects accompanying rapid depressurizations to lower operating pressures when significant primary mass depletion had occurred. As will be shown below, operational problems with uncontrolled coolant leakage from the system precluded the use of results from Test S-SR-1 for direct interpretation as to the viability of feed and bleed cooling. Rather, the test furnished data that is useful for identifying and examining phenomena that influence feed and bleed operation.

3.3.1.2 Test S-SR-1 Results. The transient was initiated at 1300 seconds into the test. (The first 1300 seconds were used to determine primary leakage and environmental heat losses.) Table 3 indicates the sequence of major events for this test. The initial conditions of important parameters prior to feed and bleed initiation are given in Table 2.

The first part of the transient simulated a "hands off" situation where the system was allowed to establish conditions at the safety relief pressure in response to a loss of feed water and loss of offsite power. Figure 9 shows the response of the pressurizer pressure and collapsed liquid level. At the initiation of the transient (1300 seconds) the pressurizer liquid level is seen to rise. This resulted from terminating pressurizer heater power with the resultant cooling of the pressurizer[a] causing collapse of the vapor space. The vapor bubble in the pressurizer continues to collapse until the pressurizer is full of liquid.

---

a. The pressurizer environmental heat loss was determined to be approximately 4.5 kW at 585 K.

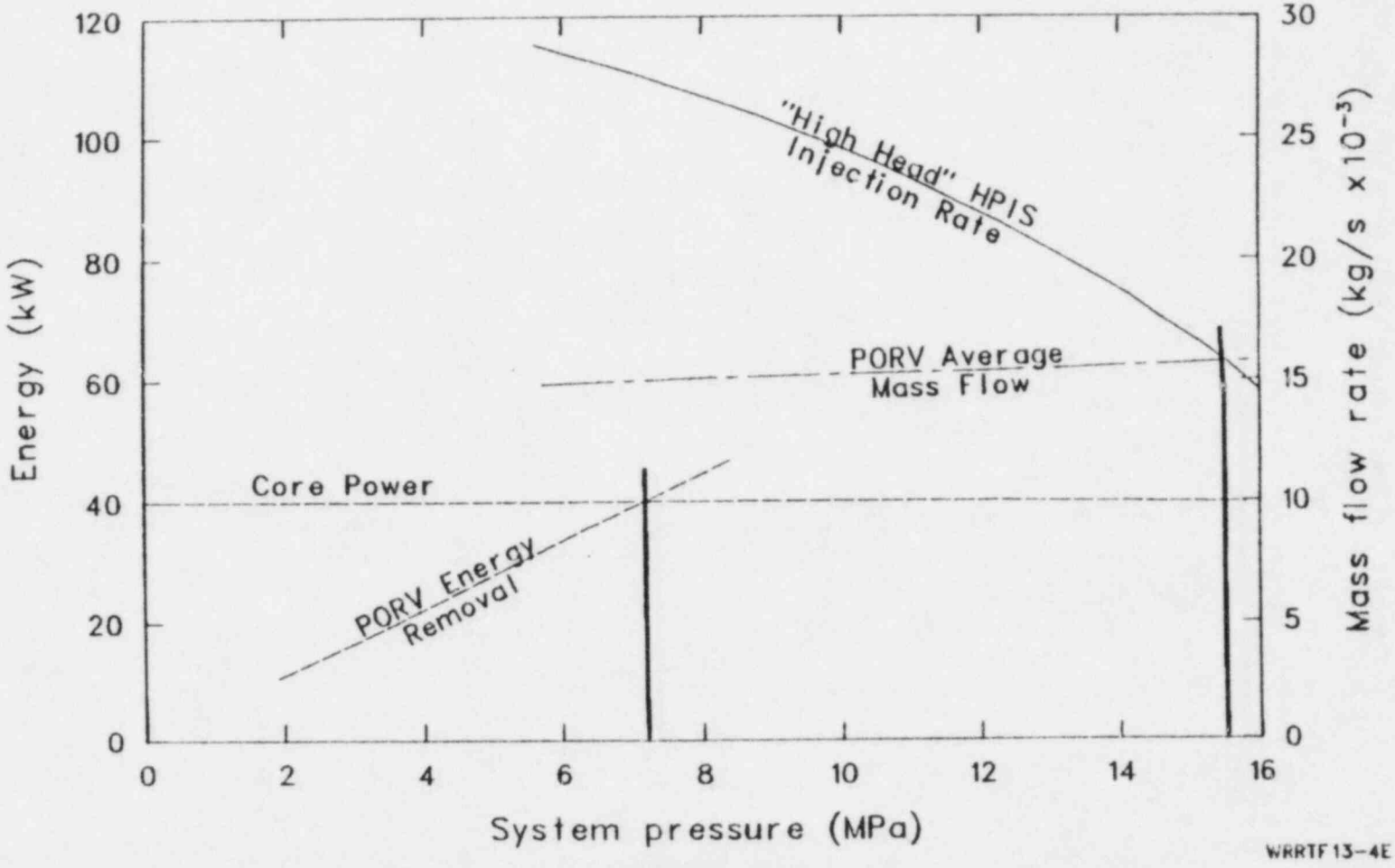

Figure 8. Semiscale Mod-2A primary feed and bleed operating map for Test S-SR-1 (high head HPIS).

TABLE 3. SEQUENCE OF EVENTS FOR TEST S-SR-1

Time (seconds)	
0-700	Determine environmental heat loss and leakage
	Pressurizer isolated from primary
	Steam generator secondaries empty
700-1300	Pressurizer and primary equilibrated and brought to initial conditions
1300	Transient initiated
	Pressurizer heaters off
	Core power increased by 40 kW
	Pressure = 17 MPa
	Leakage makeup terminated
3450	Primary system pressure reaches 15.17 MPa--setpoint of PORV
3700	HPIS enabled
6050	Depressurization to 12.41 MPa
6300	Depressurization to 11.03 MPa
6550	Termination of test

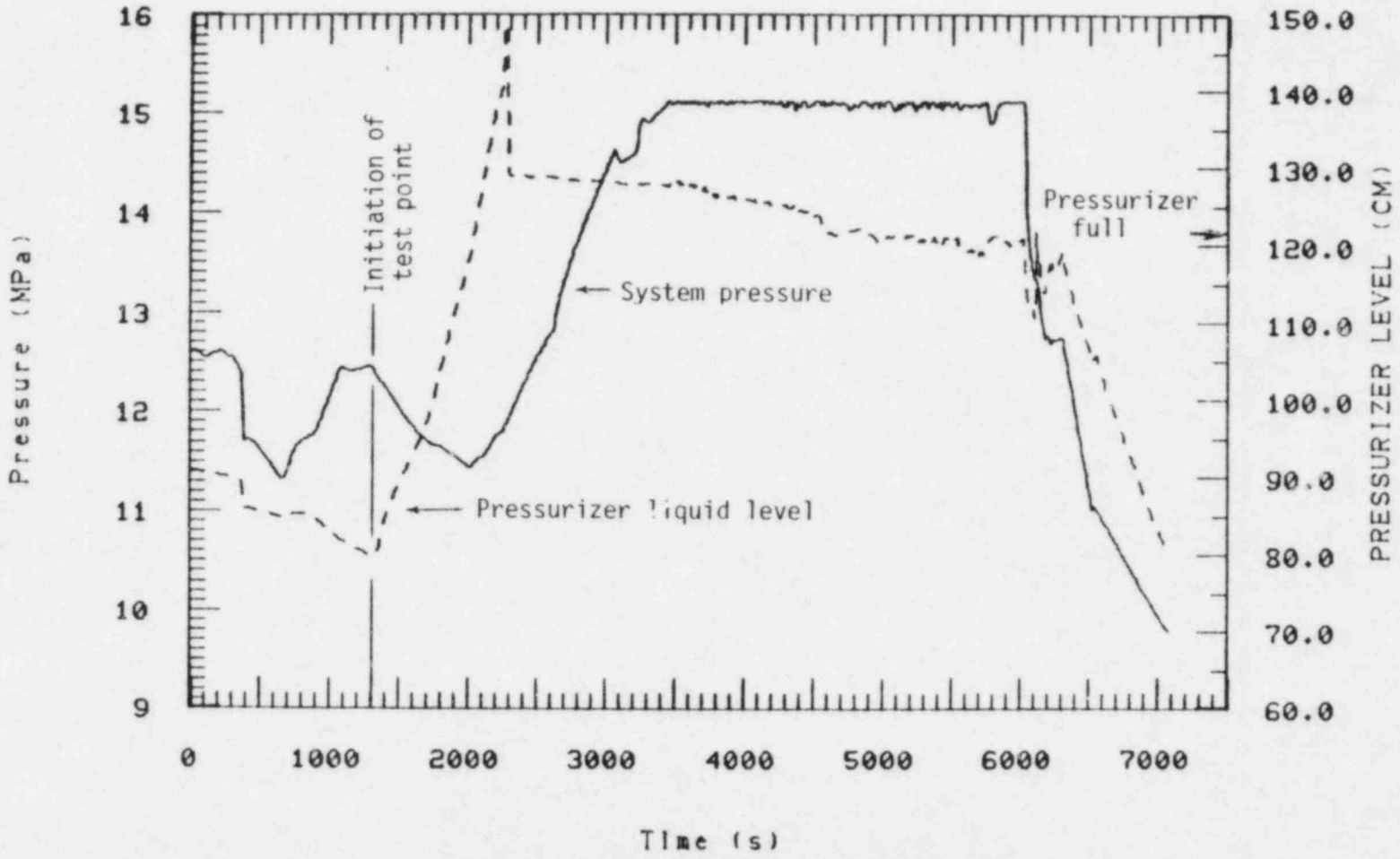

Figure 9. Test S-SR-1 pressurizer pressure and collapsed liquid level.

Figure 9 also shows the system pressure initially dropping at the onset of the test. This is also a result of the vapor bubble in the pressurizer collapsing due to the termination of power to the pressurizer heaters. As Figure 10 shows, the system pressure begins to rise when the upper head temperature reaches saturation. The system pressure continues to rise to the set pressure of the PORV (15.17 MPa). At this time (3450 seconds) the bleed portion of the operation begins. Several minutes later (at 3700 seconds) HPIS was enabled which began the feed portion of the operation.

Figure 11 shows the PORV and total HPIS mass flow rates. The PORV flow curve is not smooth due to the cycling of the PORV to maintain the system pressure at 15.17 MPa. Figure 12 shows the integrated PORV, HPIS and estimated leakage flow and the net effect on mass inventory. Beginning at 1300 seconds the mass inventory is reducing due to redistribution of mass into the pressurizer[a] (vapor bubble collapsing) and from leakage. At 3450 seconds the rate of change of inventory loss can be seen to increase due to latching open the PORV. At 3700 seconds the HPIS was enabled and the mass inventory held relatively constant, until the PORV mass flow increased. The PORV mass flow increased due to changing fluid conditions in the pressurizer. This condition continued until the collapsed liquid level in the core was just above the heated length. At that time (6050 seconds) the PORV setpoint was readjusted and the system pressure was reduced to 12.7 MPa in an attempt to recover primary mass inventory by obtaining larger HPIS flows.

The analysis of Test S-SR-2 described in the following section will show a distinct relationship between the PORV flow rate and the hot leg density (near the surge line entrance) for a situation in which the PORV is latched open. In Test S-SR-1 the PORV was cycled (with a 70 kPa hysteresis between the opening and closing pressures) to maintain selected pressures. Figure 13 shows the measured PORV flow, predicted 100%-quality steam flow

---

a. For the mass calculation shown, coolant which entered the pressurizer was subtracted from the "primary" system mass.

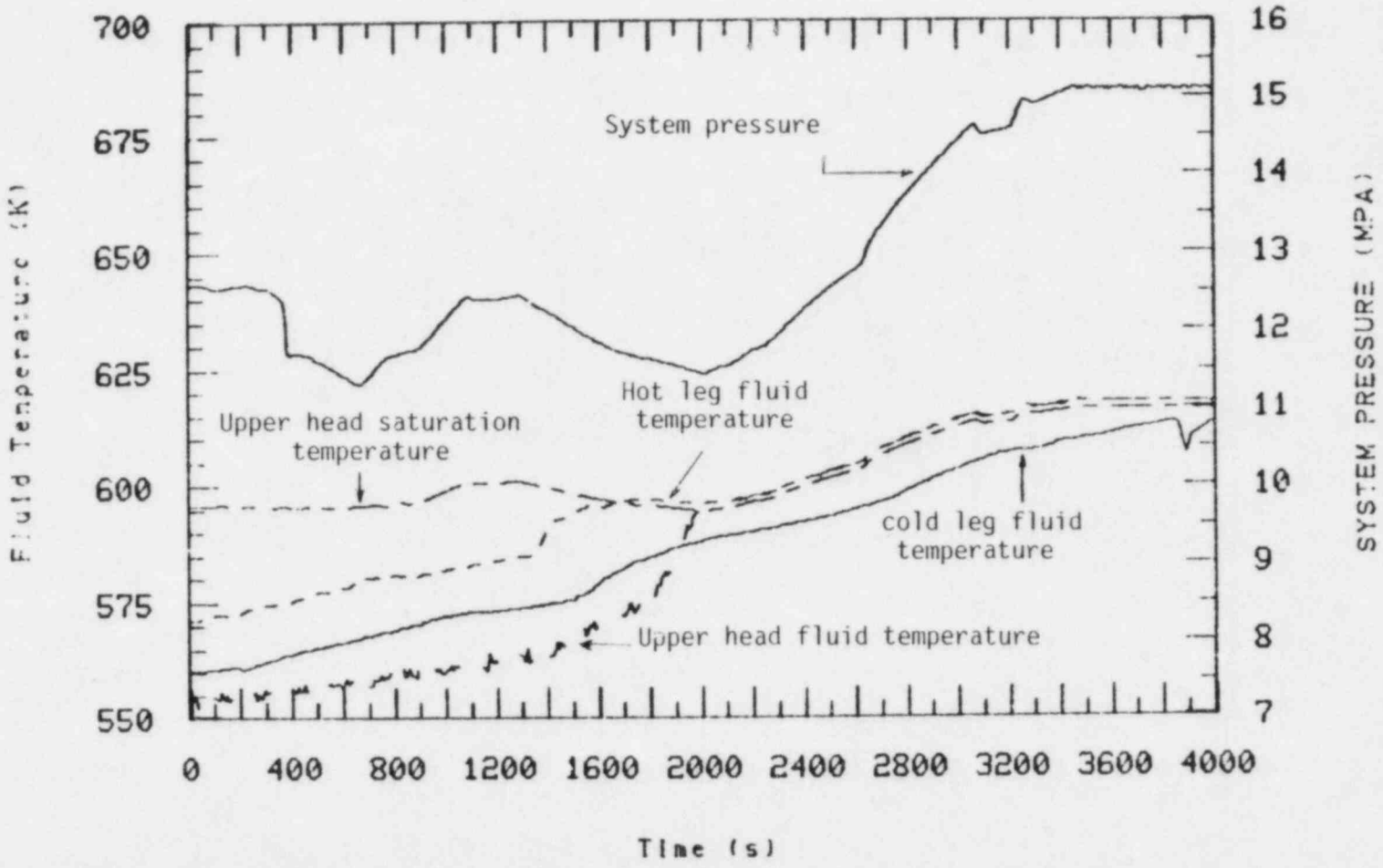

Figure 10. System pressure compared with selected system fluid temperatures for Test S-SR-1.

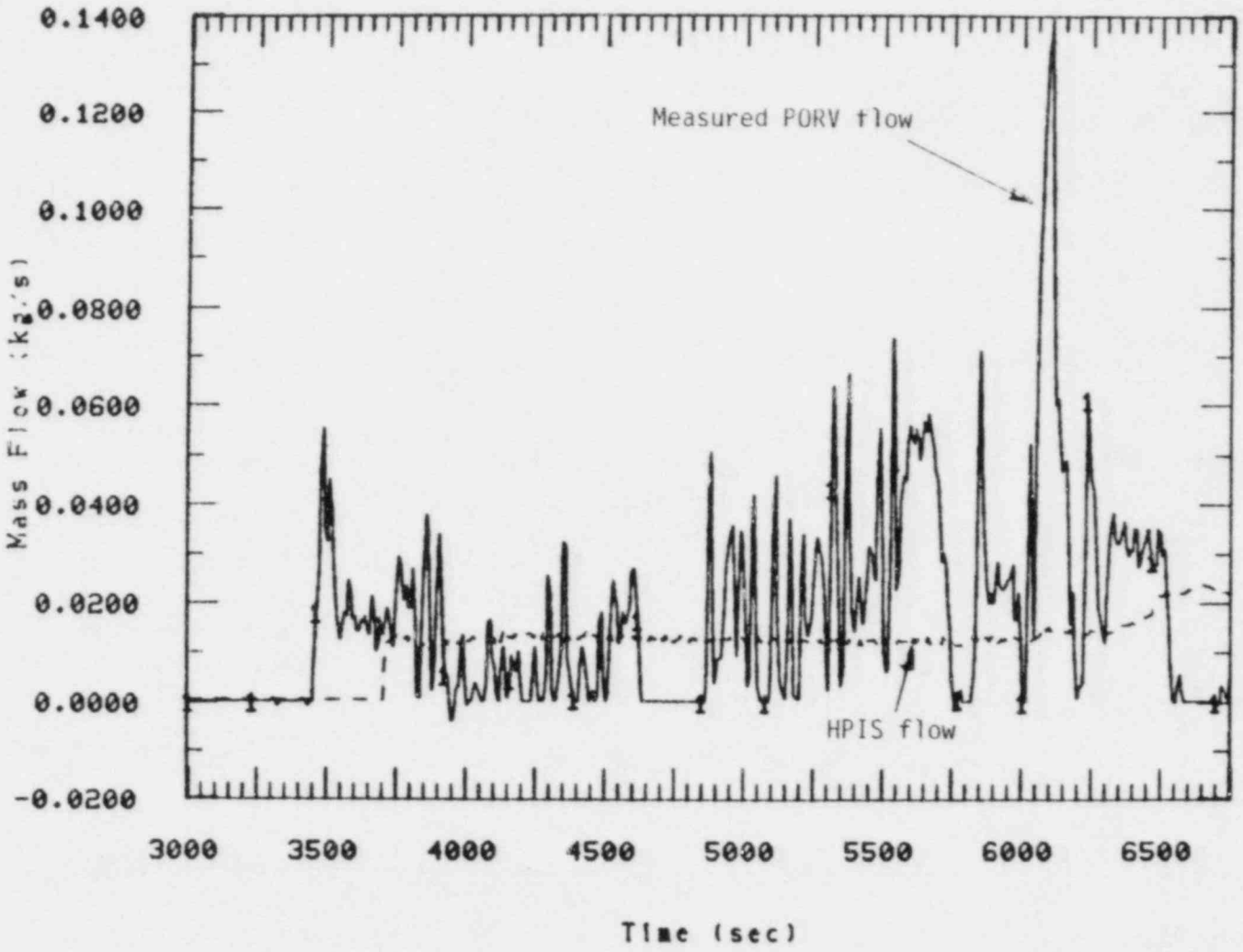

Figure 11. Measured PORV and HPIS flow for Test S-SR-1.

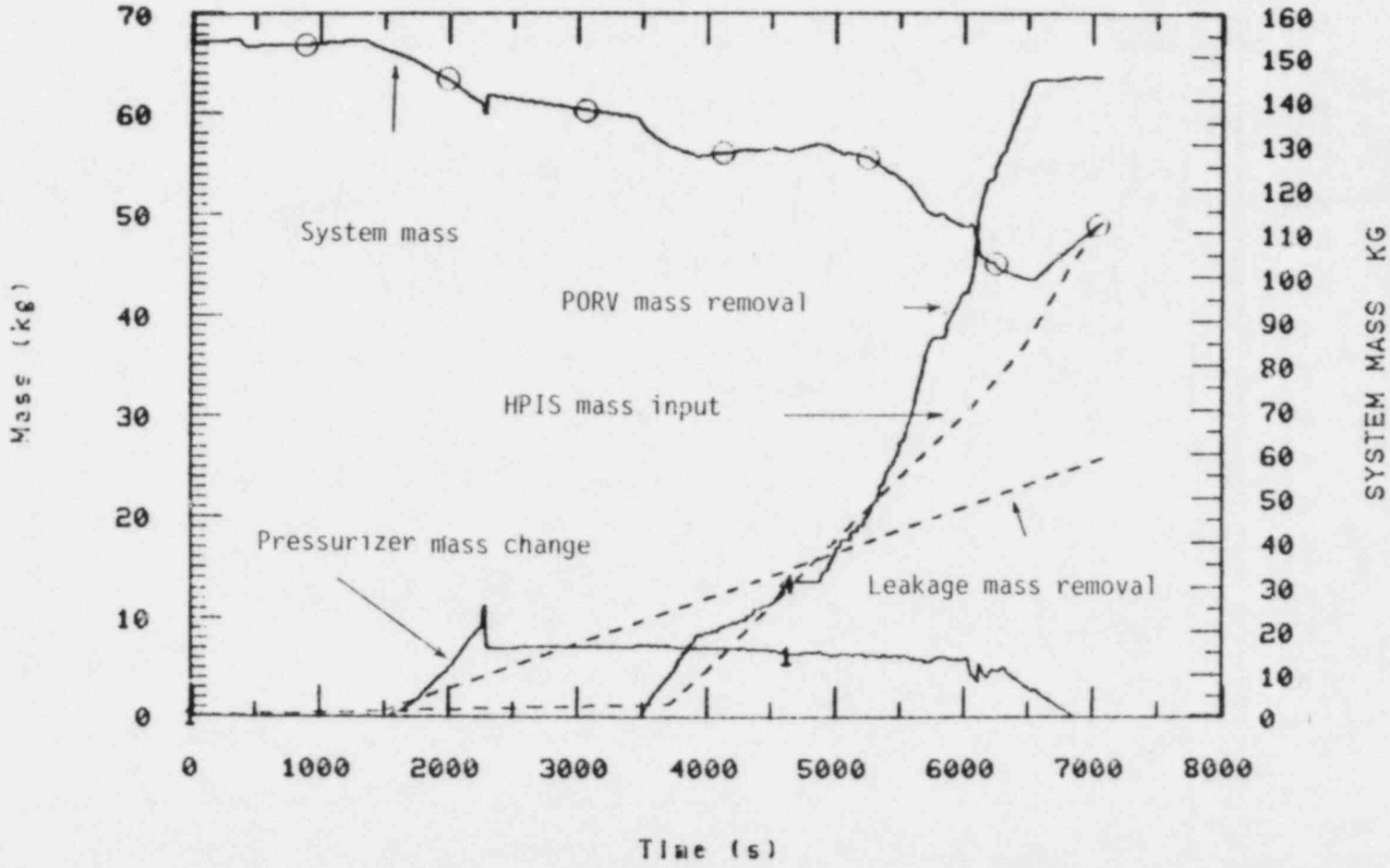

Figure 12. Primary system mass balance for test S-SR-1.

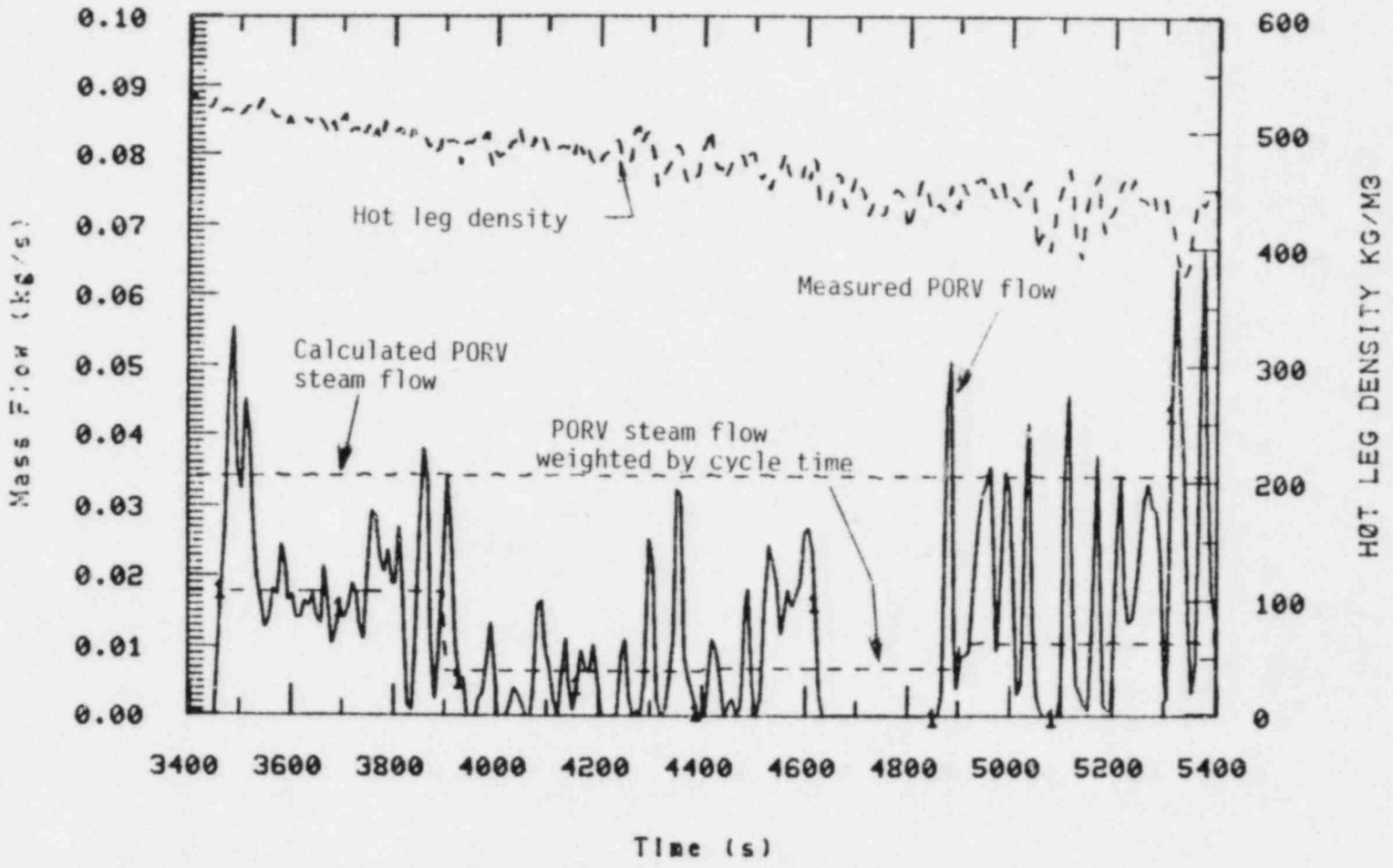

Figure 13. PORV flow rate compared to predicted values and hot leg density. Test S-SR-2.

rate, and the steam flow rate weighted by the valve cycle time required to remove the core heat, compared to the hot leg density. It is seen here that even with a low void fraction in the hot leg the flow out the PORV reflected a high quality discharge. Referring to the pressurizer liquid level of Figure 9, it appears that a vapor space existed in the pressurizer that would allow this.

At 6050 s the PORV setpoint was lowered from 15.7 to 12.41 MPa, and further lowered to 11.03 MPa at 6300 s (Figure 14). Immediately following these changes the PORV was effectively latched open until the new pressure was reached. Referring to Figures 9 and 15 at these times it is observed that the mass flow rate increased even though there was little change in pressurizer level. Also, referring to the hot leg density curve of Figure 15, the PORV flow rate was strongly dependent on the hot leg density, as is apparent by the difference in flow rates from 6100 to 6400 s. It is surmised from this behavior that closing the PORV for periods of time in the cycling process allowed a phase separation mechanism to occur in the pressurizer which maintained a steam flow discharge.

At 12.7 MPa the mass balance was still unfavorable so the pressure was reduced to 11.1 MPa in another attempt to recover primary mass inventory by increasing the HPIS injection rate. Although HPIS injection was large enough to begin to recover mass inventory, core uncovery was too extensive to prevent excessive rod temperatures. The test was terminated at 6550 seconds.

3.3.2 Test S-SR-2

3.3.2.1 S-SR-2 Predicted Response and Objectives. Test S-SR-2 was performed using a "low head" pumped HPIS injection capacity. The injection rate was powered-scaled based on HPIS flow information from the Zion plant.[7] Only the combined injection capacity of the HPIS pumps, which deadhead at 10.34 MPa, was considered. No contribution was assumed from the charging pumps, which are capable of injecting up to the safety relief pressure. The feed and bleed operating map for Semiscale based on this

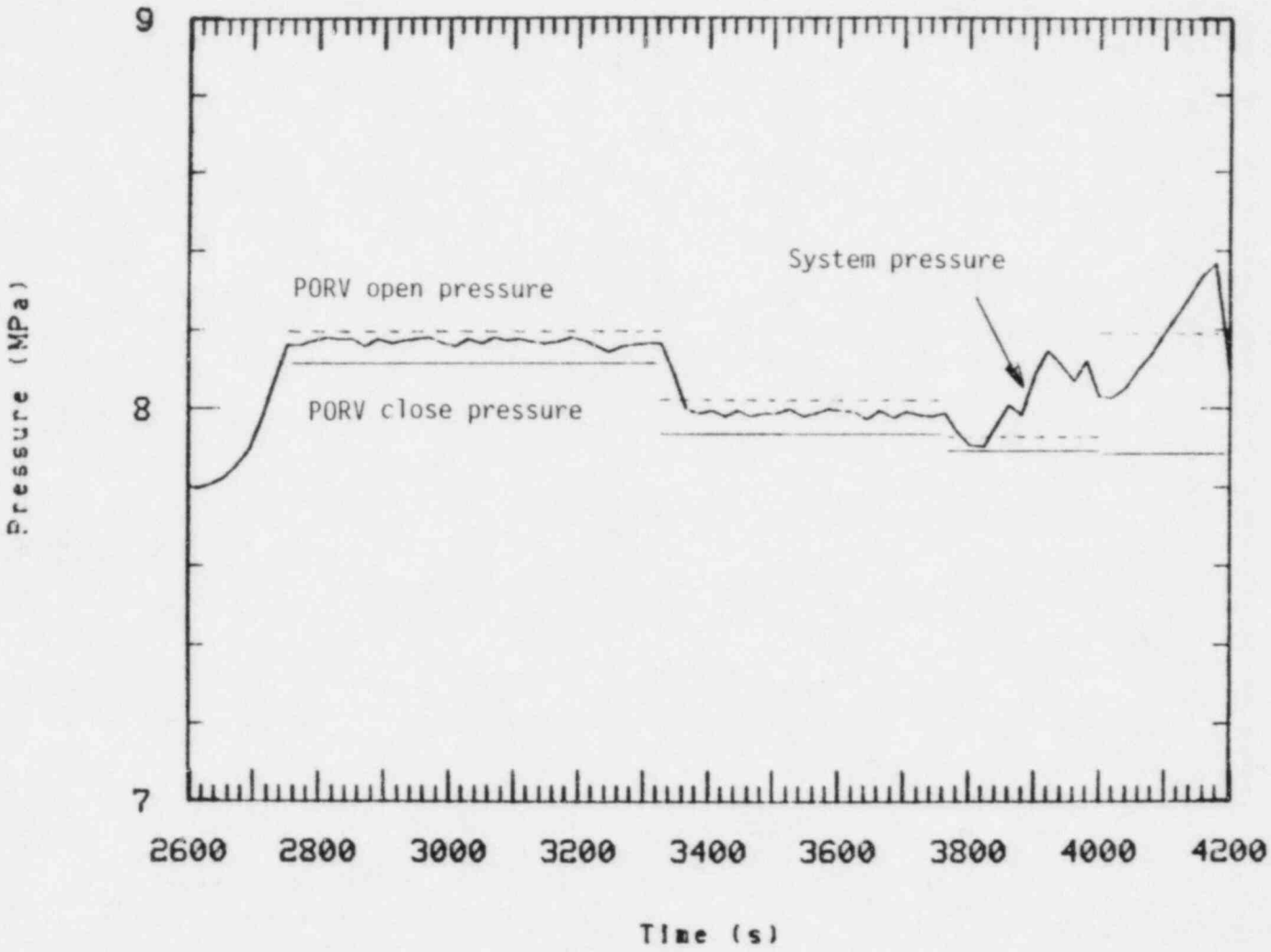

Figure 14. System pressure and PORV setpoints for Test S-SR-1 point 1.

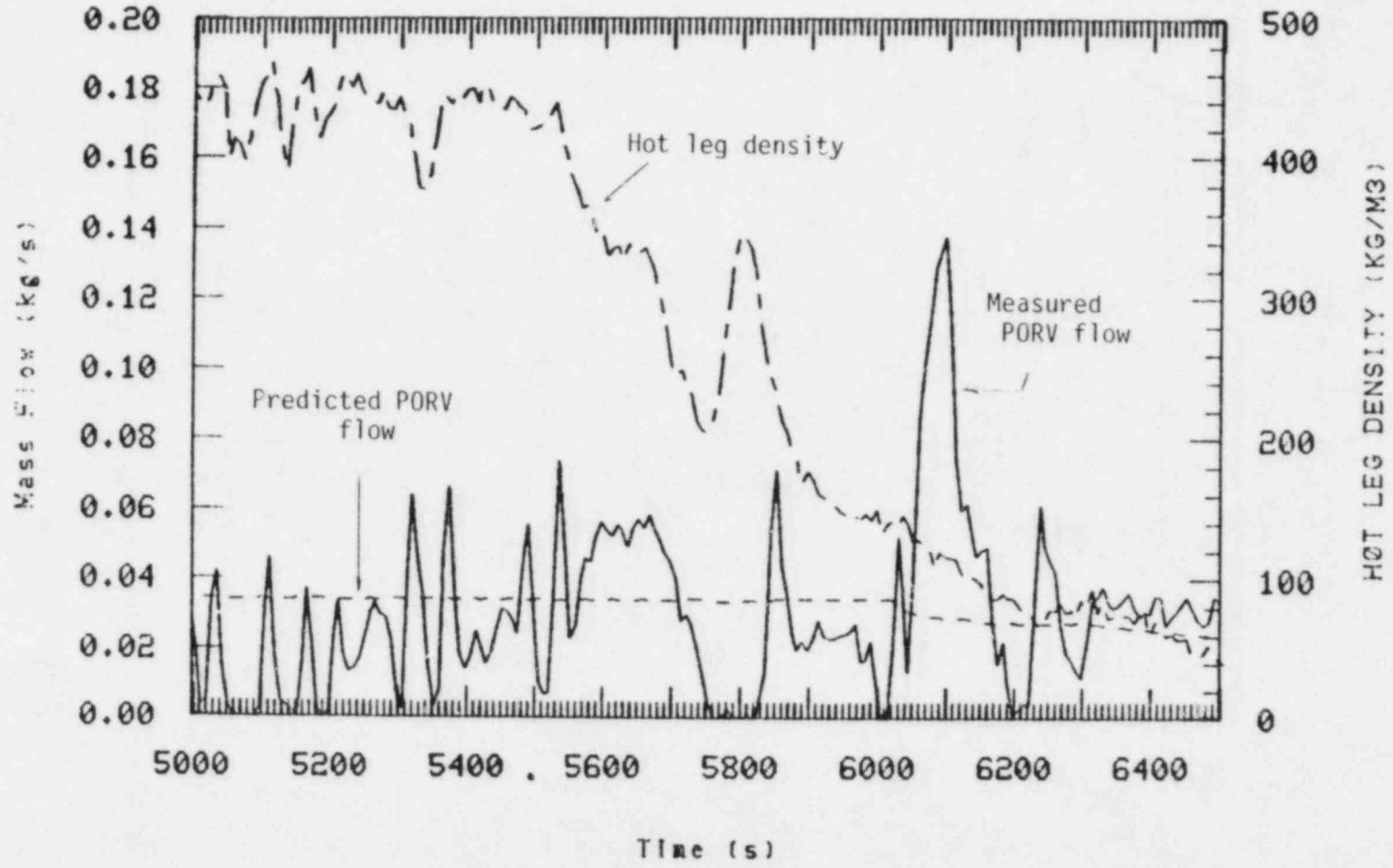

Figure 15. PORV flow rate compared to predicted value and hot leg density.

scaled HPIS flow capacity and 40 kW core power is shown in Figure 16. Figure 16 indicates that steady-state feed and bleed is theoretically possible between 7.0 and 8.2 MPa assuming 100% quality steam flow through the PORV.

The specific objectives of S-SR-2 were to determine the feasibility of operating within the predicted operating band using a representative low head pumped HPIS and to determine the feasibility of initiating a steady-state feed and bleed operation by depressurizing from a representative operating pressure.

3.3.2.2 Test S-SR-2 Results. A significant operational change for Test S-SR-2 was that the primary leakage was made up with cold water injection. This resulted in minimizing the effects of leaking mass from the primary.

Test S-SR-2 consisted of three separate feed and bleed operations. The first attempt was to try and find the upper steady-state operating limit for favorable energy removal and coolant inventory. The second operating point was below the predicted operating band for PORV steam discharge as shown by Figure 16. The third operation was a depressurization from a representative operating pressure into the predicted operating band. This operation was performed by enabling the HPIS and latching open the PORV. This maneuver is representative of feed and bleed emergency procedures specified for PWRs. Table 4 indicates the sequence of major events and the times at which the three feed and bleed operations were conducted.

The first test point consisted of operating at several pressures in an attempt to obtain a constant mass inventory. Pressure control was accomplished by setting the PORV to open and close at selected pressures. The HPIS was allowed to inject at a rate governed by the system pressure.

Figure 17 indicates the system pressures and pressurizer liquid level during the first test point. As indicated, liquid level in the pressurizer

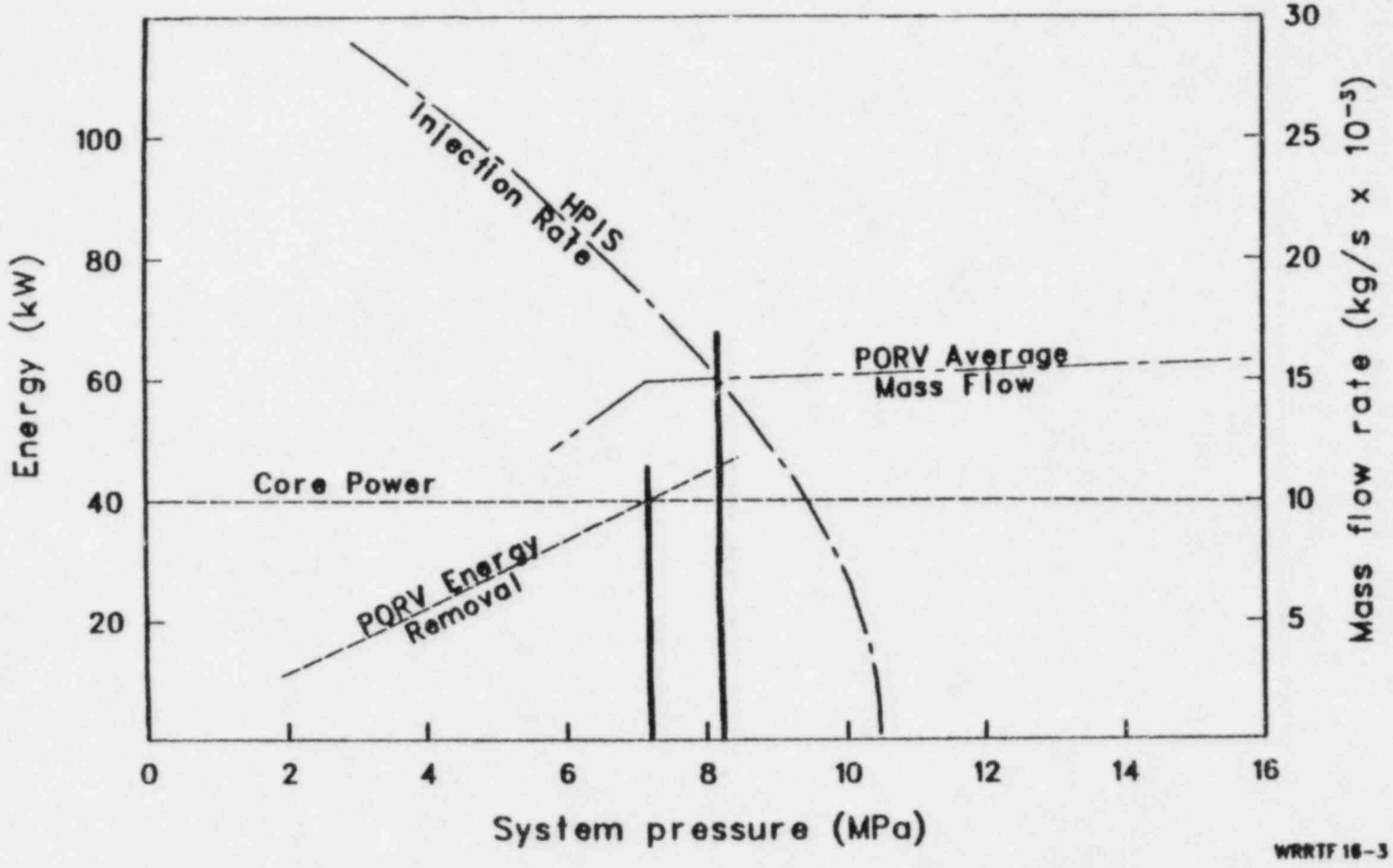

Figure 16. Predicted primary feed and bleed operating map for Test S-SR-2.

TABLE 4. SEQUENCE OF EVENTS FOR TEST S-SR-2

0-2750 seconds	Determined environmental heat loss from pressurizer and primary. Determined primary leak rate. Steam generator secondaries empty.
2750-4190 seconds	First test point
2750-3330	PORV open at 8.70. PORV closed at 8.13
3330-3750	PORV open at 8.01. PORV closed at 7.94
3750-4000	PORV open at 7.93. PORV closed at 7.86
4000-4190	PORV open at 8.19. PORV closed at 7.84
4190-8700 seconds	Reinitialize system for second test point
8700-9390 seconds	Second test point
8700-8930	PORV open at 6.38. PORV closed at 6.03
8930-9390	PORV open at 6.55. PORV closed at 6.21
9390-15,000 seconds	Reinitialize system for depressurization test point
15,000-17,500 seconds	Depressurization from representative operating pressure PORV latched open HPIS enabled

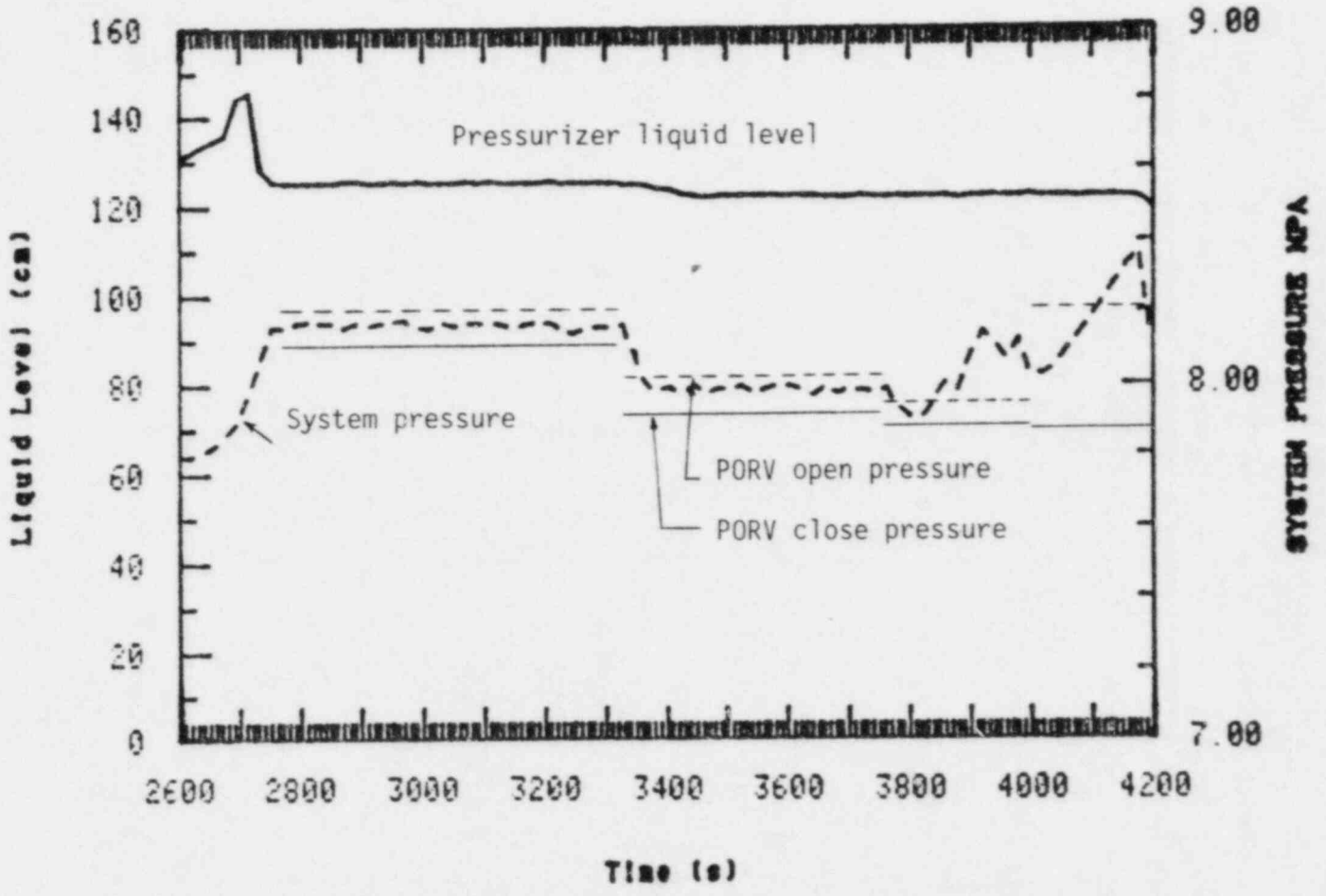

Figure 17. Pressurizer level and system pressure for Test S-SR-2, point 1.

remained full and did not change substantially during the test. Figure 18 shows PORV and HPIS flow and mass inventory. As Figure 18 indicates, initially PORV flow was approximately equal to HPIS flow resulting in no mass inventory reduction. During this time the PORV flow was approximately equal to calculated steam flows through the PORV as shown in Figure 19. The upstream conditions of the PORV then changed to a lower quality fluid as evidenced by increased mass flow through the PORV. The result of this increased PORV mass flow was to decrease the mass inventory in the system. Once this decrease was identified, the system pressure was reduced at 3325 seconds to 8.0 MPa by resetting the PORV. This pressure reduction is shown in Figure 17. The reduction in system pressure had very little effect on mass inventory loss as seen in Figure 18.

The system pressure was then further reduced to 7.58 MPa at 3750 seconds. Mass inventory was still continually lost. The PORV set point was then increased to 8.10 MPa, but as evidenced by Figure 17, the system pressure began to rise beyond this set point. As discussed in Section 2, this is an indication that insufficient energy is being removed from the system. Figure 17 indicates that the liquid level in the pressurizer did not change substantially during this time and Figure 19 indicates the PORV mass flow rate also remained unchanged. Figure 20 shows the liquid levels in the steam generator tubes were falling. It was surmised that this reduced the primary heat loss to the steam generator resulting in the pressure increase.

The second test point was an attempt to establish a steady feed and bleed operation at pressures lower than those attempted in test point 1. Figure 21 shows the system pressure and liquid level in the pressurizer during the test point. As indicated, the collapsed liquid level in the pressurizer remained full during the test. Figure 22 shows PORV and HPIS flows and corresponding mass inventory. The PORV flows are much higher than HPIS flows which results in the continuous depletion of coolant inventory. As indicated in Figure 21 several PORV pressures were attempted with continued loss of mass inventory. The last pressure range attempted was 6.21 to 6.55 MPa. Figure 21 indicates the pressure never dropped below 6.4 MPa at which time the pressure began to rise slightly. This is an

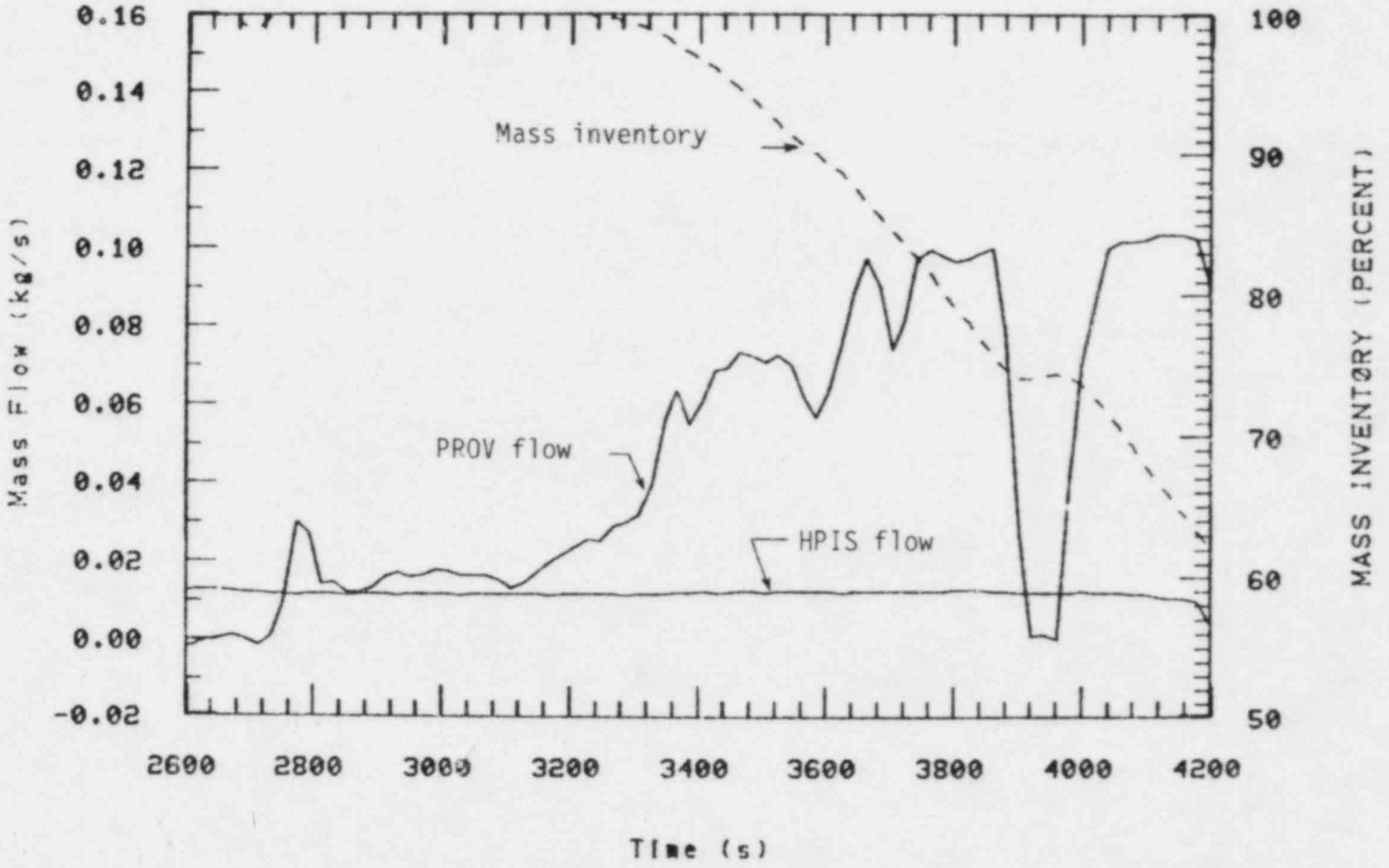

Figure 18. PORV and HPIS flow and primary mass inventory for Test S-SR-2, point 1.

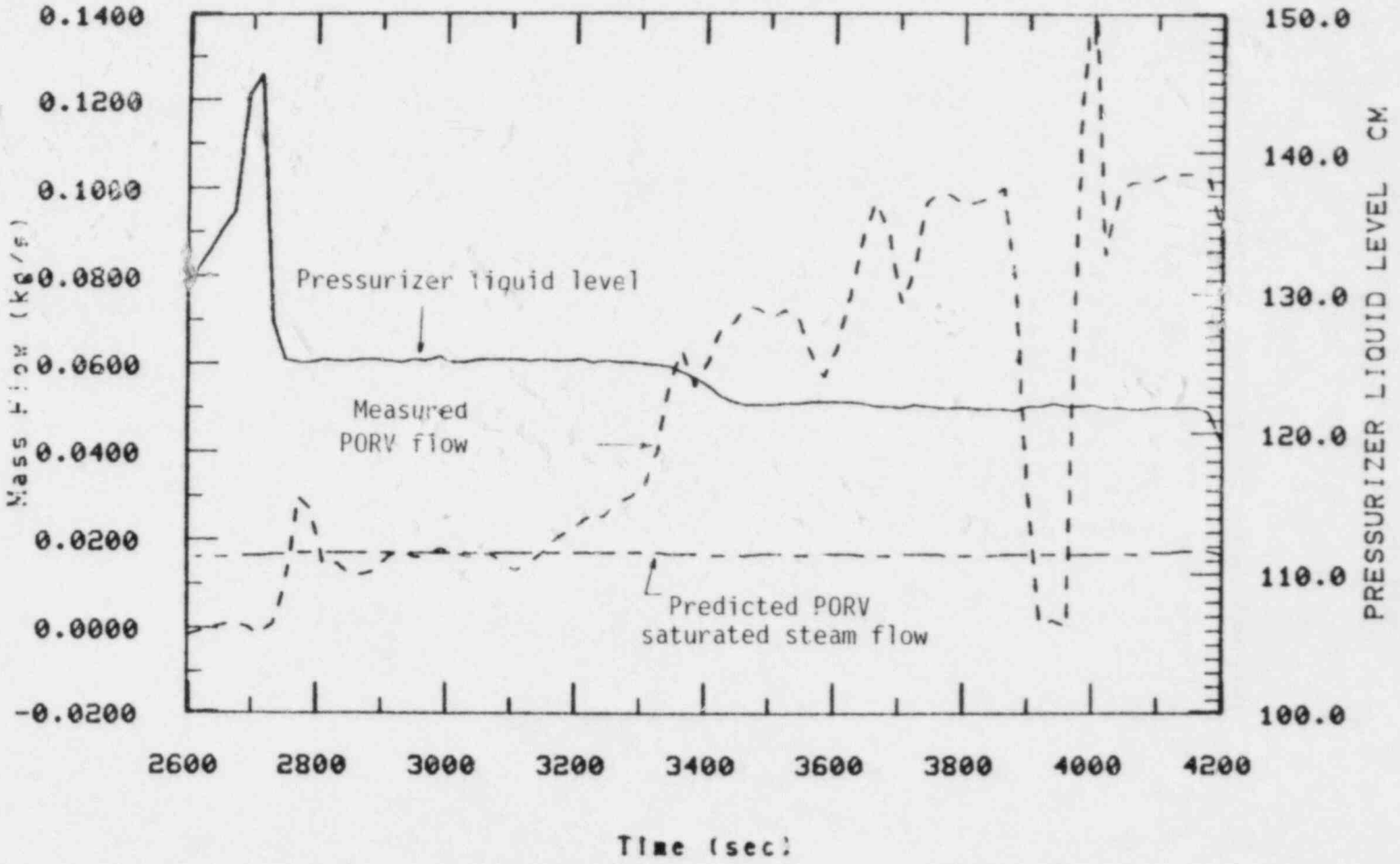

Figure 19. Measured and predicted (assuming 100% steam) PORV flow comparison with pressurizer collapsed liquid level for Test S-SR-2, point 1.

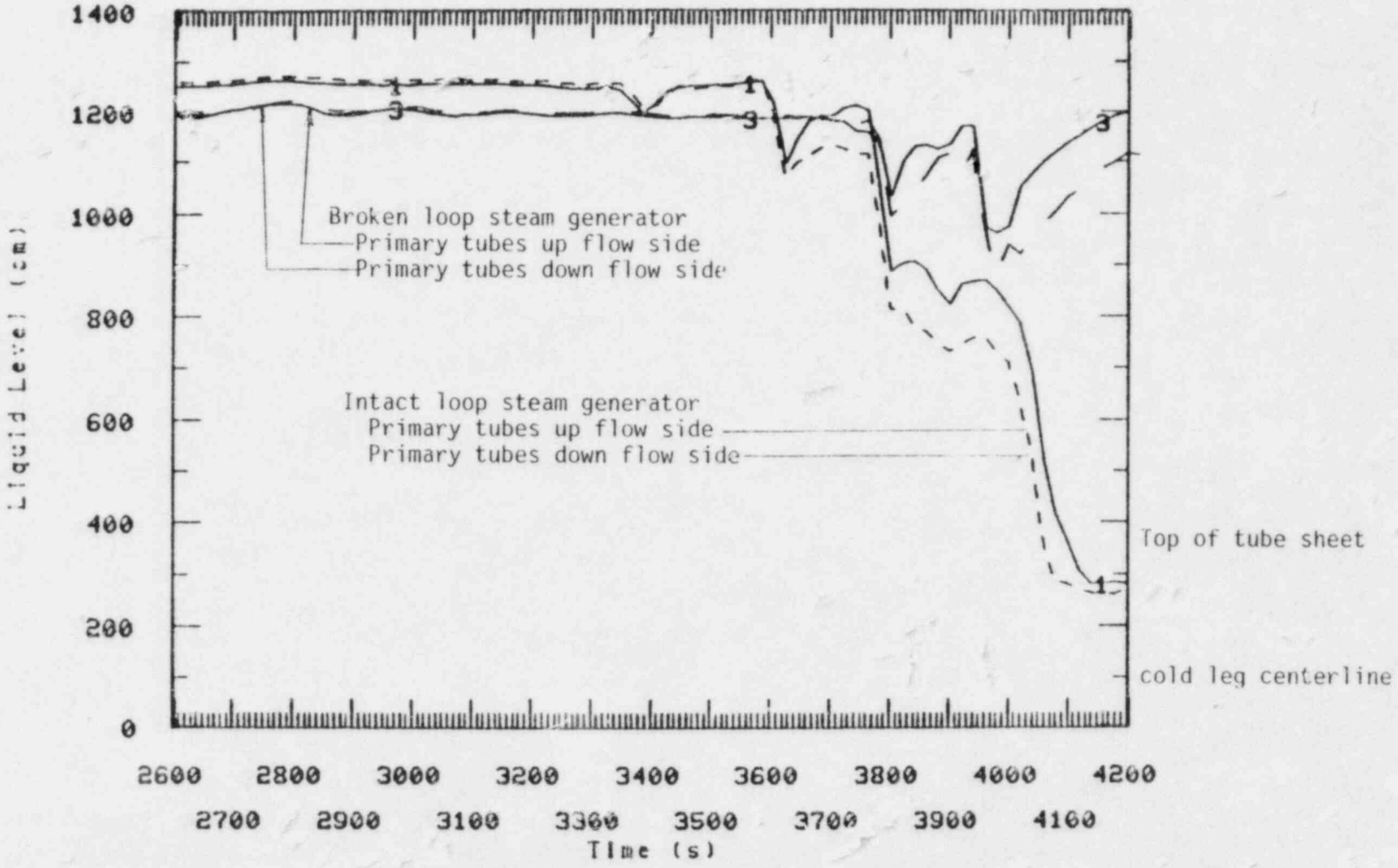

Figure 20. Collapsed liquid levels in steam generator tubes for Test S-SR-2, point 1.

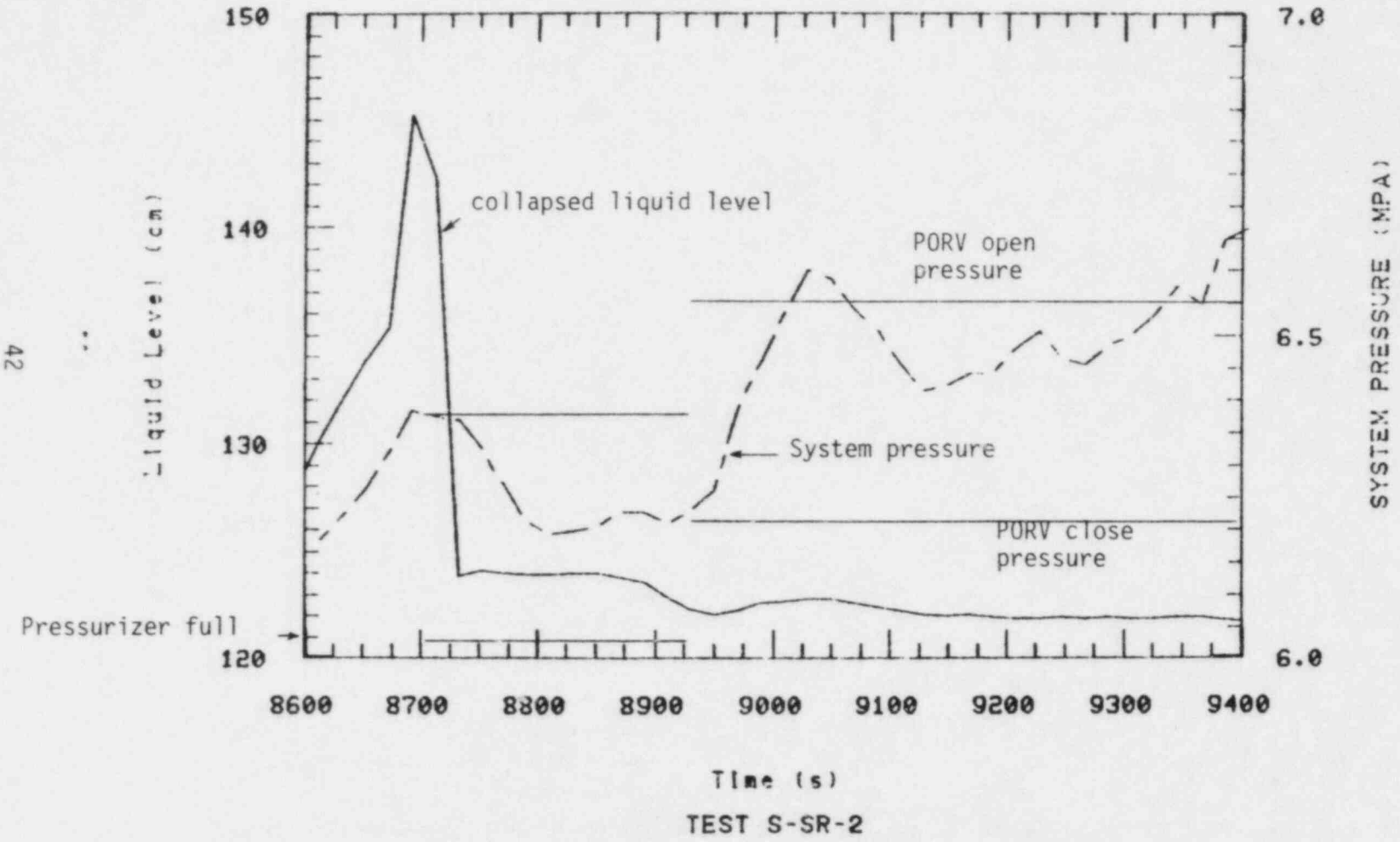

Figure 21. Pressurizer collapsed liquid level and system pressure for Test S-SR-2, point 2.

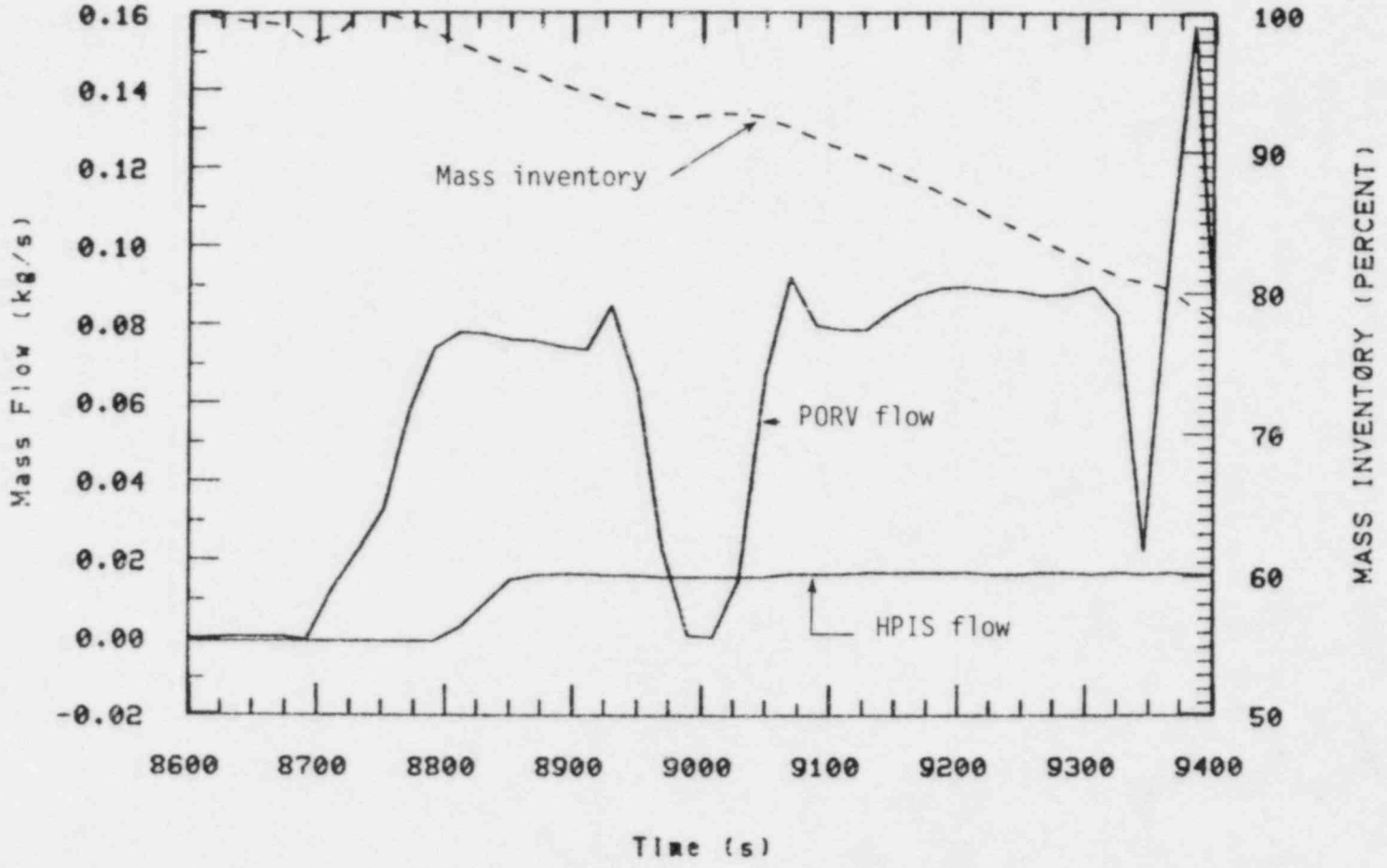

Figure 22. PORV and HPIS flow and primary mass inventory for Test S-SR-2, point 2.

indication that the energy being removed from the primary system is being reduced. Since PORV mass flow and pressurizer liquid level remain constant during the same period it is assumed that the energy removal rate of the PORV is also unchanged. Another possible energy path is to the environment. Figure 23 shows that liquid level in the intact loop steam generator is falling at the same time the pressure increases even with an open PORV valve. The falling liquid level in the steam generator tubes may have caused reduced heat transfer to the empty secondaries causing the system pressure to rise.

Figure 24 shows actual and calculated PORV flows (assuming 100% quality steam) and hot leg coolant density in the intact loop. The reduction in hot leg coolant density indicates minor voiding occurring in the hot leg due to loss of mass in the primary. The minor voiding had little effect on PORV mass flow rate as shown in Figure 22.

The objective of the last test point was to determine the feasibility of obtaining a steady state feed and bleed operation (using a low head pumped HPIS) initiated from a representative operating pressure. The procedure for this test point consisted of depressurizing the primary by latching open the PORV. Immediately prior to the depressurization the pressurizer heaters were turned off and the HPIS enabled.

Figure 25 indicates the pressurizer pressure and collapsed liquid level response during this test point. As can be seen, the pressurizer level initially dropped and then recovered to a level indicating a liquid full pressurizer. The initial level reduction is a result of flashing of the pressurizer liquid. Initially the pressurizer is the hottest volume in the primary and this fluid flashes first when the PORV is opened. As the steam bubble is vented through the PORV the pressurizer inventory depletes, and cooler hot leg liquid flows into the pressurizer filling the pressurizer. After the initial drop and rise the indicated level remained constant at a near full value. The system pressure dropped rapidly from the initial pressure of (15.17 MPa) to 8.0 MPa which was approximately the saturation pressure of the hot leg fluid. The pressure then slowly decreased to 6.8 MPa.

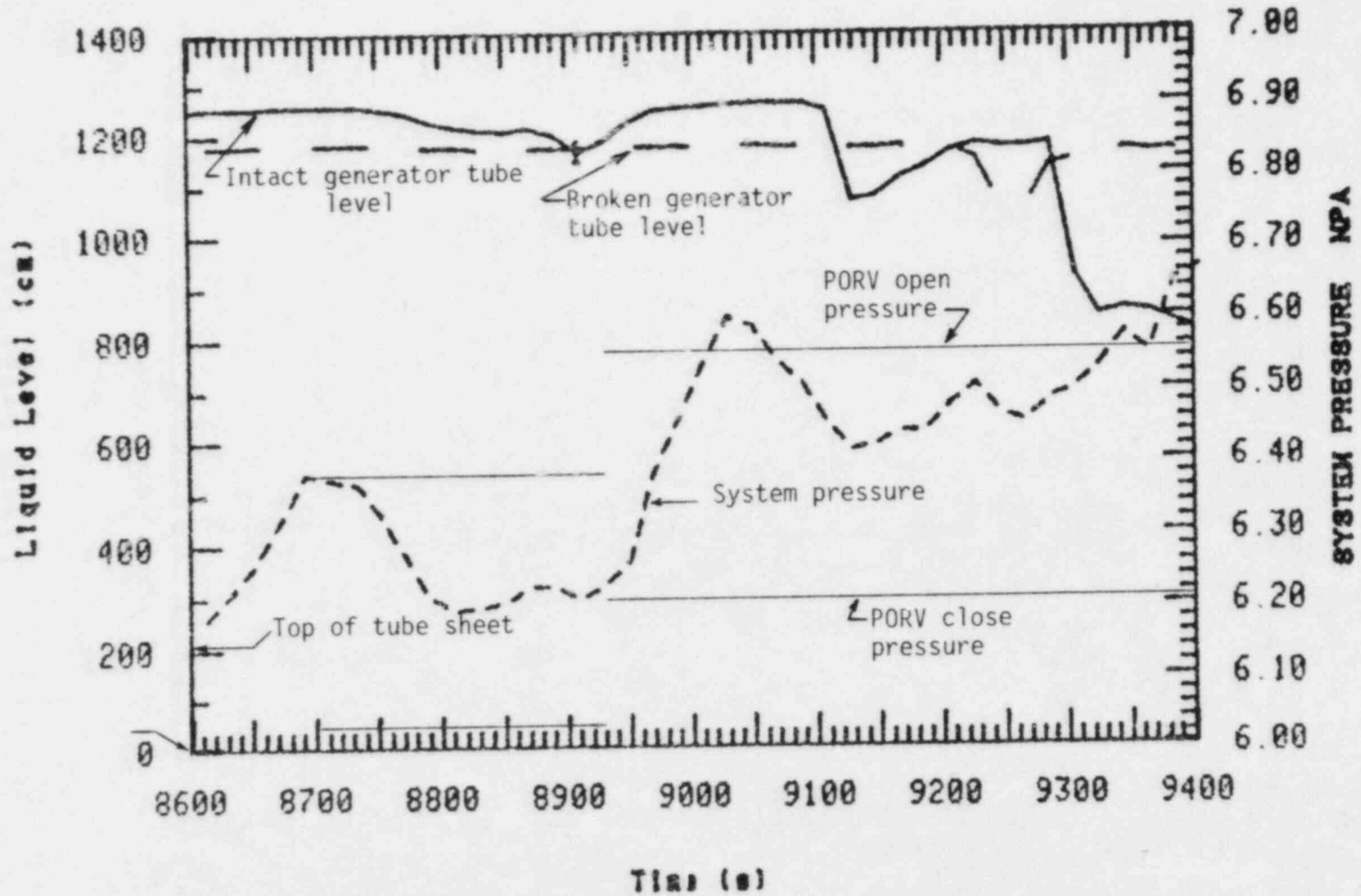

Figure 23. Steam generator tube collapsed liquid levels and primary system pressure. Test S-SR-2, point 2.

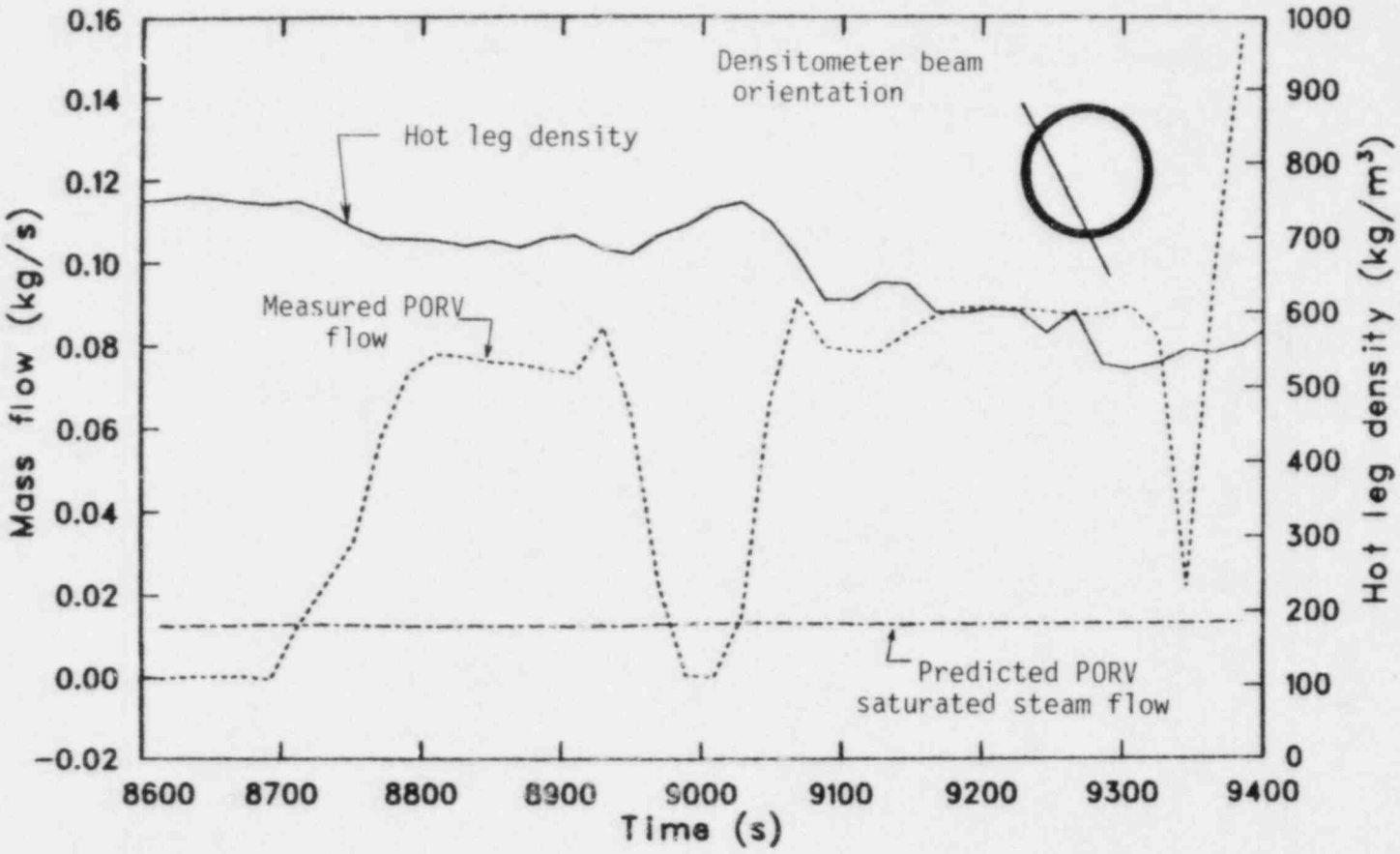

Figure 24. Measured and predicted (100% quality steam) PORV flow comparison to hot leg density for Test S-SR-2, point 2.

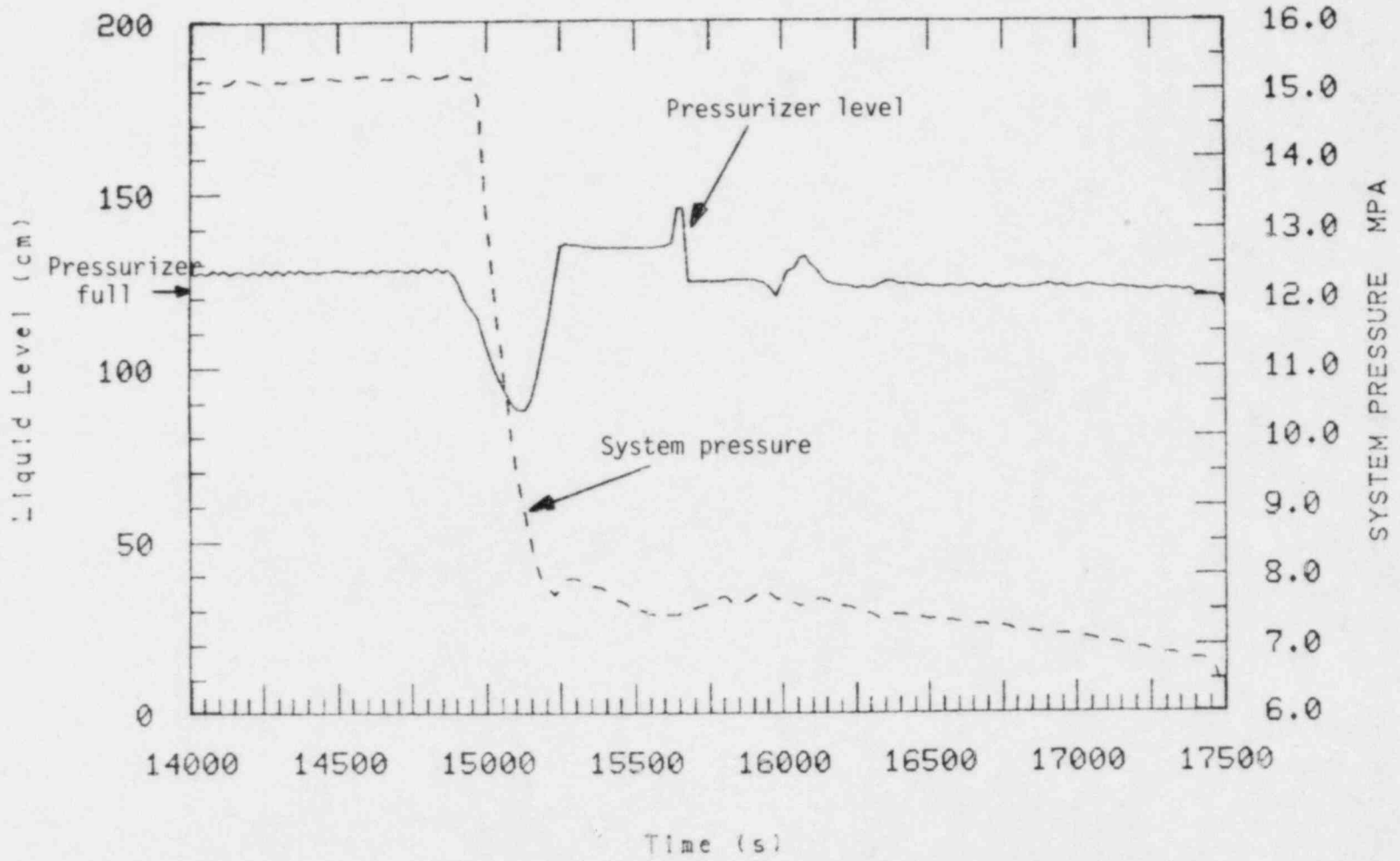

Figure 25. Pressurizer pressure and collapsed liquid level during Test S-SR-2, point 3.

Figure 26 shows both the actual and the calculated (assuming 100% quality steam) PORV flow compared to the hot leg density. An interesting point observed here is that the PORV mass flow rate remains high (indicating low quality fluid upstream of the PORV) until the hot leg substantially voids. After the hot leg had voided the PORV flow rate indicated that high quality steam was being discharged. Referring back to Figure 25 it is seen that the pressurizer still remained nearly full of liquid at that time. Flooding calculations presented in Section 4.2 predict that the steam velocities in the surge line were high enough to prevent countercurrent draining of pressurizer liquid into the voided hot leg.[a] It is apparent from these behaviors that there is a close coupling between the conditions in the hot leg and the quality of fluid that enters the PORV, irrespective of pressurizer inventory. Due to this coupling, until there was substantial voiding of the hot leg the PORV mass discharge rate remained much higher than values typical of 100% quality steam flow. Since the HPIS injection capacity was on the order of the PORV steam discharge rate, the higher discharge resulted in a net deficit in the inflow/outflow mass balance. Figure 27 compares the measured PORV flow rate to the HPIS injection rate and shows the net influence on system mass inventory.

The primary system fluid distribution resulting from the mass depletion was generally characterized by a draining of fluid from the upper elevations. Figures 28 and 29 show the collapsed liquid levels in the loop components; the steam generator tubes and the pump suction piping. Figure 30 shows the collapsed liquid levels for different regions of the vessel. The upper head and upper plenum regions of the vessel voided rapidly. Drainage of the steam generator tubes exhibited a delay that was most likely caused by the residual heat transfer discussed earlier. This acted to promote condensation in the tubes and kept voids from forming. Once the inventory has decreased to about 60 to 50% the intact loop steam

---

a. Section 4 will address particular hydraulic phenomena that bear on the typicality of the Mod-2A pressurizer behavior.

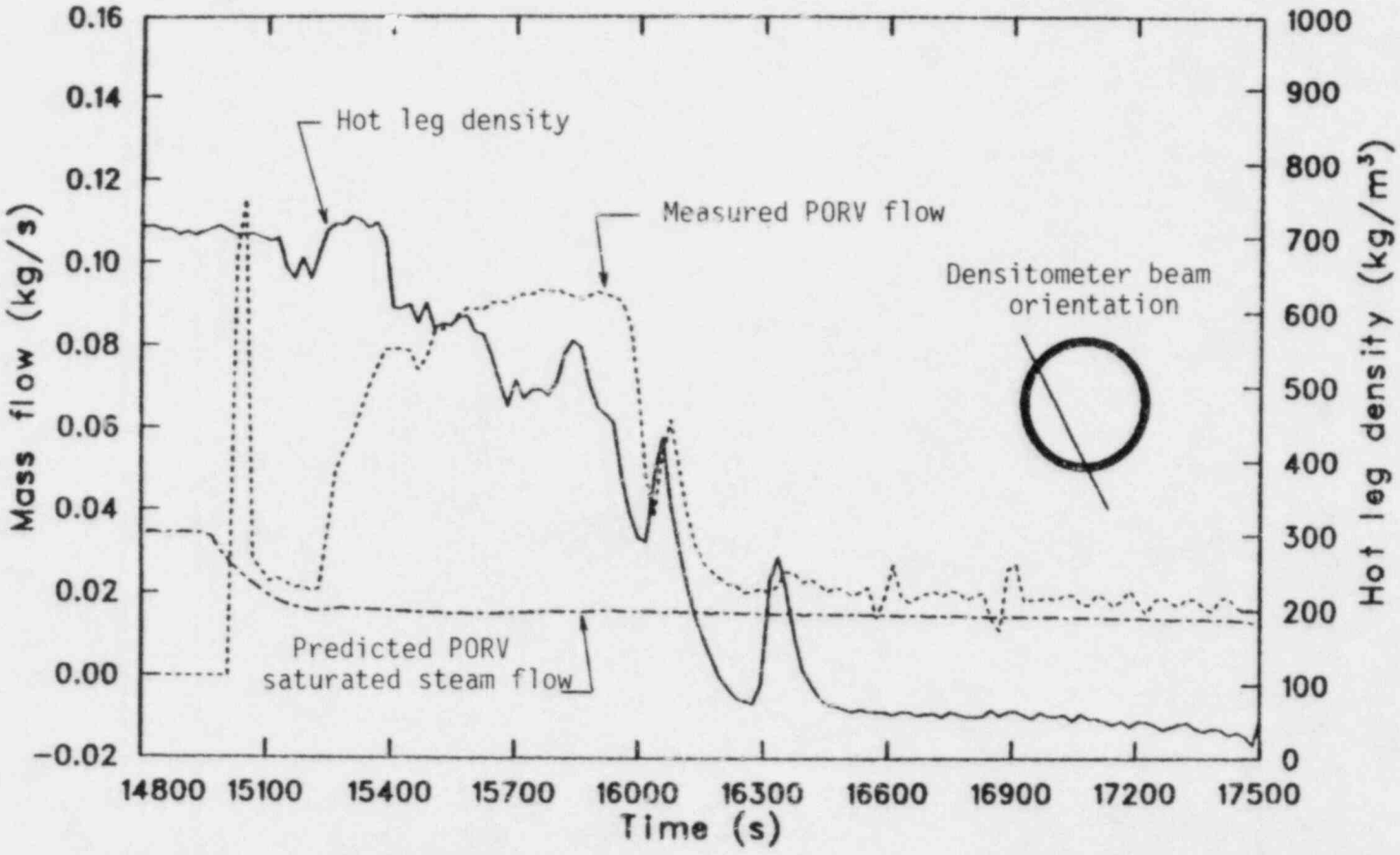

Figure 26. Measured and predicted (100% quality steam) PORV flow comparison to hot leg density for test S-SR-2, point 3.

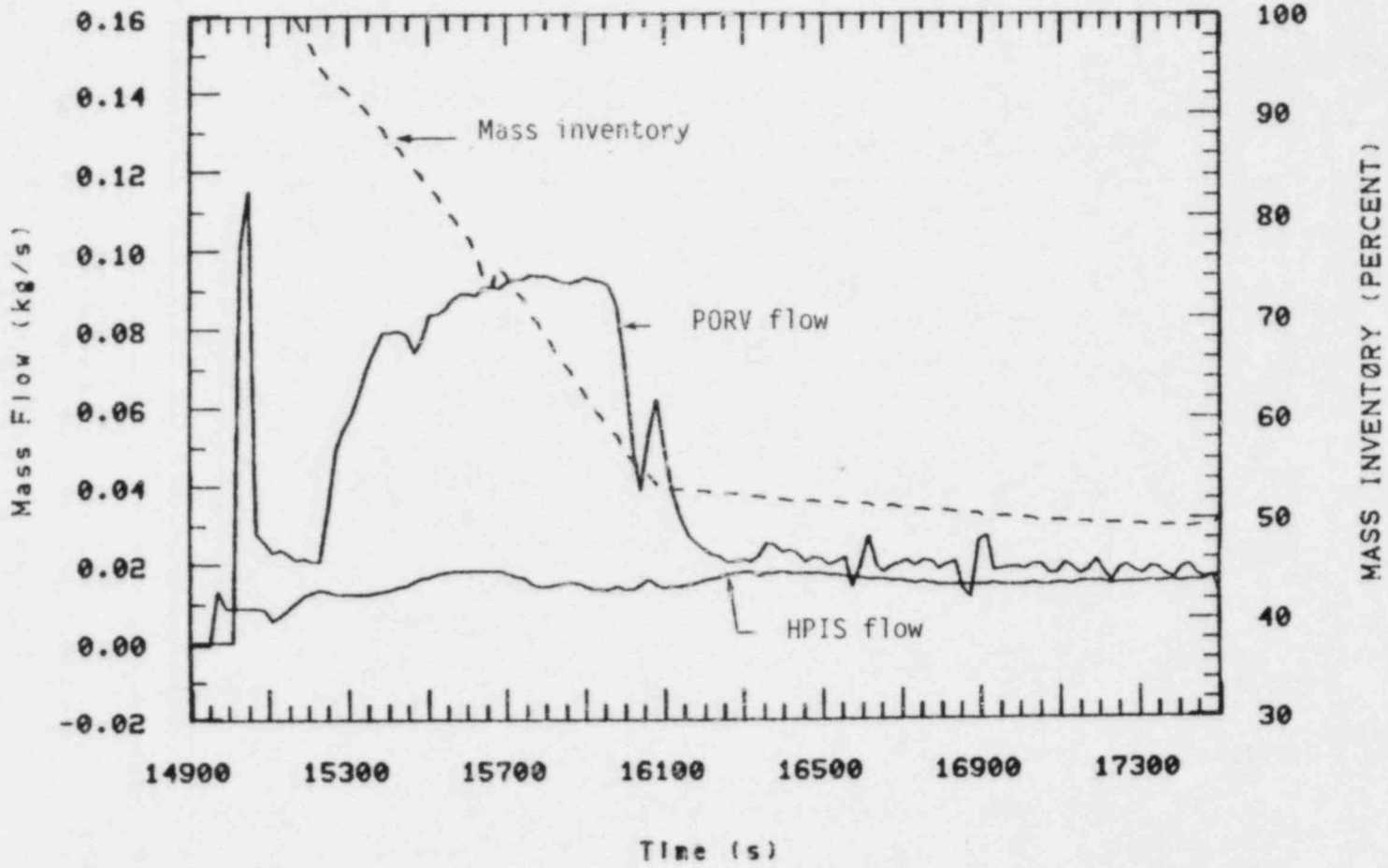

Figure 27. PORV and HPIS flow and primary mass inventory for Test S-SR-2, point 3.

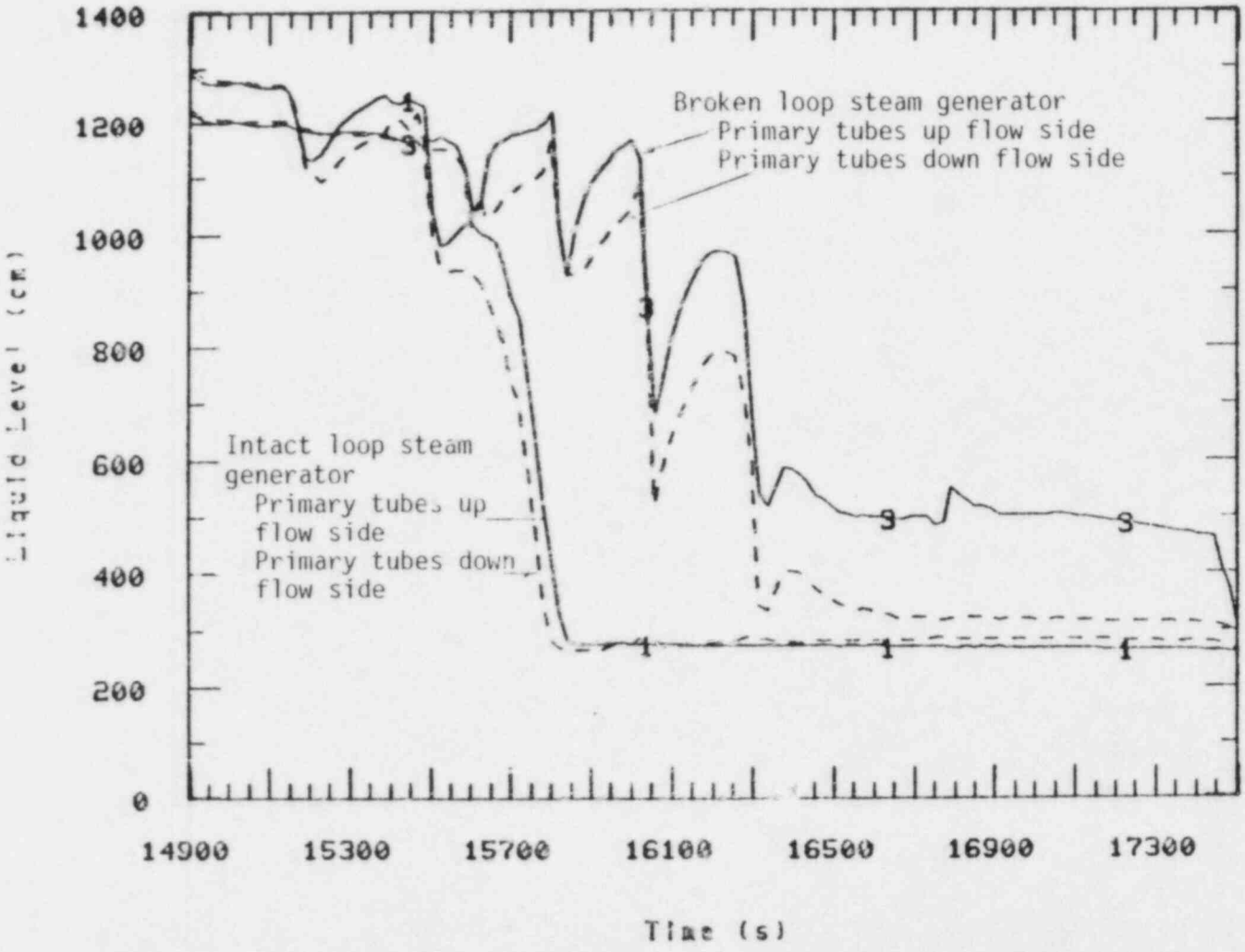

Figure 28. Steam generator tube collapsed liquid levels.

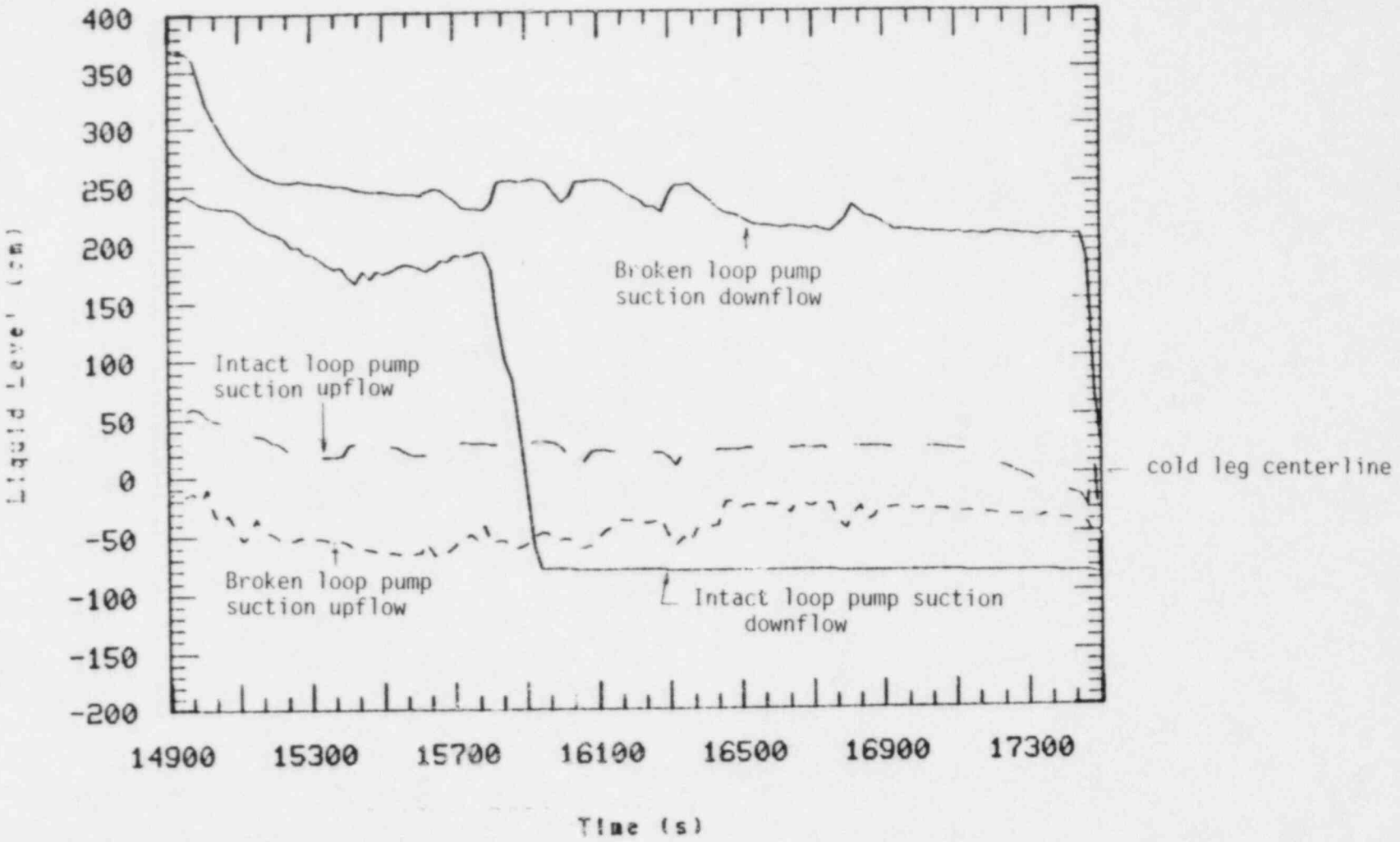

Figure 29. Pump suction levels. Test S-SR-2, point 3.

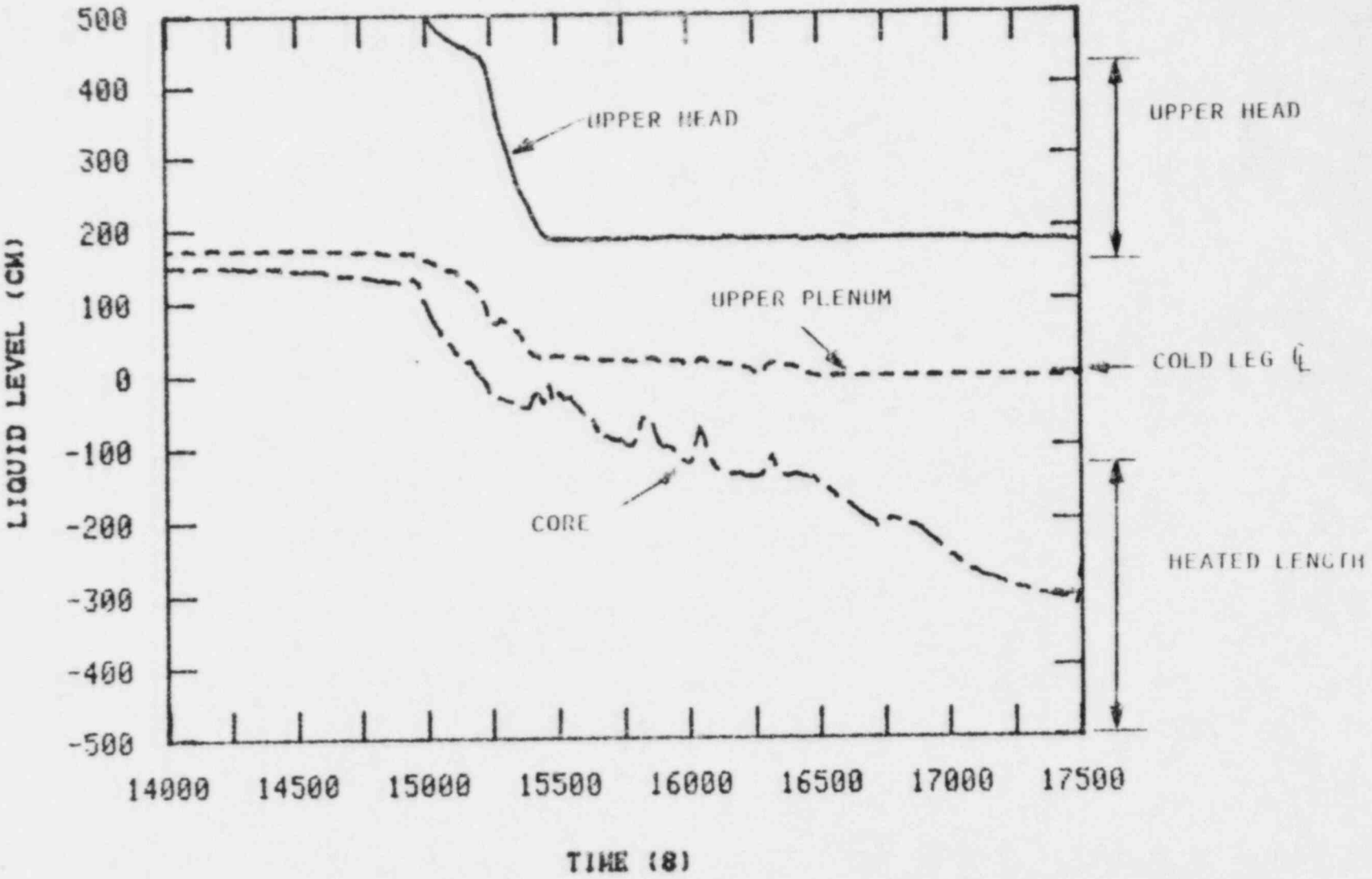

Figure 30. Vessel collapsed liquid level.
Test S-SR-2, point 3.

generator tubes had emptied. As seen in Figure 28 there appears to have been sufficient heat loss to the broken loop generator to cause a slow, large amplitude fill and dump behavior out to 16300 s. Temperature fluctuations from this phenomena were observed around the system.

The overall liquid level in the system dropped to about cold leg elevation. Due to heat losses in the loop piping and lack of a driving mechanism to force water from the loops, a stagnant volume of subcooled water remained in the pump suctions. Further depletion of fluid was at the expense of the saturated liquid in the vessel. As seen by examining Figure 27, even after the hot leg had voided there was a small deficit in the PORV/HPIS mass balance. This resulted in a slow depletion of vessel inventory and eventual dryout of the core. Incipient core dryout for this feed and bleed transient occurred at a system mass inventory of 55% as opposed to inventories of typically 35% for small cold leg break experiments. The reason for this higher value is that a substantial quantity of water remained in the loop pump suction piping, and also levitated in the pressurizer, where it did not contribute to core cooling. Comparison of the core dryout behavior versus vessel inventory response found that the inventory at which incipient dryout occurred was consistent with the two-phase level swell behavior reported for small cold leg break LOCA's.[8]

Figure 31 shows the response of selected fluid temperatures relative to a rod temperature and the collapsed liquid level in the core. Note that the temperatures remain near saturation until the core begins to uncover. These fluid temperatures do therefore not provide an accurate reflection of vessel liquid levels other than indicating superheated vapor following dryout of the core.

3.3.3 Conclusions from Semiscale Experiments

The inability of the Mod-2A experiments to attain steady-state feed and bleed operation once hot leg voiding had occurred is subject to

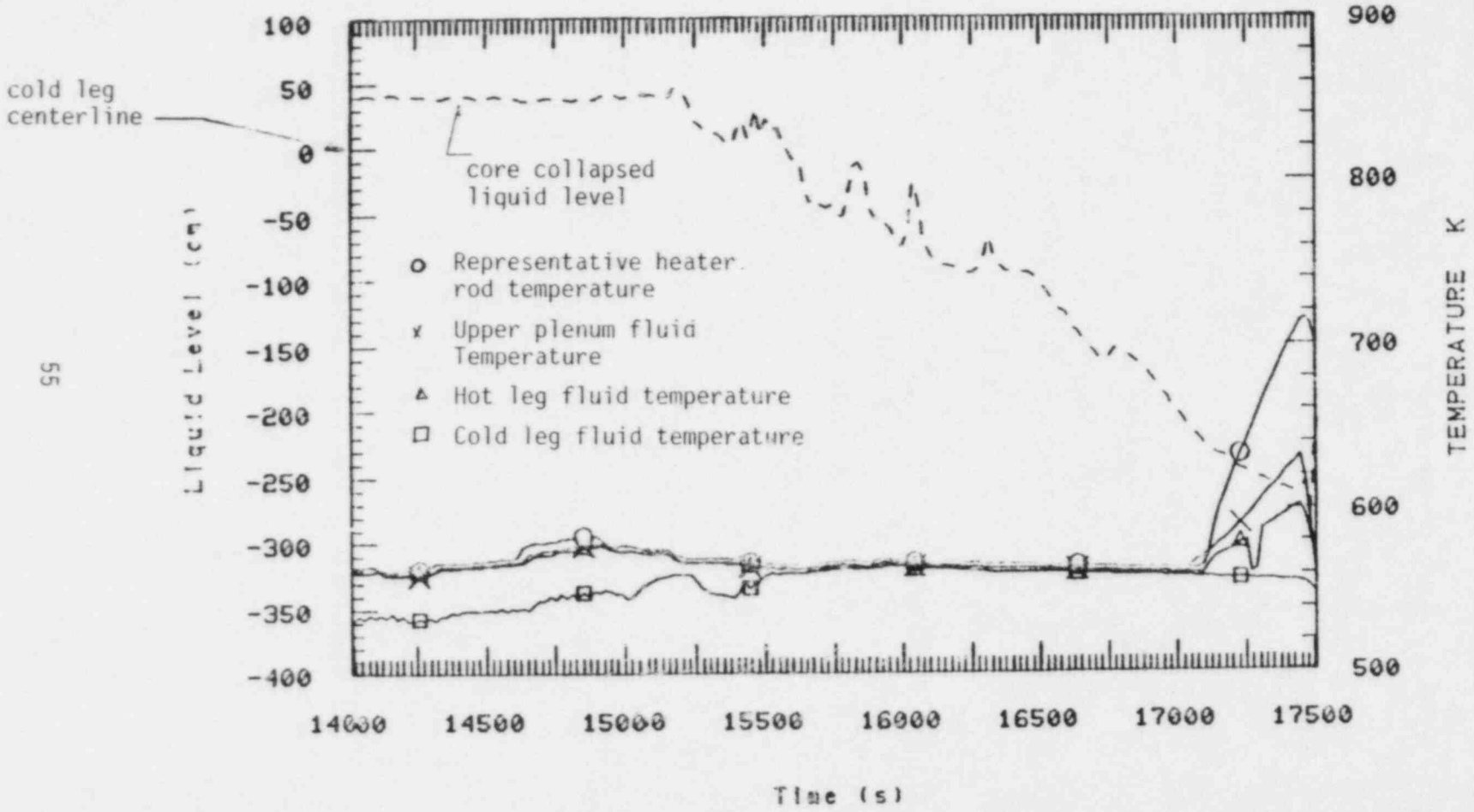

Figure 31. Core liquid level compared with representative temperatures during Test S-SR-2, point 3.

numerous experimental uncertainties. The results will be examined in terms of system typicality in the following section. The conclusions that can be directly drawn from these experiments are as follows:

1. PORV discharge rates dominate primary feed and bleed capability, and are more variable than the ability to select either a given core power or representative HPIS injection capacity.

2. PORV flow rates are very dependent on upstream fluid conditions which in turn may be directly affected by the conditions in the hot leg, particularly in a situation where the PORV is continuously latched open for an extended period. However, cycling of the PORV to maintain a constant system pressure appeared to promote phase separation and allow high quality steam flow even with low quality hot leg conditions.

3. Temperature response in the hot leg, upper plenum, and upper head do not appear to be good indicators for determining liquid level in the vessel. As evidenced by test data, the hot leg, upper plenum, and upper head temperatures did not respond to local liquid levels.

4. TYPICALITY OF SEMISCALE RESULTS

In and of themselves, the results from the Semiscale experiments do not indicate the existence of a problem regarding primary feed and bleed. The importance of the results from the Semiscale experiments lies in demonstrating the dominance of the PORV discharge rate on primary feed and bleed capability and the dependence of the PORV discharge on hot leg conditions, and consequently system coolant inventory.

4.1 Experimental Uncertainties

The inability to maintain system inventory in Semiscale during periods when the PORV flow was in near agreement with the predicted steam flow rate is subject to experimental uncertainties. Uncertainties exist in the actual PORV orifice characteristics, HPIS injection rate and measurement thereof, system heat losses, and fluid leakage.

Each of the parameters that create the operating maps of Figures 8 and 16 are subject to experimental uncertainties. Taking the conditions of Test S-SR-2 (Figure 16) as an example, due to the narrow steady-state operating band, the uncertainty in almost any individual parameter can eliminate the operating band. (Or, likewise, expand the band.) The calculated or estimated uncertainty in each parameter is listed in Table 5 and plotted in Figure 32. It is seen by examing the figure that the uncertainties in either the net core power or HPIS injection rate could have acted to eliminate the steady-state operating band.

However, the observed PORV mass discharge relationship to hot leg conditions during the transient depressurization, with a factor of 5 increase above the predicted steam flow rate, lies outside the effects of the uncertainties mentioned above. Given that all the other parameters could have been accurately imposed, then, this phenomena would still have acted to eliminate the steady-state band until such time as the hot leg had voided. It is therefore concluded that with the PORV latched open a steady-state mass inventory could not have been established until after sufficient primary coolant inventory had been lost so as to void the hot

TABLE 5. SEMISCALE EXPERIMENTAL UNCERTAINTIES

Parameter	Uncertainty	Basis for Uncertainty
Net Core Power	±25%	Component heat losses from Reference 6, structural heat transfer, and interpretation of heat loss checks prior to testing.
Average PORV Mass Flow Rate	±25%	Based on uncertainty in net core power.
Predicted PORV Mass Flow Rate	±3%	Uncertainties in flow area, discharge coefficient and compressibility factors.
Predicted PORV Energy Removal Rate	±3%	Based on uncertainty in predicted PORV mass flow rate.
HPIS Injection Rate	±.008 kg/sec	Reported accuracy of turbine meter flow mesurement.

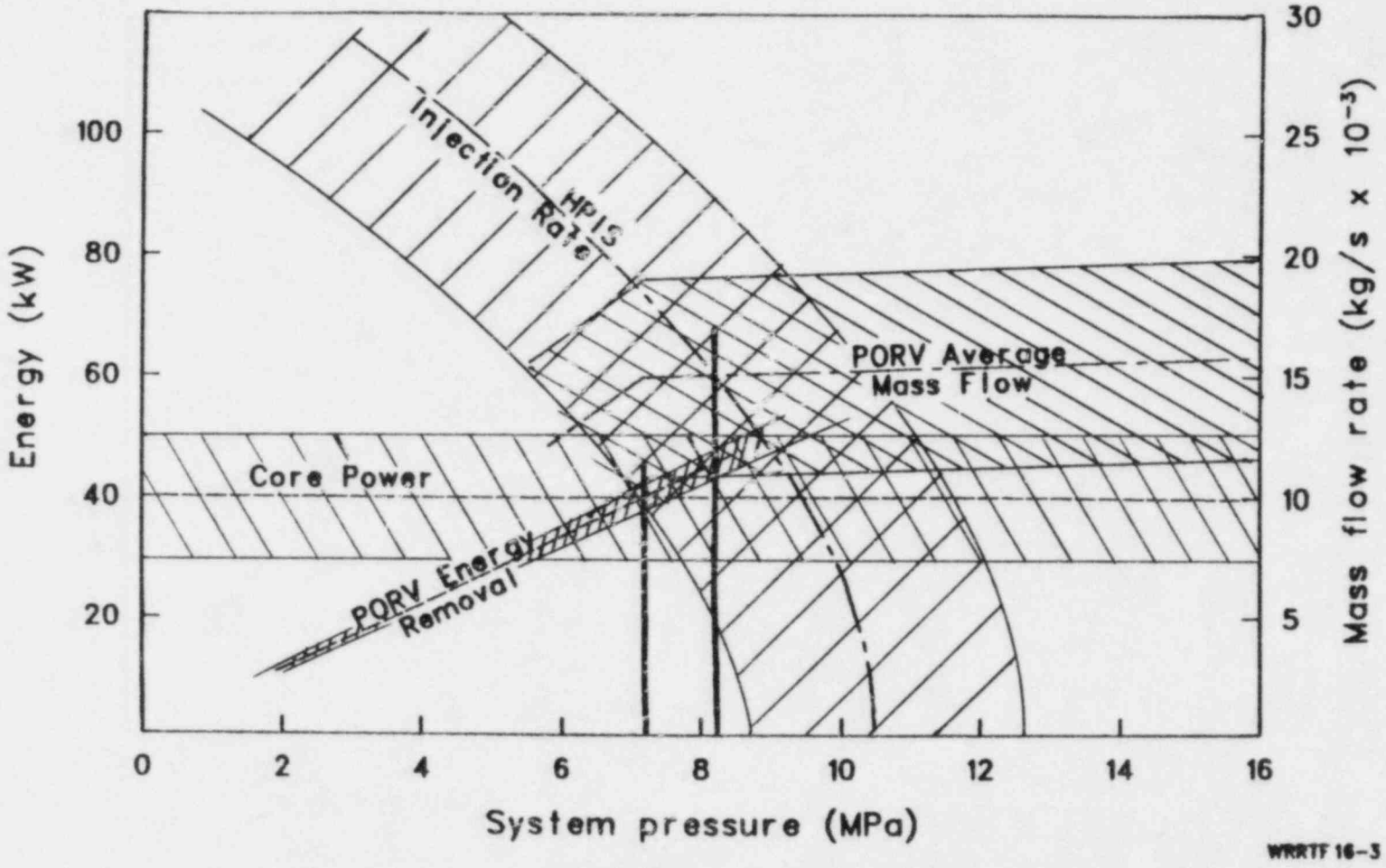

Figure 32. Semiscale Mod-2A primary feed and bleed operating map for 2% core power with uncertainties.

leg, given the imposed HPIS boundary conditions. Once the hot leg had voided the ability, or inability, to maintain coolant inventory is highly subject to uncertainties in the actual HPIS injection rate and PORV discharge characteristics. With the relatively narrow operating band defined for Test S-SR-2 small changes in core power, PORV flow, or HPIS injection rate could influence the ability to obtain a steady-state condition. The questions remaining as to the typicality of the Semiscale results deal with geometry and scaling and are addressed in the following sections.

4.2 Surge Line Flooding

As discussed in Section 2.2.2, although one could postulate some liquid/vapor separation mechanisms that would be influenced by the pressurizer tank geometry, the net effect could be negated if the vapor velocity in the surge line resulted in flooding conditions. Any water thus separated in the pressurizer tank would therefore remain in the tank until eventually discharged out the PORV. Figure 33 shows the velocity for 100% quality steam flow through the Semiscale surge line (ID=0.94 cm) as a function of time for the transient depressurization of Test S-SR-2, compared to the calculated flooding velocity. Also shown is the scaled flooding velocity for a range of typical PWR surge line sizes.[a] As seen from these curves the velocities expected in the surge line are significantly above the flooding limit. From these calculations, supplemented by the fact that such apparent flooding behavior has been observed in actual reactor transients[10] it would appear that this phenomena was not significantly distorted by any Semiscale geometrical atypicalities.

4.3 Surge Line Orientation

As discussed in Section 2.2.3 the orientation of the surge line connection to the hot leg may have an influence on the PORV discharge by

---

a. The flooding curves were calculated with the correlation from Reference 9 which unifies the Wallis and Kutateladze correlations and appears very useful for scaling the effect of pipe size.

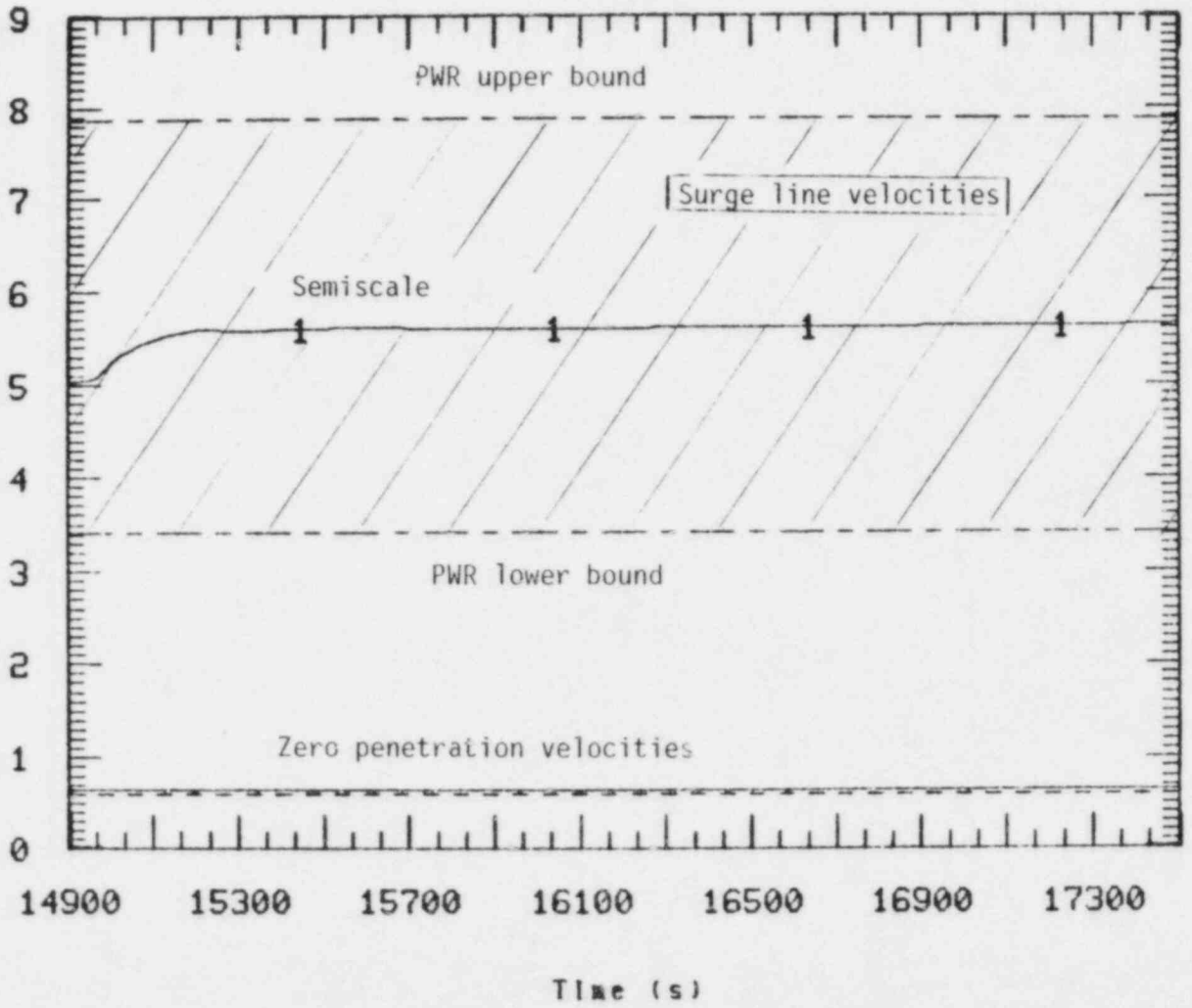

Figure 33. Comparison of flooding correlations with surge line steam velocities for Semiscale and range of PWR geometries.

promoting phase separation at the hot leg. The Semiscale surge line-to-hot leg connection geometry is shown in Figures 7 and 34. As shown, the surge line connects to the side of the pipe on the horizontal centerline. Results from Semiscale natural circulation experiments have shown that minimal loss of primary inventory results in substantial voiding of the hot leg. As an example from Reference 11, a loss of only about 5 to 10% coolant inventory results in a void fraction of 40% in the hot leg. (This result must be tempered by the fact that there was a secondary heat sink that induced natural circulation loop flow.) Due to the horizontal side connection of the existing Mod-2A surge line, substantial voiding of the hot leg is necessary to uncover the surge line entrance.[a] This degree of hot leg voiding must be preceeded by voiding of the steam generator tubes and the upper regions of the vessel. Results from the experiments showed that a coolant inventory loss on the order of 30 to 40% was required to uncover the surge line.[b] Since substantial loss of primary inventory was found to be necessary to void the hot leg to the extent that high quality steam entered the surge line in the feed and bleed experiments, it appears that surge line orientation can dramatically affect the inventory and timing at which steady-state feed and bleed becomes feasible.

A worst case for mass loss from the system when stratified flow exists in the hot leg is a two-phase flow until the surge line uncovers and then continued entrainment of liquid by the vapor flow. If sufficient entrainment potential existed at typical discharge rates it would reduce the importance of surge line orientation. Figure 35 shows the steam flow velocity (assuming 100% quality) into the surge line as a function of the hot leg stratified liquid level measured with gamma densitometers[c] for

---

a. A void fraction of 61% in stratified conditions will void the Semiscale hot leg to the bottom of the surge line.

b. The ratio of surge line diameter to hot leg pipe diameter for Semiscale Mod-2A is 0.17 whereas that for PWR's ranges from approximately 0.3 to 0.4. Surge line uncovery in a PWR would therefore require even more voiding.

c. The flow regime for typical conditions during feed and bleed is stratified flow as determined with correlations of Reference 13. During portions of the experiment however, the natural circulation flow rates induced by environmental heat losses can shift conditions close to the intermittent (slug) flow regime.

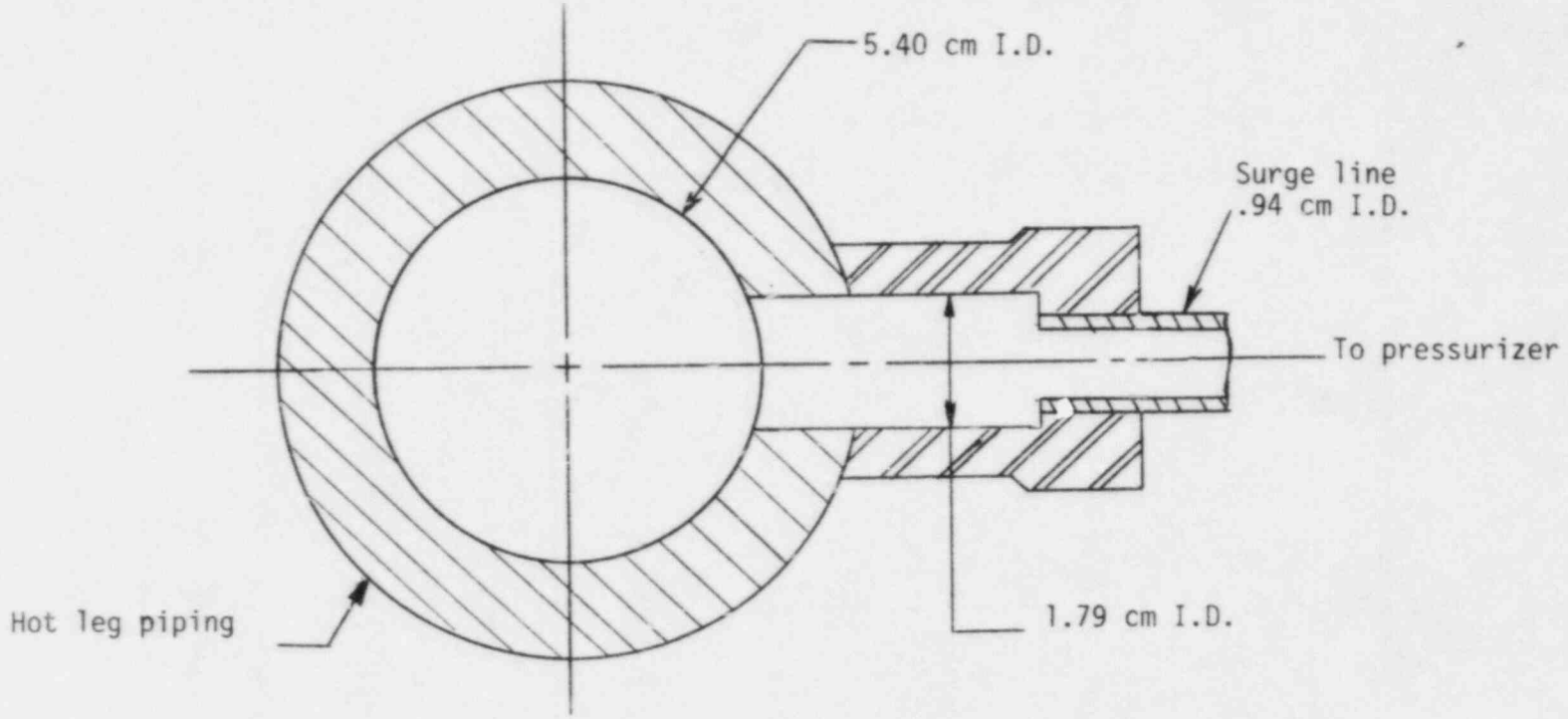

Figure 34. Semiscale Mod-2A hot leg/surge line configuration for Feed and Bleed tests. (not to scale.)

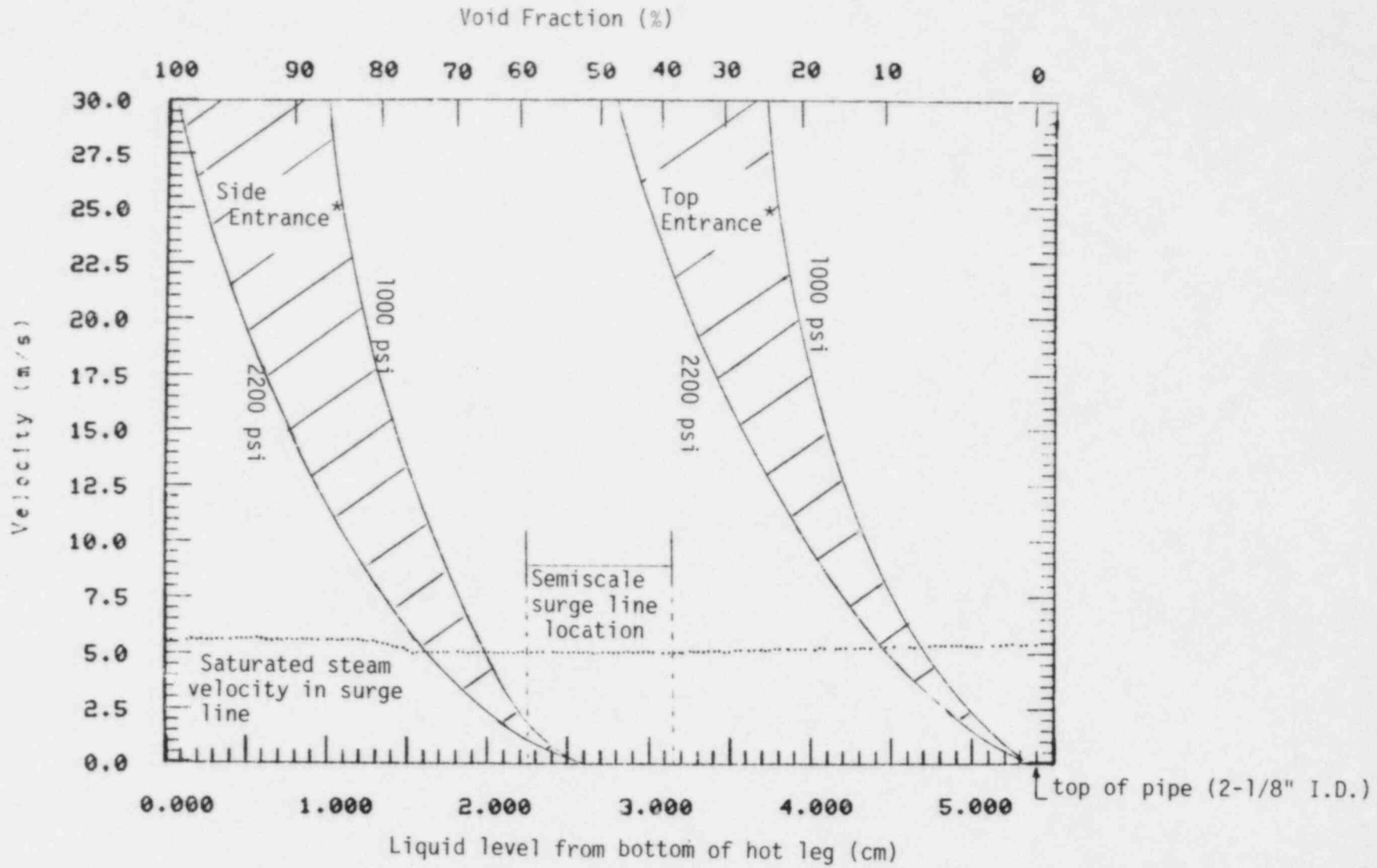

Figure 35. Liquid entrainment predictions for side and top entry surge lines.

*Correlation band denotes pressure range of transient

Test S-SR-2, point 3. Also shown are the velocity boundaries for entrainment for both a side and top exit (Reference 12). (Ranges indicated are for pressures occurring during the test.) It is evident that while there is some chance for entrainment with both geometries there is a very broad difference between the hot leg liquid level (void fraction) at which phase separation is plausible for a top versus side entrance. Also, results presented in the next section show that separation apparently occurred during a feed and bleed operation in the LOFT facility which has a top entrance surge line.

4.4 Supporting Analysis, Applicable LOFT Data

To examine the effects of scale on these various phenomena and to obtain independent data to check Semiscale results, applicable data generated in the Loss-of-Fluid Test (LOFT) pressurized water reactor were also examined. In April 1981, a Loss-of-Feedwater Accident (LOFW)[14,15,16] simulation as well as simulations of two LOFW recovery procedures were conducted in LOFT, a 50 MW(t) integral nuclear experimental facility. The LOFT configuration for these simulations[a] is shown in Figure 36 and detailed descriptions of LOFT and its scaling basis are available in References 17 and 18. Of particular interest to this report with respect to scaling are the following:

a. The LOFT pressurizer is of cylindrical geometry with internal dimensions 0.85 m diameter and 2.02 m height. The L/D of 2.38 compares with 7.13 for the Zion pressurizer. Thus, the LOFT pressurizer has a larger cross-sectional area (relative to height) than Zion. This will affect, for example, the velocity of steam in the pressurizer and, consequently, the amount of carryover into the PORV line.

---

a. Test L9-1/L3-3.

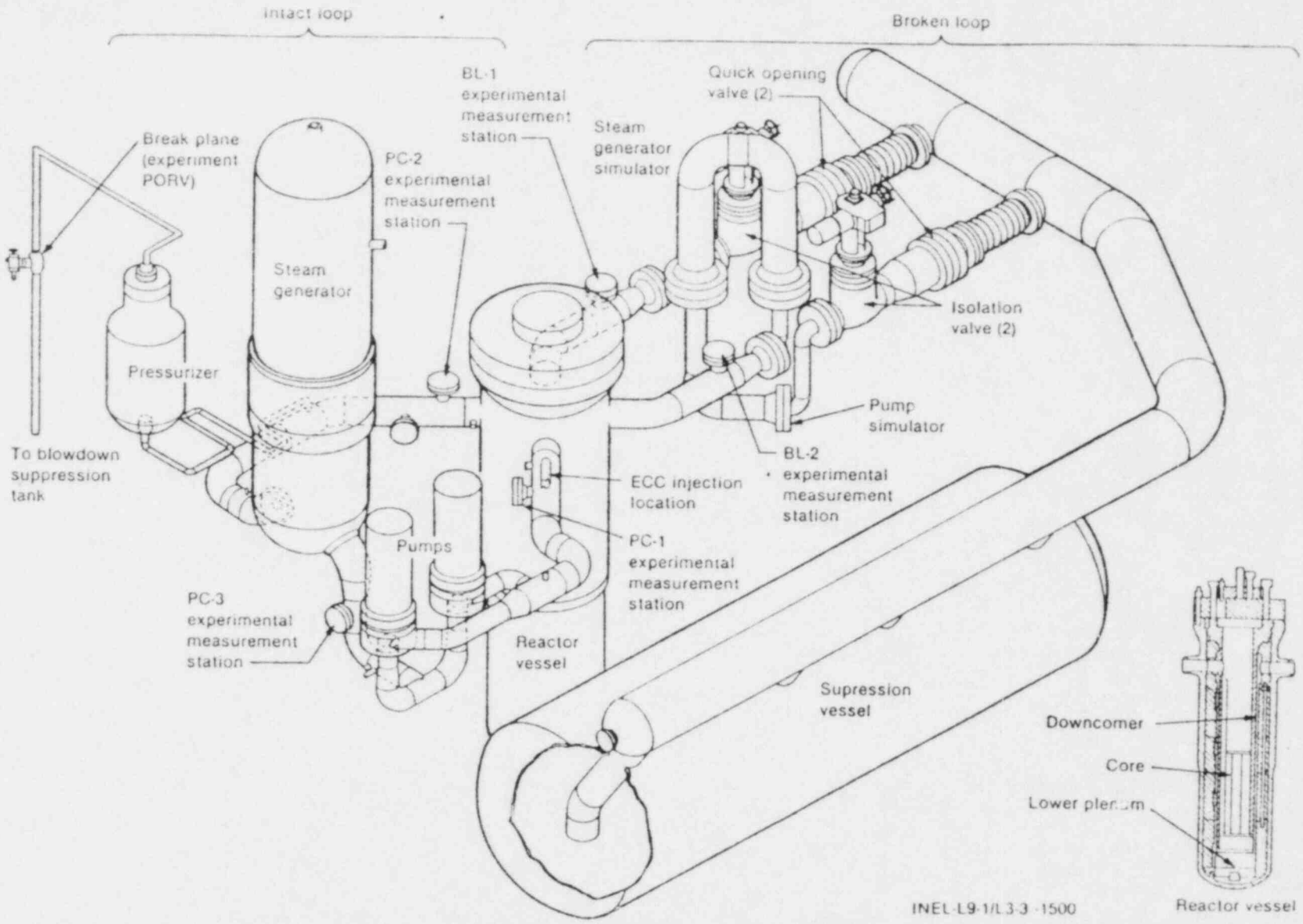

Figure 36. Axonometric projection of LOFT system.

b. The LOFT pressurizer surge line is a 2 in. Schedule 160 pipe which leads vertically upward from the horizontal hot leg which is a 14 in. Schedule 160 pipe.

c. The power operated relief valve (PORV) installed for the LOFW simulation has a relief capacity of 0.66 kg/s saturated steam at the relief setpoint of 16.2 MPa. This corresponds to a Westinghouse plant type with minimum PORV relief capacity (1.32 kg/s·MW(t).

The LOFW simulation was initiated with the reactor at full power (50 MW) by stopping all secondary feedwater flow. Reactor scram was delayed to 65 s to maximize the depletion of secondary water inventory. The plant was allowed to react to the LOFW for 3270 s (54.5 min) with no operator intervention. During this time, the primary system heat imbalance caused the coolant to swell into the pressurizer and collapse the steam bubble. The primary system was liquid solid by approximately 1250 s (20.8 min) and remained solid throughout this phase with the PORV automatically cycling to control pressure.

At 3270 s (54.5 min), the PORV was manually latched open to initiate the first LOFW recovery simulation, a primary feed and bleed operation with severely degraded primary to secondary heat transfer. The decay heat level was approximately 0.53 MW or 1.1% of initial power. The PORV remained open for 1580 s (26.3 min), dropping the primary system pressure rapidly to saturation and then continuing to depressurize the system. In order to obtain maximum primary system voiding for the second LOFW recovery simulation, no primary feed was initiated. However, based on the measured PORV mass flow and known high pressure injection capacity, it is estimated that a steady state primary system heat and mass balance could theoretically have been achieved.

When the PORV was latched open, the mass flow out the valve initially transitioned from low quality to a high quality flow as the subcooled primary system was unable to expand fast enough to keep up with the increased volumetric flow. When the pressure reduced to saturation, voids

started to form outside the pressurizer and this increased the surge rate into the pressurizer. The PORV mass flow transitioned back to a low quality flow which persisted for a while and then continued to gradually decreased to even lower quality. Figure 37 shows the PORV mass flow during this time. Also shown in the figure are PORV mass flows for saturated liquid and saturated steam (fluid quality = 0.0 and 1.0, respectively) calculated using the Homogeneous Equilibrium Model critical flow model[19] as well as fluid density in the upper part of the hot leg. As shown, the fluid in the hot leg started to stratify after the pumps were stopped and primary system voiding occurred. Since the pressurizer surge line is connected vertically to the top of the hot leg, as soon as voids started to occur there, the surge line flow quickly transitioned to a higher quality and the PORV mass flow followed suit. This is similar to the PORV mass flow transition in Semiscale although that transition was delayed until more hot leg voiding occurred. This supports the conclusion that the surge line/hot leg connection geometry has a strong influence on phase separation and PORV flow rate.

Figure 38 shows the response of the LOFT pressurizer liquid level. The pressurizer was liquid full prior to latching open the PORV. The level then decreased into the indicating range and remained approximately constant while the PORV was open. The rapid drop in level in 5100 s (85 min) was a response to restoration of steam generator auxillary feedwater injection.

An as yet unresolved question about the PORV mass flow concerns the flow oscillations after 4000 s (67 min). Apparently, there was a rapid fluctuation of the fluid density upstream of the PORV with the density oscillating between saturated liquid and saturated steam densities. The cause of this phenomena is as yet not clear.

To summarize, the LOFT data exhibit a correlation between the PORV mass flow and hot leg density which is qualitatively similar to that measured in Semiscale. The pressurizer volume itself does not appear to significantly affect this correlation though the correlation is very

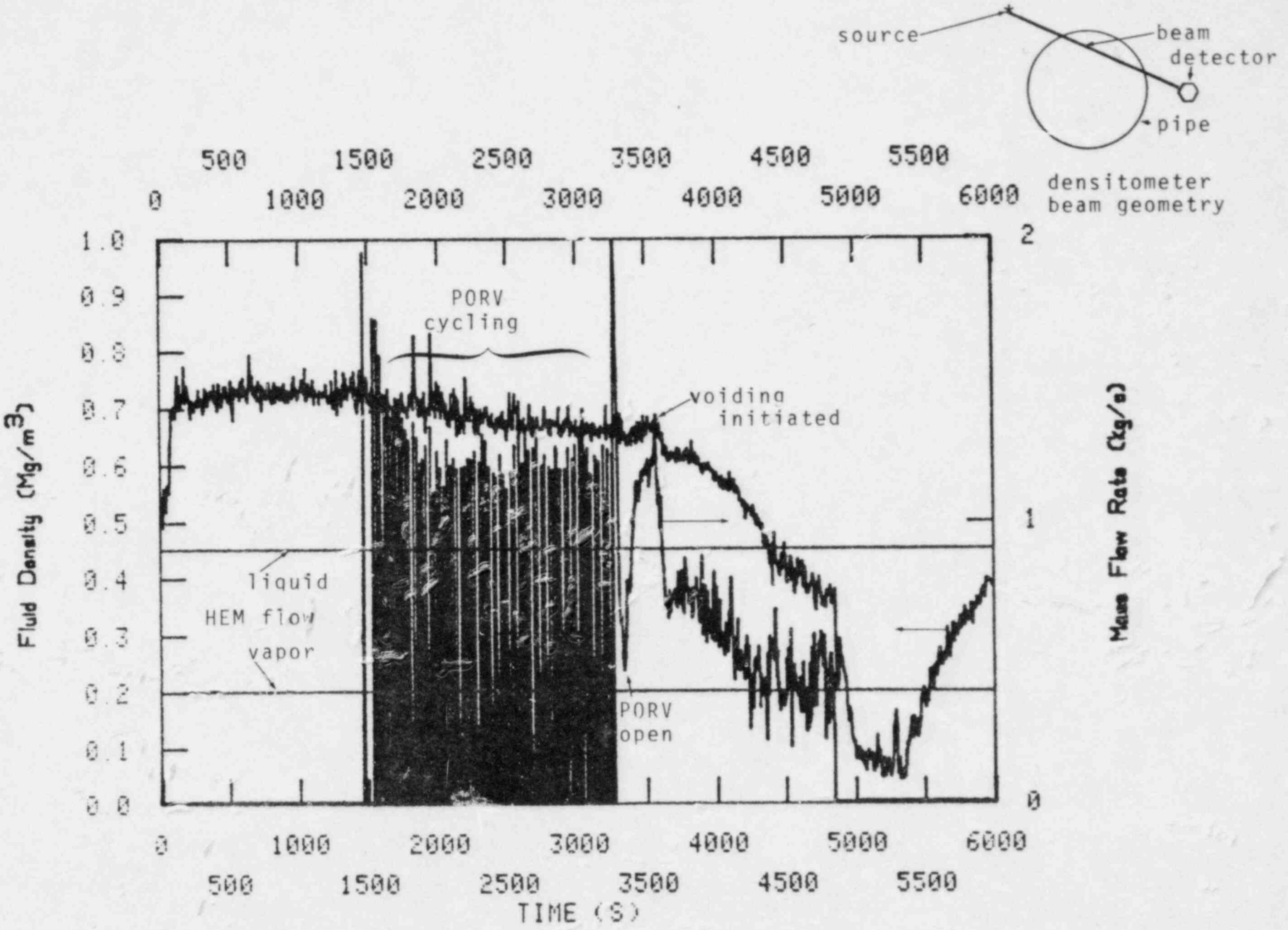

Figure 37. LOFT Test L9-1 PORV mass flow and intact loop hot leg density.

Figure 38. Pressurizer liquid level response.

sensitive to the surge line/hot leg geometry. PORV mass flow oscillations, which occurred after the transition to higher quality flow, are currently not explained.

5. RELAP5 ANALYSIS OF SEMISCALE TEST S-SR-2

A RELAP5 analysis of Semiscale Test S-SR-2 was performed to demonstrate the ability of the code to calculate the phenomena observed in the test. Comparisons of data and calculations established the ability of RELAP5 not only to accuractely predict the overall system response, but also to predict local responses, such as PORV mass flow rate, pressurizer liquid level, and primary system mass inventory depletion. The conclusions drawn from this analysis provide confidence in similar calculations performed for a large pressurized water reactor discussed in the next section.

5.1 Model Description

The computer analysis of Semiscale Test S-SR-2 was performed with the RELAP5[20] computer code.[a] The model shown in Figure 39 was based largely on the standard RELAP5 model for Semiscale,[21] with the following modifications to make it specific to Test S-SR-2:

1. The intact loop pump model was removed and replaced with piping to represent the actual test configuration.

2. Pressurizer noding was increased from eight to sixteen nodes to give better detail to the fluid conditions immediately upstream of the PORV

3. Steam generator secondary sides were simplified to a single volume riser and single volume downcomer. The steam generators were filled with saturated steam at the measured initial primary side outlet temperature

4. All primary system outer surfaces, with the exception of the pressurizer were considered adiabatic for the baseline

---

a. MOD1, Cycle 18, Configuration Control No. F00885

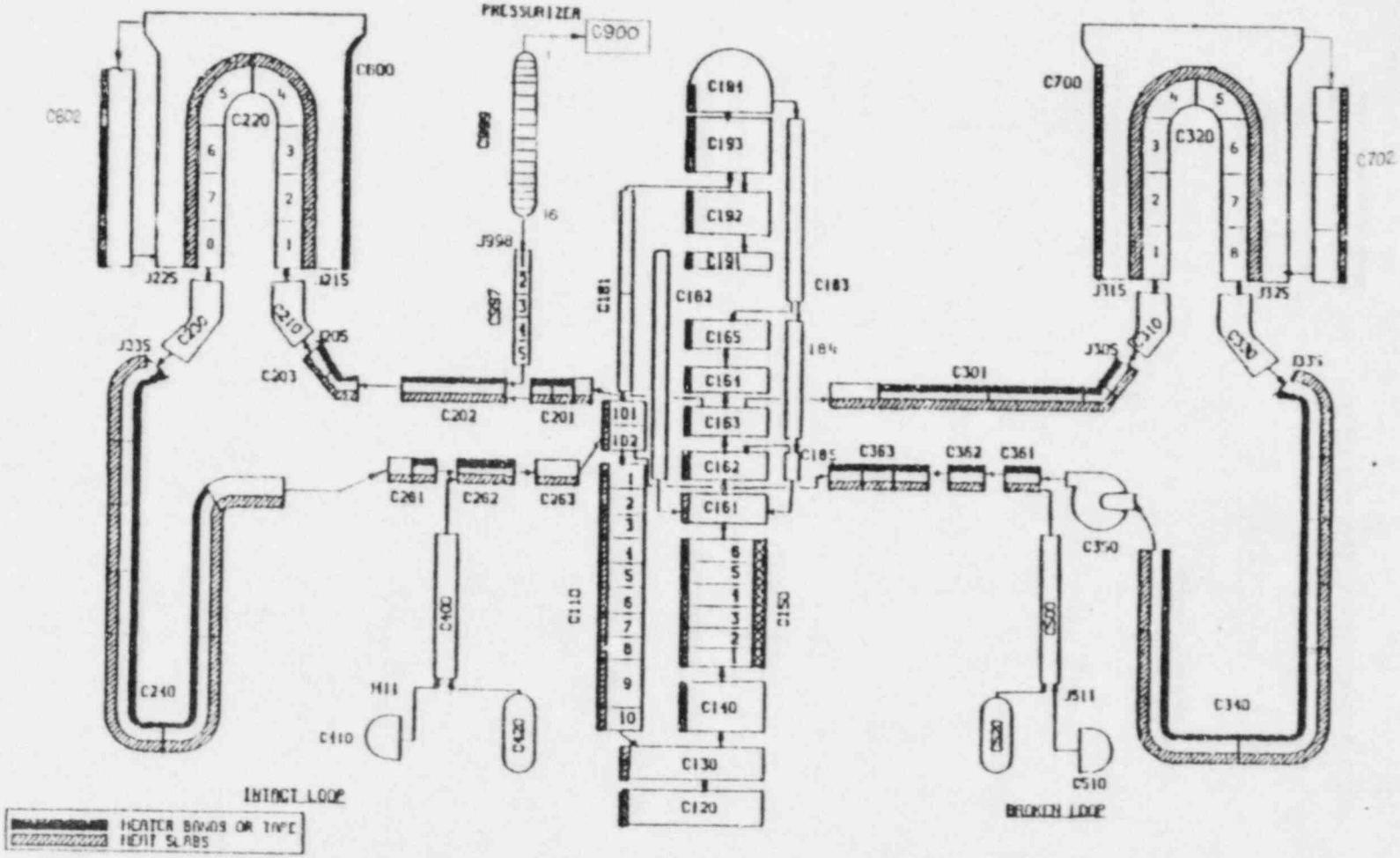

Figure 39. RELAP5 nodalization of the Semiscale Mod-2A system.

calculation. This approximation was based on the use of piping and vessel external heaters to supply local system heat losses. Modifications to this boundary condition are described in the specific analysis later in this report. The result of the heat loss assumptions was the selection of 40 kW as the baseline calculation core power.

5. A break junction representing the PORV was modeled on the top of the pressurizer. The piping leading to the flow limiting orifice used to simulate the PORV was not modeled, but rather was represented with a two-phase discharge coefficient of 0.84 on the PORV junction. The selection of this value is discussed later with the sensitivity studies.

6. Pressurizer wall heat loss was modeled mechanistically. A separate pressurizer model was used to modify the thermal conductivity of the insulation material until the calculated heat loss from the pressurizer agreed with the measured heat loss at test conditions.

7. High pressure injection system flow was set to EOS[3] specified values, rather than actual values delivered during the test. The smoother function with respect to pressure in the EOS specification made the results easier to generalize.

5.2 RELAP5 Analysis of Test S-SR-2

The RELAP5 analysis of Test S-SR-2 addressed the transient beginning at 14975 s. A baseline calculation was first performed with a simplified system model to determine whether measured test parameters and corresponding calculated values were in qualitative agreement. The baseline calculation used adiabatic conditions at all external primary coolant system boundaries with the exception of the pressurizer.[a] The

---

a. Pressurizer heat loss, as determined in sensitivity studies with a separate pressurizer model, was included in all three stages.

baseline calculation also included a two-volume secondary side for each steam generator, with an adiabatic boundary between the steam generator secondaries and the environment. The success of the baseline calculation warranted a further calculation that included heat loss from the steam generator secondaries to the environment. Core power was augmented for this calculation by the heat loss to the environment at initial conditions. All other primary system boundaries remained the same as the baseline calculation. In neither case was primary system leakage modeled.

The following discussion will focus on the baseline calculation. That calculation provided a sufficiently good representation of the test that the remaining calculation could be treated as a sensitivity study to indicate the importance of modeling spatially dependent heat losses. In that regard, the discussion of the additional calculation will be directed toward the differences from the baseline calculation.

5.2.1 Case 1--Baseline Calculation

The system transient which occurred upon opening the PORV was essentially a continuous mass depletion in which the mass added to the system via the high pressure injection system was less than that lost through the PORV. The calculated PORV mass flow rate shown in Figure 40 exhibited the same characteristics as observed in the test. Notably, the initial small decrease in mass flow was followed by a sharp rise beginning at about 300 s and continuing until about 1000 s.[a] Referring to the pressure trace in Figure 41 the initial decrease in PORV mass flow was a function of the decreasing system pressure. The decrease in mass flow rate reversed, however, as the pressurizer inventory lost through the PORV was replaced with liquid from the hot leg. Figure 42 shows that the increase in pressurizer liquid level was consistent with the increase in mass flow which became saturated liquid flow at about 300 s and remained so until about 1000 s. The calculated mass flow was somewhat higher than observed

---

a. 14975 s experiment time corresponds to 0 s in the RELAP5 calculation.

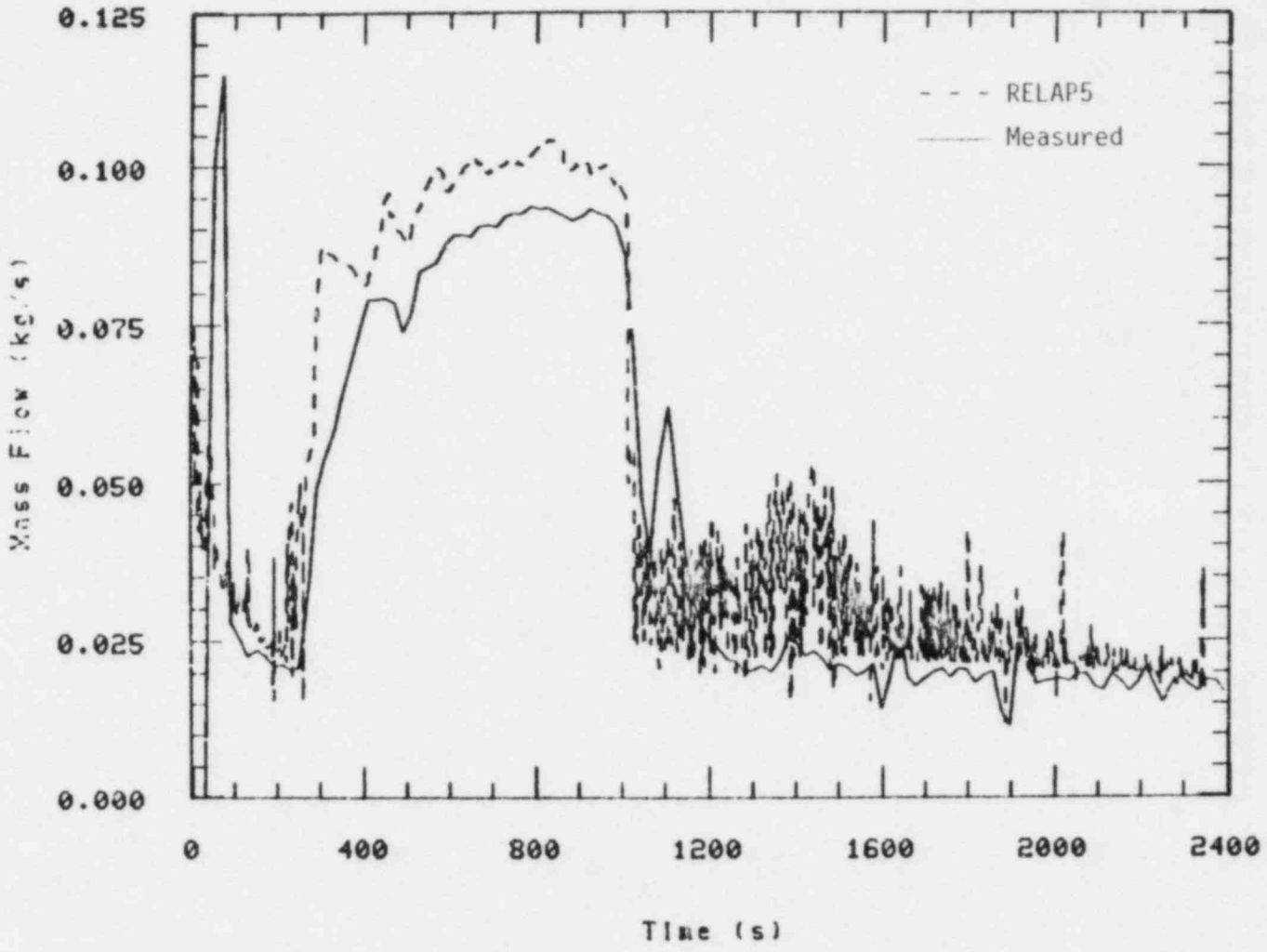

Figure 40. Comparison of measured PORV flow with RELAP5 predicted PORV flow. Test S-SR-2, point 3.

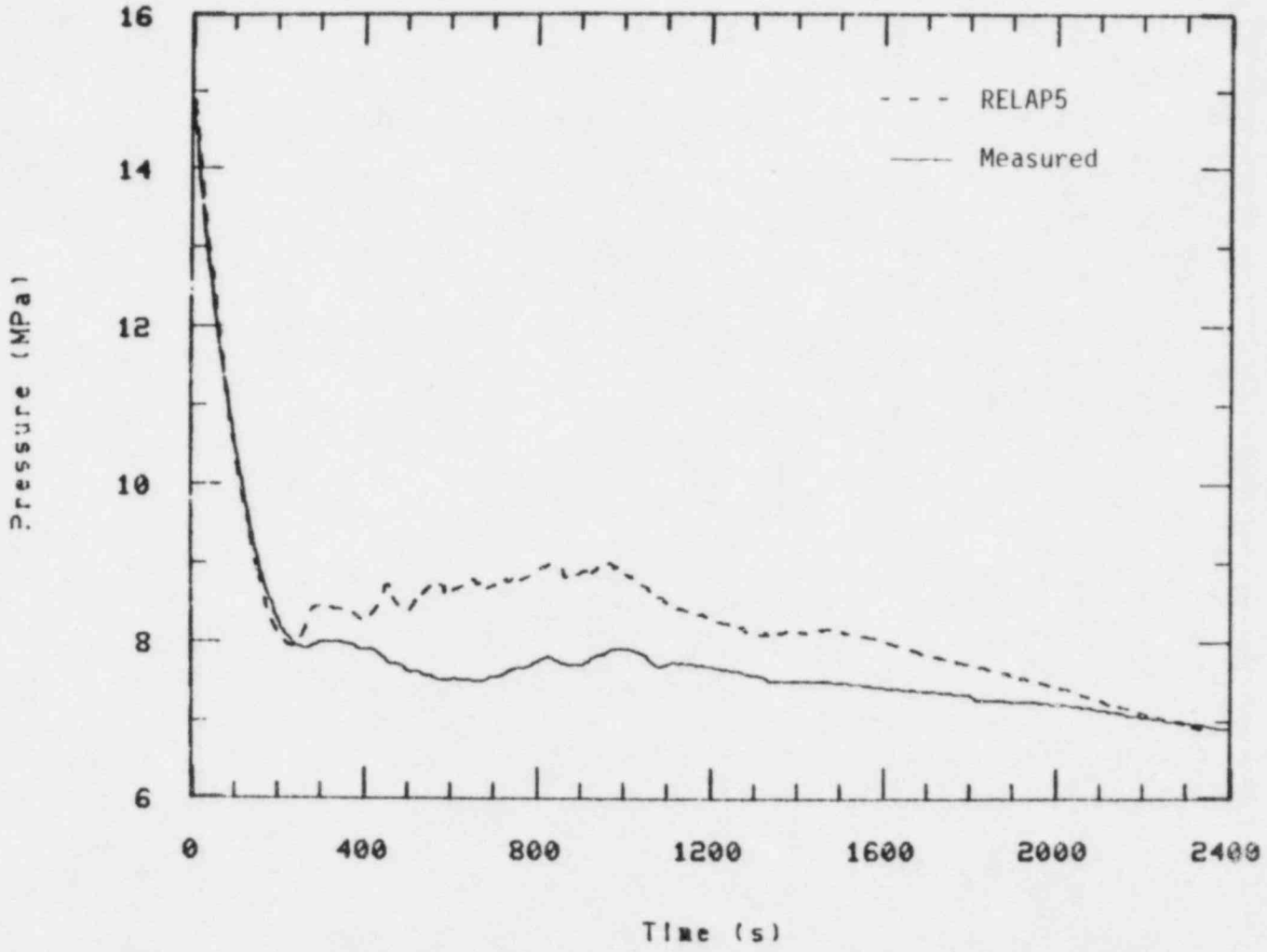

Figure 41. Comparison of measured and RELAP5 predicted upper plenum pressures. Test S-SR-2, point 3.

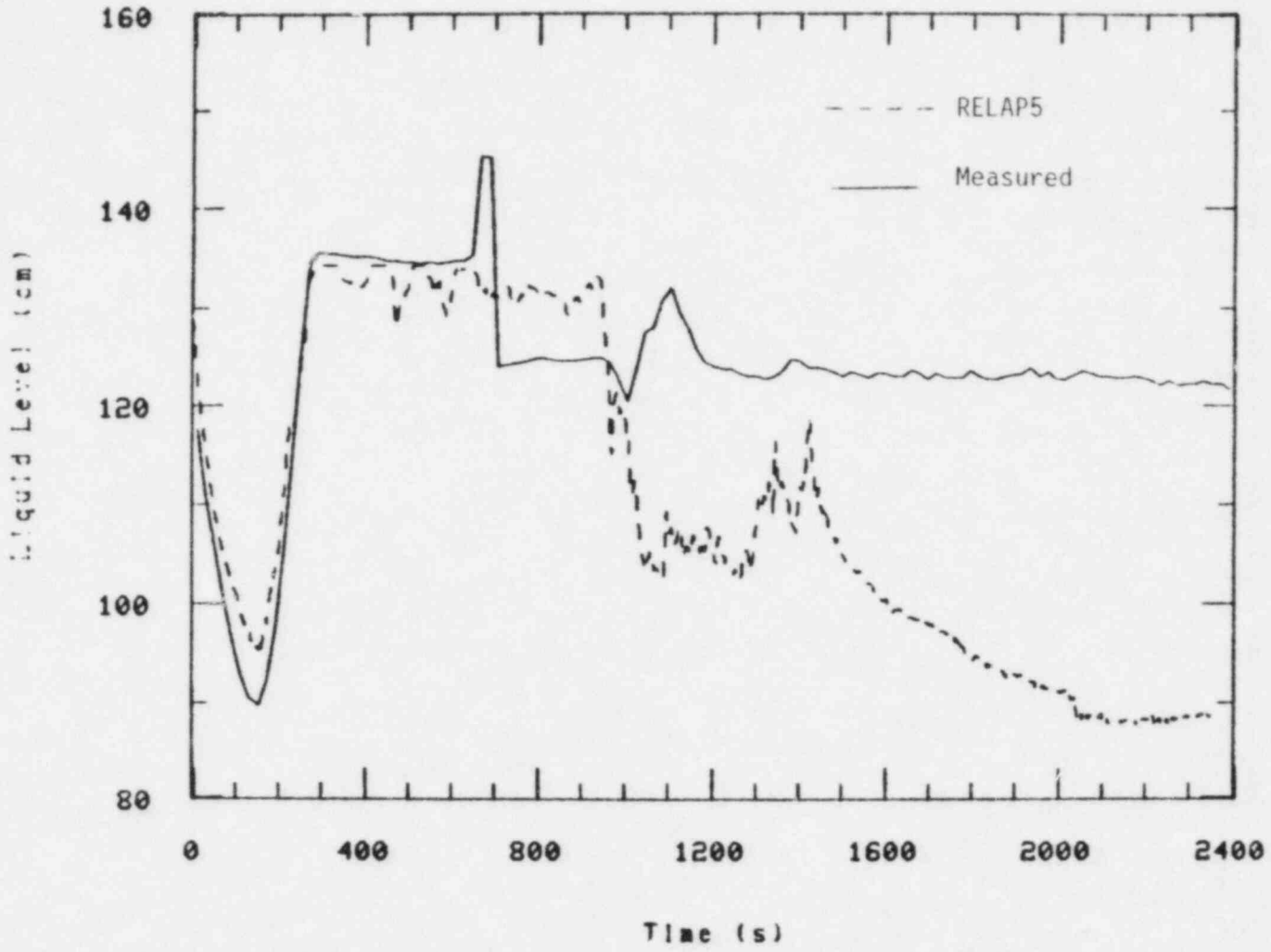

Figure 42. Comparison of measured and RELAP5 predicted pressurizer liquid level. Test S-SR-2, point 3.

in the test, a result of the calculated system pressure being higher than data. It will be shown later that these slight differences from data were quite sensitive to the assumption of adiabatic system boundaries.

As observed in the experiment, by 1000 s enough system inventory had been lost to drain the steam generator U-tubes and begin to drain the intact loop hot leg. At that time, both the PORV mass flowrate and the pressurizer liquid level dropped abruptly. In the test when the hot leg void fraction was great enough to drop the liquid level below the surge line elevations, surge line flow changed from low to high quality. RELAP5/MOD1 predicted the same phenomenon, but the transition from surge line liquid flow to mostly vapor flow was not a function of surge line geometry. RELAP5/MOD1 does not track a liquid level within a single homogeneous control volume unless the flow is in a horizontal stratified regime. Instead, the flow regime in the surge line junction with the hot leg was calculated to be in the transition region between bubbly and slug flow, closer to the bubbly regime, which has higher interphase frictional drag. The transition regime calculation is quite sensitive to void fraction, and as the hot leg void fraction increased, the flow regime proceeded rapidly to slug flow characteristics. This resulted in a rapid reduction in the interphase frictional drag coefficient by a factor of about 3 to 10. Subsequently the vapor velocity entering the surge line was greater than twice the liquid velocity, the effect being predominantly vapor flow into the surge line. Because the length of time needed to void the hot leg was rather short, the specific mechanism causing the flow transition in the surge line was not too important.

Transition to steam flow in the surge line caused a rapid drop in pressurizer liquid level and a transition from liquid flow to steam flow at the PORV. Though the mass flowrate through the PORV decreased significantly, it was still greater than the HPIS flowrate. Therefore, the inventory depletion process continued, ultimately being manifested as a decrease in the vessel collapsed liquid level. The comparison of observed and calculated vessel liquid levels in Figure 43 shows reasonably good agreement during the transient, although RELAP5 calculated somewhat greater voiding in the upper plenum early in the transient than was observed in the

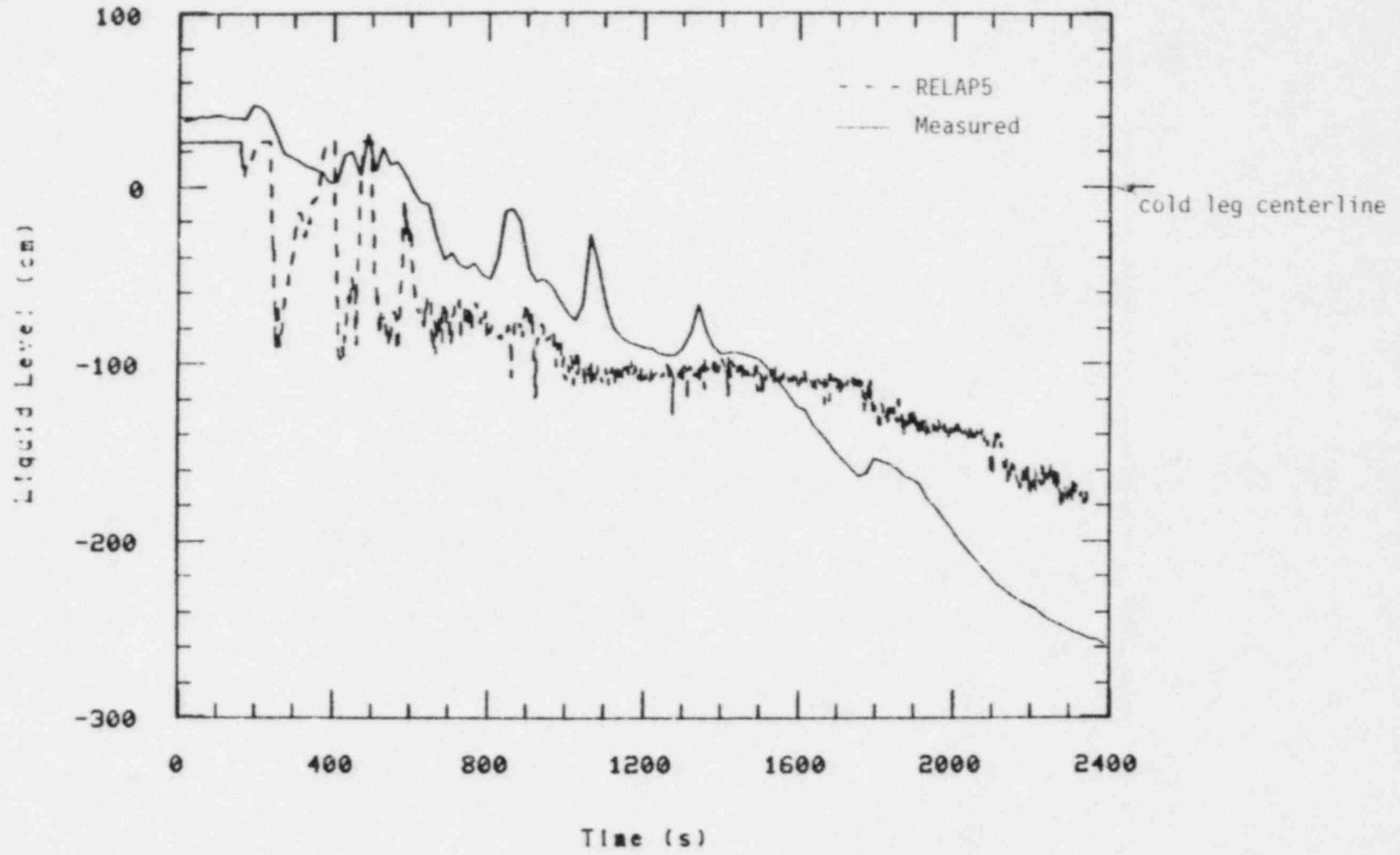

Figure 43. Comparison of measured and RELAP5 predicted vessel liquid levels. Test S-SR-2, point 3.

test. Analysis of the vessel liquid level comparison is confounded somewhat by the difference in system mass inventory depletion rates. Figures 41 and 44, PORV mass flowrates and HPIS mass flowrate, can be compared to show that the calculated drop in vessel liquid level is consistent with the difference in the mass flow rates. A higher than actual HPIS flowrate[a] resulted in a more gradual reduction of system inventory than observed in the test. The comparison of PORV mass flow rate and HPIS mass flow rate calculated by RELAP5 (Figure 45) shows that the flow imbalance was nearly zero at the time the calculation was terminated. One would expect, therefore, that a steady-state operating point was nearly established. At the same time, the calculated vessel liquid level was nearly low enough to uncover the core.

5.2.2 Case 2--Steam Generator Secondary Heat Loss

Heat loss from the system, other than through the pressurizer walls, was not modeled in the baseline calculation. An approximation of adiabatic boundaries was expected to be good because of the external heaters and augmented core power used in the experiment to offset the carefully characterized heat loss.[22] The close agreement between the test and the baseline calculation showed the assumption to be reasonable. A second calculation was performed to investigate the effect of the spatial distribution of heat loss. As a first step to incorporate spatial effects, the steam generator heat loss, based on an estimation of natural convection heat transfer from a circular cylinder to air[21] and the initial calculated heat transfer rates in RELAP5, was taken as 5 kW initially. Core power was augmented by this 5 kW to offset the heat loss and to maintain a net 40 kW input to the system. No other changes were made from the baseline calculation.[b]

---

a. As stated previously, HPIS flow was modeled according to the EOS specified value, rather than actual values delivered in the test.

b. A minor correction was made to an internal pressurizer junction. Sensitivity calculations showed the effect to be small.

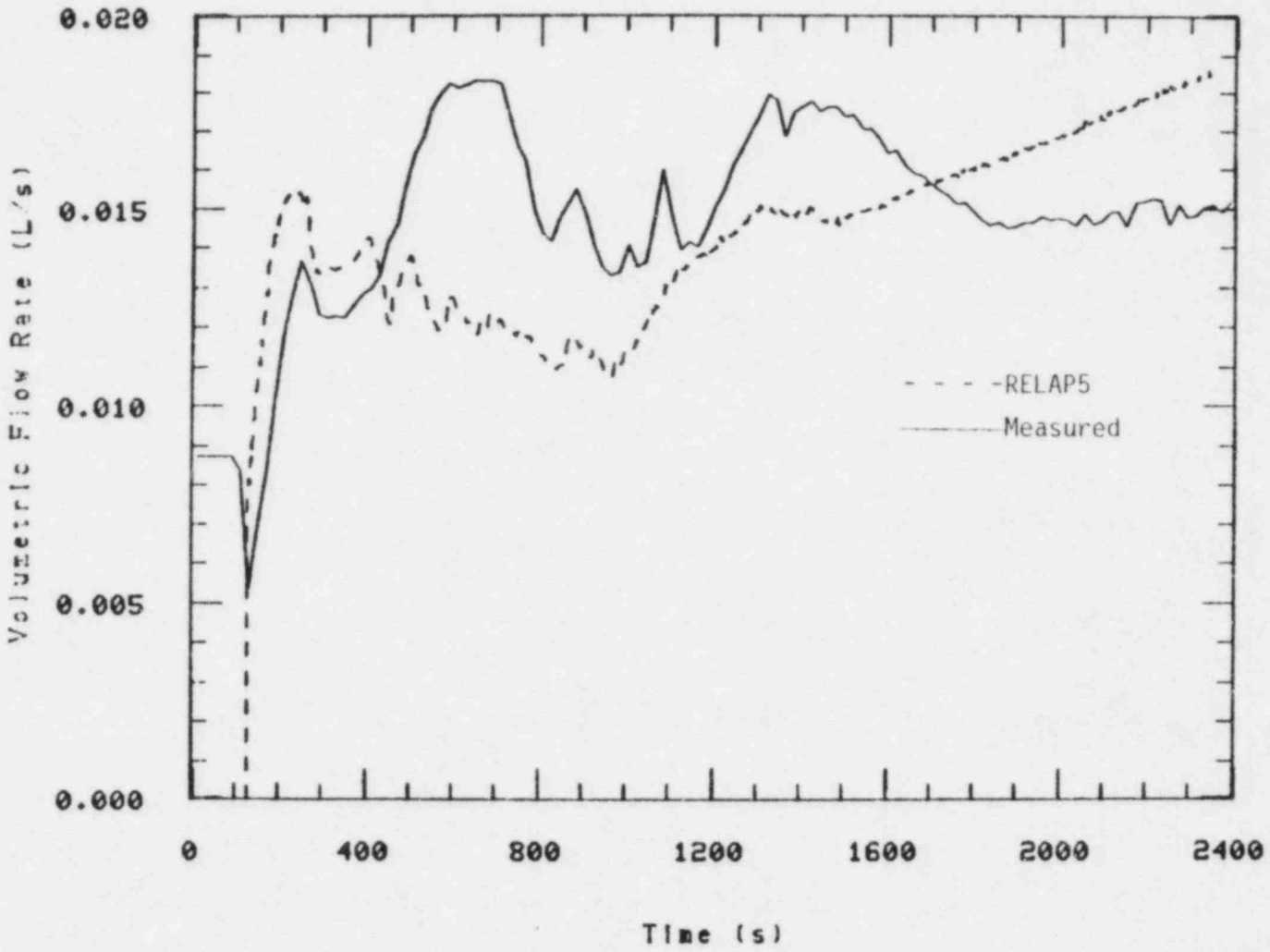

Figure 44. Comparison of measured and RELAP5 predicted HPIS flow. Test S-SR-2, point 3.

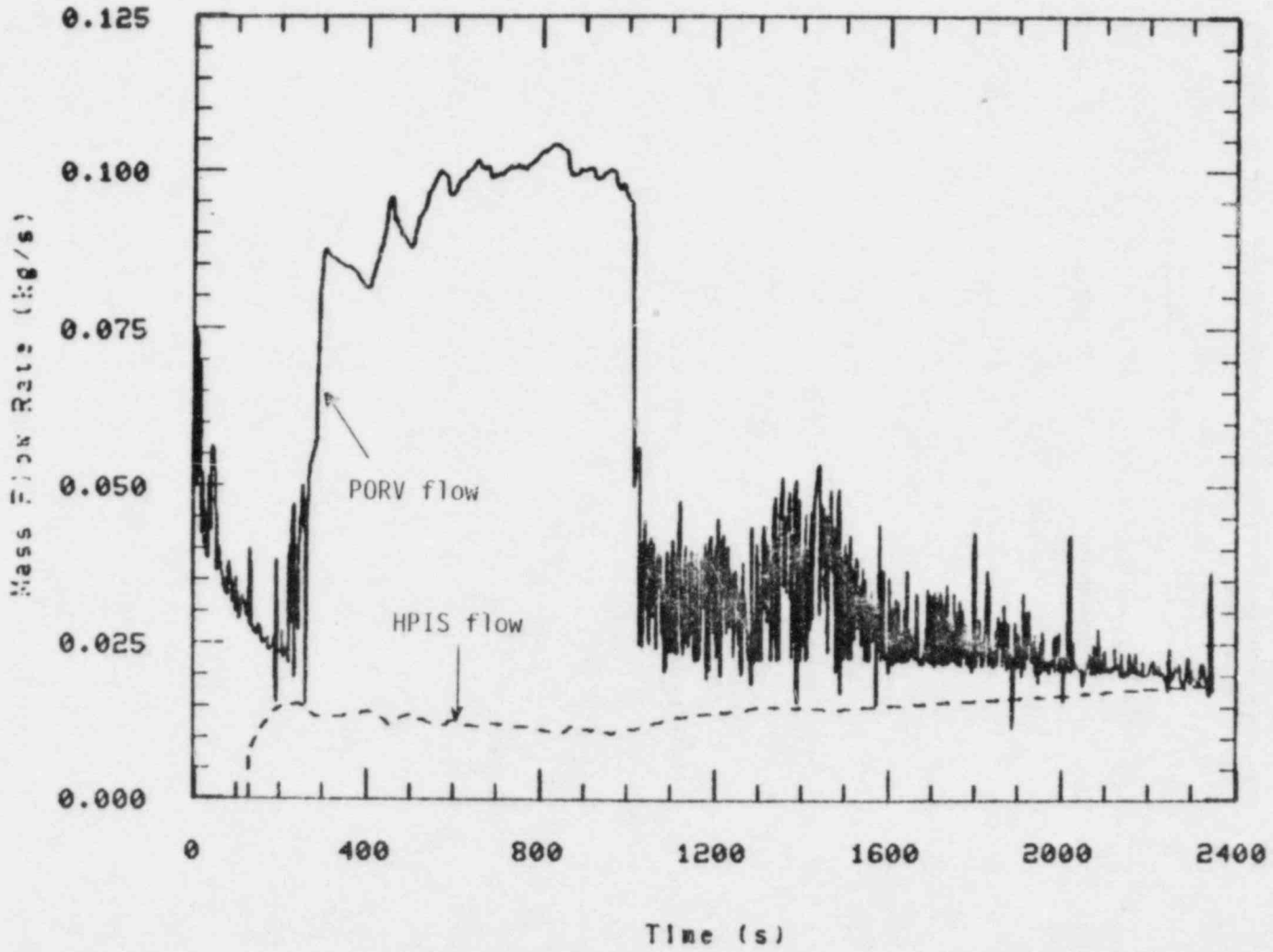

Figure 45. RELAP5 predicted PORV and HPIS flow rates. Test S-SR-2, point 3.

Figure 46 shows an improvement in the calculated PORV mass flow rate during the first 1000 s of the transient. This was the result of closer agreement between the calculated and observed pressures as shown in Figure 47. The reduction in calculated pressure as compared to the baseline calculation is the result of an increase in the steam generator heat transfer rates. This reduction was increased somewhat by an underestimate of the initial steam generator heat loss.[a]

The pressurizer liquid level, Figure 48, showed the same characteristics as the baseline calculation, the only exception being a somewhat later drop in level due to hot leg voiding. This result was consistent with the lower PORV mass flow rate. Similarily, the vessel liquid level calculation, Figure 49, showed the same characteristics as the baseline calculation.

The sensitivity of a steady-state operating point to core power can be seen in the vessel liquid level calculation. The underestimate of secondary system heat loss mentioned above resulted in an effective reduction in the net power driving the transient calculation. As a result, the PORV mass flowrate was reduced because of lower system pressure. The imbalance between PORV and HPIS mass flowrates was therefore reduced and a constant vessel liquid level resulted. It should be noted that the underestimate of steam generator heat loss resulted in a slightly low net power compared to the baseline calculation. A better estimate would have resulted in a higher net power and probably a delay in the time at which the constant vessel liquid level was established.

5.3 Sensitivity Studies

Analyses using a separate RELAP5 pressurizer model driven by time dependent input conditions were performed to determine the most appropriate

---

a. Subsequent calculations showed that 10 kW would have been a better estimate of steam generator heat loss.

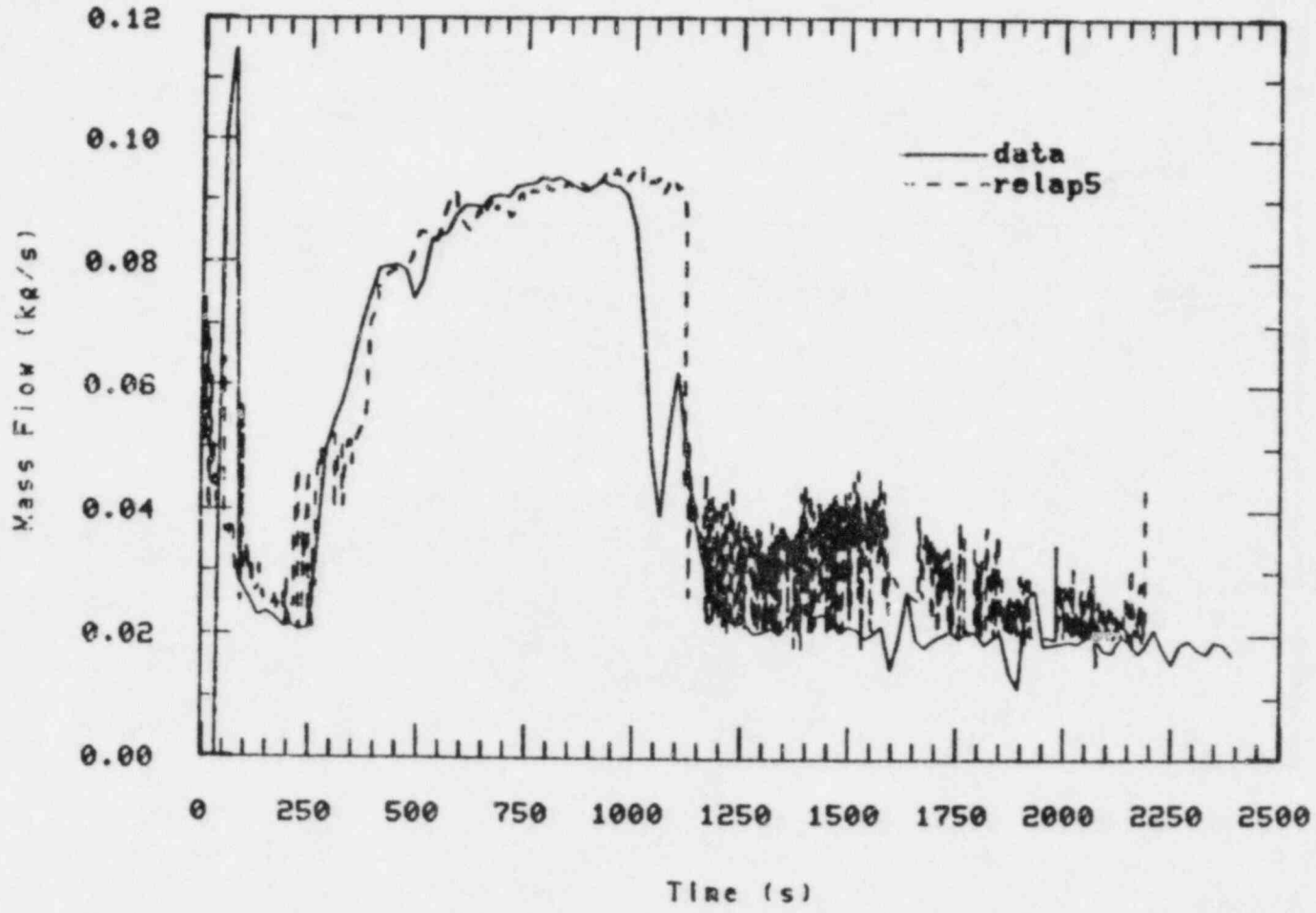

Figure 46. Comparison of measured and RELAP5 predicted PORV mass flow rate. Test S-SR-2, point 3.

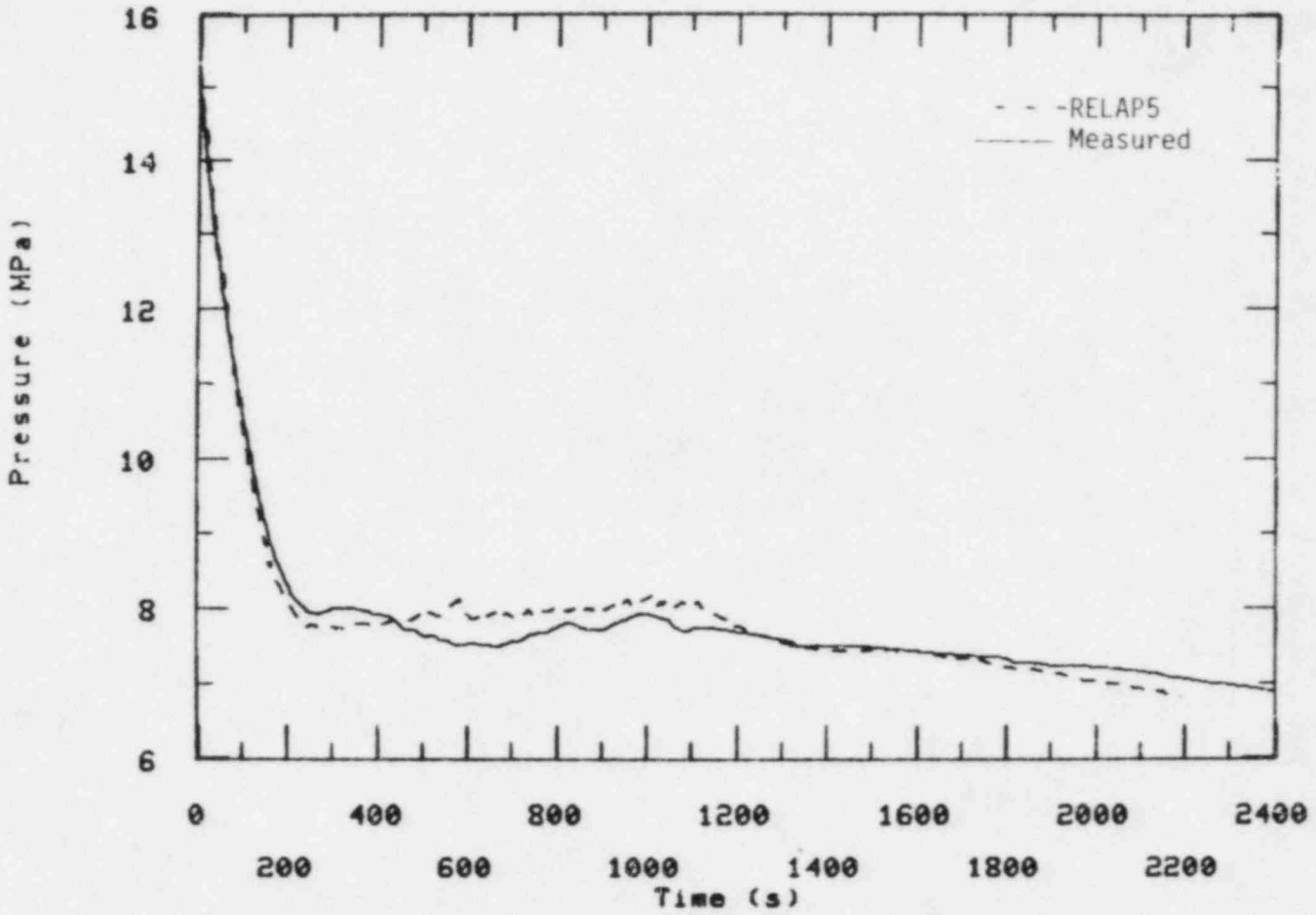

Figure 47. Comparison of measured and RELAP5 predicted system pressure. Test S-SR-2, point 3.

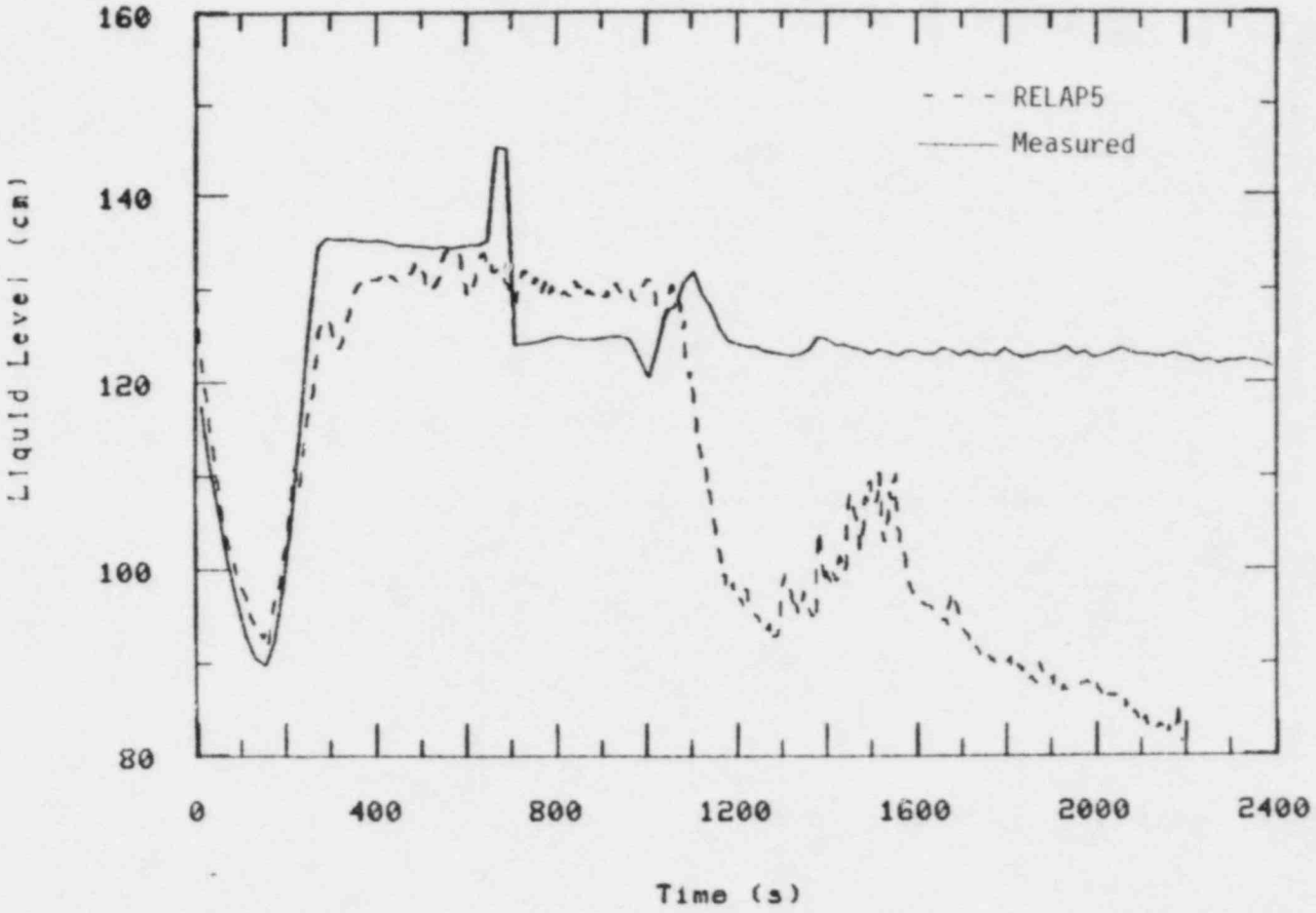

Figure 48. Comparison of measured and RELAP5 predicted pressurizer liquid level. Test S-SR-2, point 3.

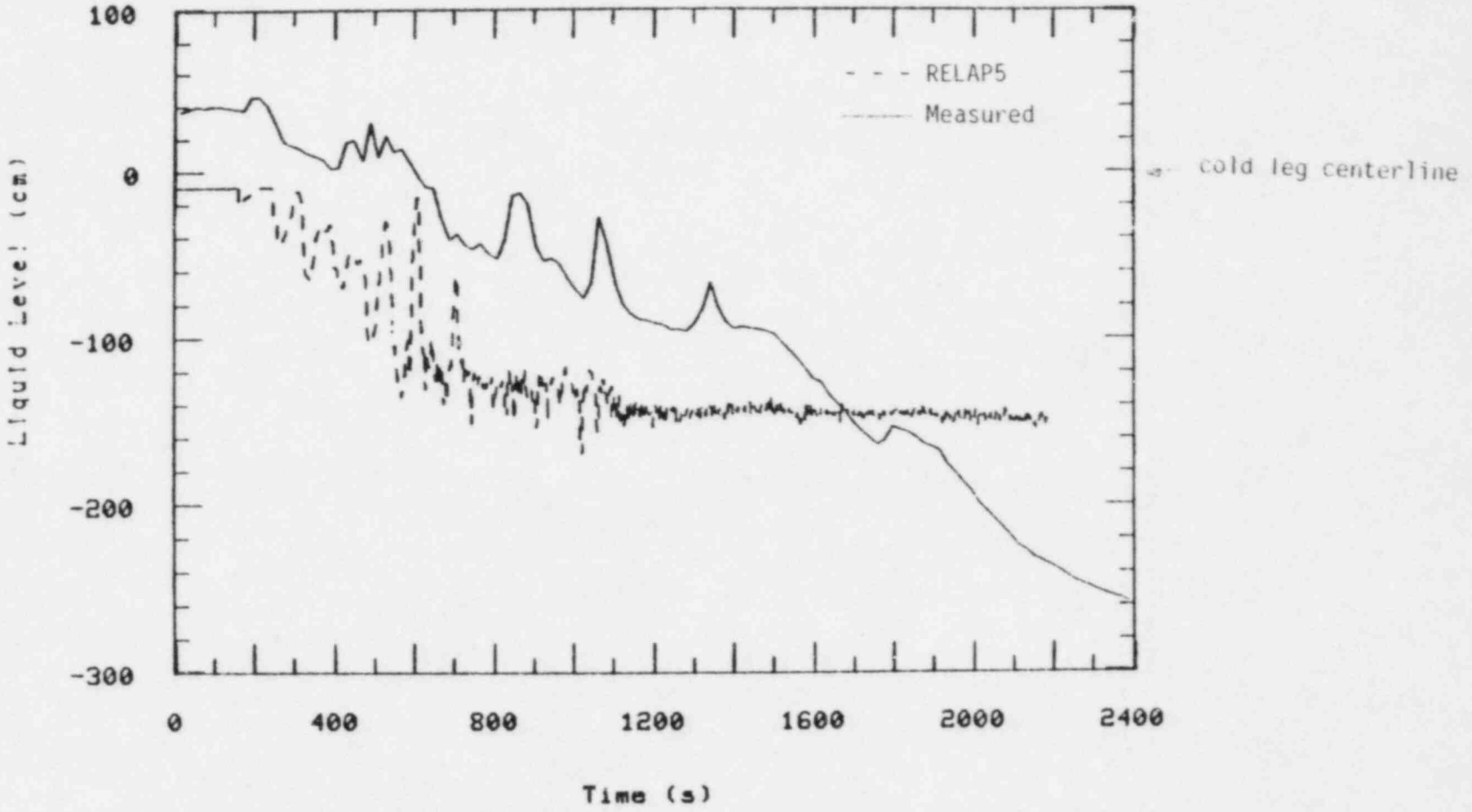

Figure 49. Comparison of measured and RELAP5 predicted core liquid levels. Test S-SR-2, point 3.

modeling assumptions for the system calculation. The boundary conditions used to represent the primary system were hot leg pressure and quality determined from data taken during Test S-SR-2. The results of the sensitivity studies are as follows:

1. Pressurizer noding had a small but noticeable effect on discharge mass flow and on pressurizer quality. Calculations using 8, 16, and 20 nodes[a] showed the finer noding to result in a slightly higher mass flow rate through the PORV and a slightly lower quality in the uppermost control volumes. Calculations using finer noding also showed more condensation and a higher collapsed liquid level than the 8-node model.

2. Pressurizer wall heat transfer resulted in a PORV mass flow rate about 20% greater than that calculated with an adiabatic boundary condition on the outer wall surface. The adiabatic wall calculation was noiser than that with heat transfer and gave worse agreement with data.

3. Calculated PORV mass flow rates were compared with data for steam flow at 8 MPa to determine a value for the discharge coefficient in the RELAP5 model. The calculated flows were a linear function of the discharge coefficient and showed 0.82 to give the best comparison with data.[b]

4. Doubling and halving the pressurizer surge line resistance, R', produced no noticeable changes in the pressurizer response.

---

a. The 20-node model was developed by halving the top four nodes in the 16-node model.

b. The system analysis used CD2 = 0.84 instead of 0.82. However, the estimated value of 0.84 was so close to the derived value of 0.82 that no system calculations were repeated.

5.4 Conclusions from the RELAP5 Analysis

1. RELAP5 correctly calculated the overall system response observed in Test S-SR-2. In addition, it gave a good representation of both the magnitude and timing of the PORV flow, system pressure, and pressurizer and core liquid level transients.

2. RELAP5 showed agreement with the test result that establishment of a steady-state feed and bleed operating point is sensitive to the exact PORV and HPIS flow characteristics.

3. Modeling sensitivity studies showed that pressurizer wall heat transfer and node size upstream of the discharge junction have small but noticeable effects on the pressurizer response.

6. FULL-SCALE PLANT FEED AND BLEED CALCULATIONS

Conclusions based upon the analysis in the previous section indicated that the RELAP5 code successfully predicted the occurrence and effects of phenomena controlling feed and bleed in the Semiscale system. The code was next used to extend the analysis to a full-scale system, and for a representative transient that might incorporate a feed and bleed cooling operation. A RELAP5 primary feed and bleed calculation was performed with a model of a standard, Westingnouse, four-loop, 3411 MW(t), pressurized water reactor (RESAR). The following transient scenario was assumed which eventually led to the feed and bleed operation. The plant was assumed to be operating at 100% power at best-estimate initial conditions when a loss-of-offsite power occurred with the coincident failure of all auxiliary feedwater systems. The steam generator heat sink was lost after the steam generator secondaries dried out. The loss of secondary heat sink caused the primary coolant system to heat up and pressurize until the PORV setpoint was reached. The operators were then assumed to initiate a feed and bleed operation by latching open both pressurizer PORVs and starting both charging and both HPIS pumps.

Important differences are worth noting in boundary conditions between the full-scale plant calculation and the Semiscale experiments covered earlier. The Semiscale experiment used a constant core power that was representative of decay heat levels within the first half hour after a scram. The full-scale plant calculation used a best-estimate, continually decreasing, decay heat curve, and the feed and bleed operation was calculated to begin more than one hour after scram. The full-scale plant calculations allowed charging pump injection in addition to the HPIS pumps, thereby resulting in higher injection rates and shutoff heads than the corresponding values used in Semiscale. Finally, the PORV was sized for the actual reported flow rate versus the 20% oversizing used in the Semiscale experiments. The operating map for the RESAR calculation is shown in Figure 50 and may be compared to Figure 16 to illustrate the aggregate effect of the differences.

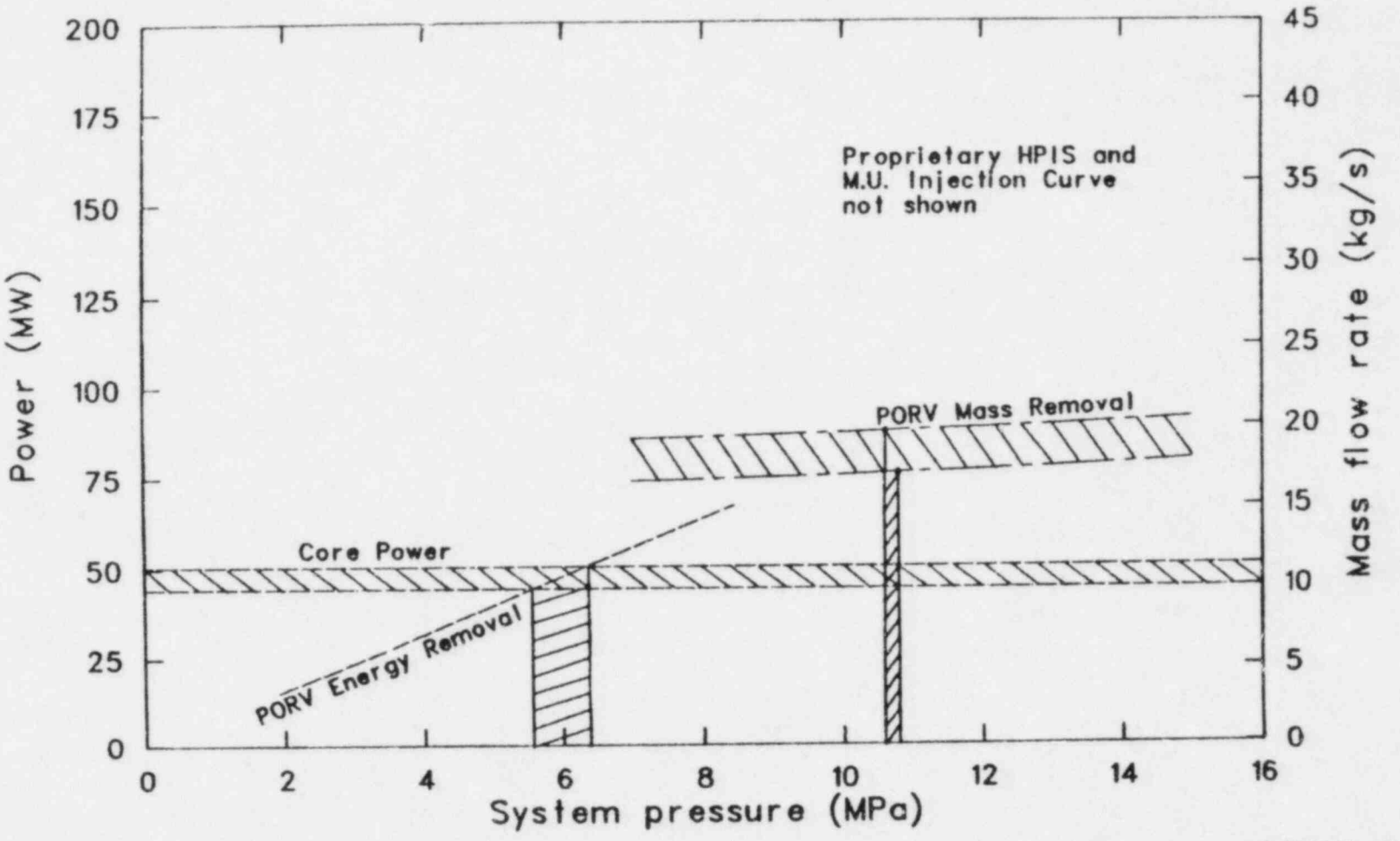

Figure 50. Primary feed and bleed operating map for RESAR calculation.

6.1 Model Description

The RELAP5 RESAR model was originally developed to perform small cold leg break calculations. The model represents the primary coolant system, ECCS, steam generator secondaries, and portions of the feedwater and steam piping (Figure 51). The four reactor coolant loops in the plant were modeled with two coolant loops in the RELAP5 model. One loop in the RELAP5 model represented a single primary coolant loop while the other loop, designated the triple loop, represented the three remaining coolant loops in the plant.

The RELAP5 RESAR model is described in detail in Reference 23. Modifications to the referenced model were made in order to perform the feed and bleed analysis. The pressurizer was modeled with sixteen volumes, rather than eight, to provide additional detail in the pressurizer and to be consistent with the Semiscale model described in Section 5. The pressurizer surge line was attached to the single loop. The two PORVs in the plant were represented with one junction attached to the top of the pressurizer. The PORV junction area (0.001772 m^2) was sized to pass a steam flow rate of 26.46 kg/s per valve at 16.20 MPa using the RELAP5 critical flow model. A steam mass flow rate versus pressure curve was used to represent the five safety relief valves on each steam generator secondary. A curve of core power versus time, illustrated in Figure 52, was used to represent control rod insertion (scram) and decay heat. The decay heat corresponds to the 1973 ANS standard[24] plus actinide decay. The auxiliary feedwater system was deleted. Trips were modified to represent a loss-of-offsite power transient. Calculated steady-state conditions which define the best-estimate state of the plant prior to the loss-of-offsite power are shown in Table 6.

6.2 Best Estimate Calculation Results

The times at which significant events occurred in the calculation are given in Table 7. The thermal-hydraulic response of the system is illustrated in Figures 53 through 55. Emphasis in the following discussion is placed on the feed-and-bleed portion of the transient; the loss-of-offsite power and failure of the auxiliary feedwater merely provided a plausible scenario resulting in feed-and-bleed operation.

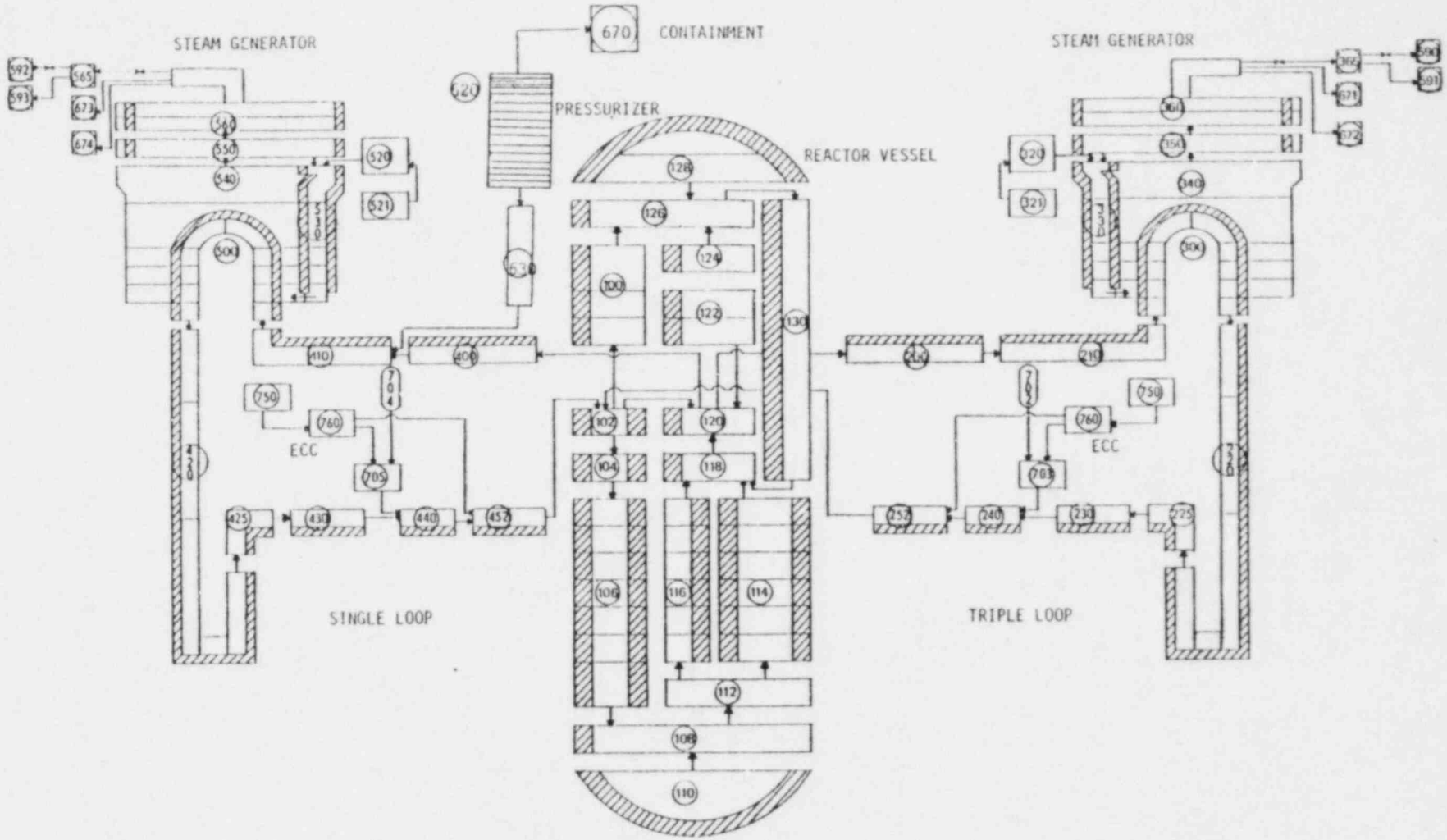

Figure 51. RELAP5 model of RESAR.

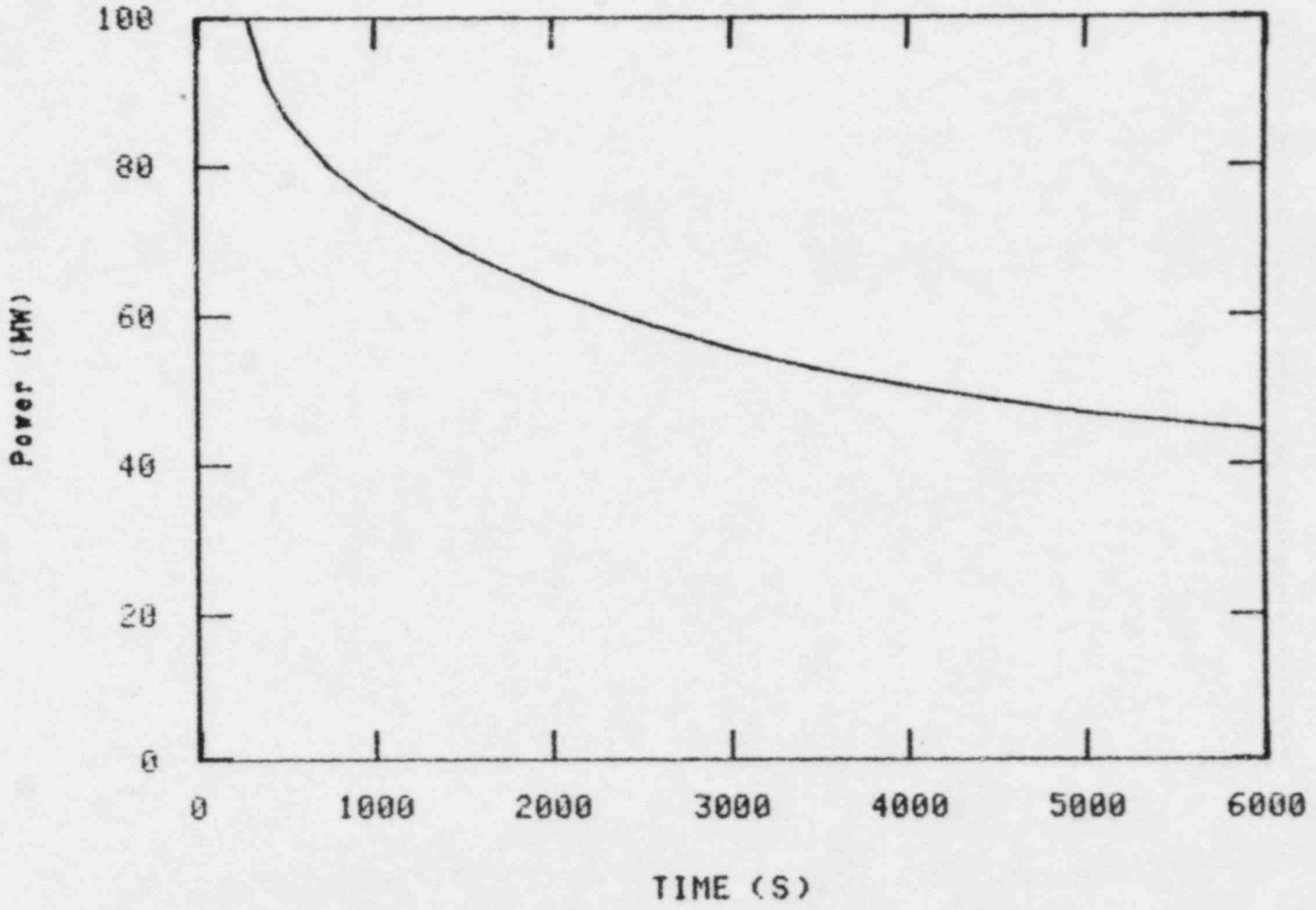

Figure 52. Core power for the RESAR feed and bleed calculation.

TABLE 6. INITIAL CONDITIONS FOR THE RESAR CALCULATION

Parameter	Initial Value
Core power, MW(t)	3411
Pressurizer pressure, MPa	15.56
Hot leg fluid temperature, K	
Single loop	598.6
Triple loop	598.6
Cold leg fluid temperature, K	
Single loop	565.2
Triple loop	565.2
Cold leg mass flow rate, kg/s	
Single loop	4435.
Triple loop	13,300
Steam generator secondary pressure, MPa	
Single loop	6.474
Triple loop	938.47 psia (6.470)
Feedwater mass flow rate, kg/s	
Single loop	475.9
Triple loop	1428.
Feedwater temperature, K	499.8
Steam generator secondary liquid mass,[a] kg	
Single loop	46,190
Triple loop	142,400
Pressurizer liquid mass,[b] kg	17,360

a. Includes the liquid in the feedwater line.

b. Includes the liquid in the surge line.

TABLE 7. SEQUENCE OF EVENTS IN THE RESAR CALCULATION

Time (s)	Event
0.0	Loss-of-offsite power, reactor coolant pumps tripped
0.5	Control rod drop initiated
1.0	Turbine stop valves closed
3.1	Control rods fully inserted
5.0	Feedwater valves closed
59	Steam generator secondary relief valves opened (single loop)
73	Steam generator secondary relief valves opened (triple loop)
3875	Steam generator secondaries dryout
4052	PORV setpoint pressure reached; both PORVs latched open; charging initiated
4100	HPIS initiated
4150	Flashing in upper plenum and upper head
4500	Pressurizer 95% liquid full; subcooling reestablished in hot legs
5260	Calculation terminated

Calculated pressurizer pressure during the loss-of-feedwater/feed and bleed transient is shown in Figure 53. The loss-of-offsite power at 0 s caused reactor scram, reactor coolant pump trip, and steam generator isolation. The pressurizer pressure initially decreased and then increased in response to the combination of reactor scram and pump coastdown. By 200 s, natural circulation flow was sufficient to transfer the core decay power to the steam generators with the secondary liquid inventory providing a heat sink. The secondary liquid was boiled to steam which exited the steam generators through the safety relief valves. The pressurizer pressure remained nearly constant after 200 s until the steam generator secondaries dried out at 3875 s. The subsequent loss of the secondary heat sink caused the primary coolant to heat up which increased the pressure until the PORV setpoint was reached at 4052 s. The operators were then assumed to latch open both PORVs and start both charging and both HPIS pumps. The resulting steam flow out the PORVs caused the pressure to decrease rapidly until 4150 s when fluid in the stagnant portions of the upper plenum and upper head began flashing. Flashing in the vessel reduced the depressurization rate directly through the effect of steam generation, but more importantly by causing a liquid insurge into the pressurizer which lowered the volumetric flow out the PORVs. The primary coolant system depressurized relatively slowly for the remainder of the calculation.

The calculated pressurizer liquid level during the transient is shown in Figure 54. The liquid level initially decreased and then increased similar to the pressure transient shown in Figure 53. The pressurizer level remained nearly constant between 200 s and 3875 s when the steam generator secondaries dried out. The pressurizer level then increased slightly as the primary coolant heated up and expanded until the PORVs were latched open at 4052 s. The pressurizer level increased at a slightly greater rate until 4150 s when flashing began in the upper plenum and upper head. Fluid expansion due to flashing in the vessel caused a rapid insurge of fluid into the pressurizer and a corresponding rise in pressurizer level. The pressurizer was 95% liquid full, by volume, at 4500 s. The pressurizer remained nearly liquid full for the remainder of the calculation.

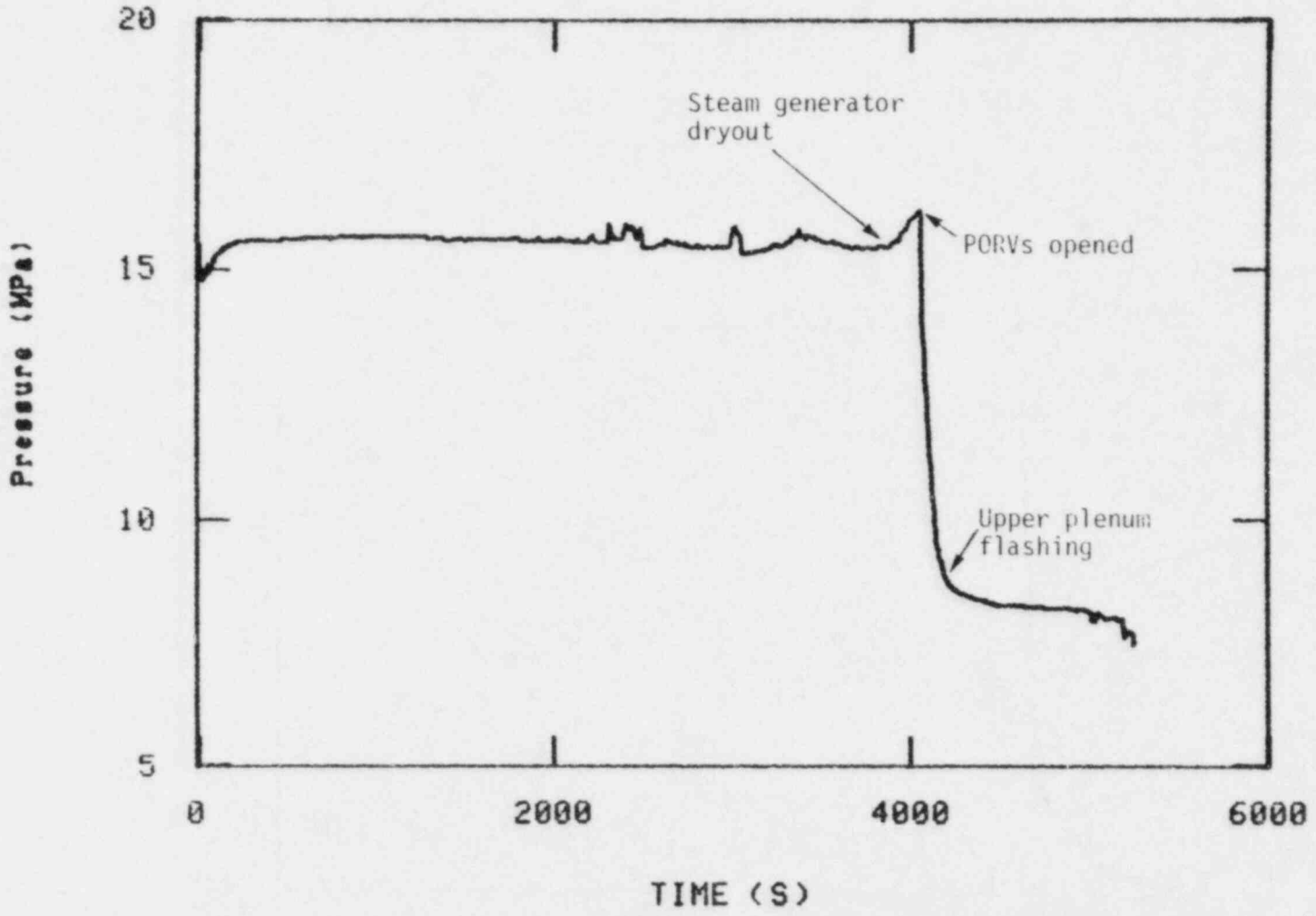

Figure 53. Calculated pressurizer pressure for RESAR feed and bleed.

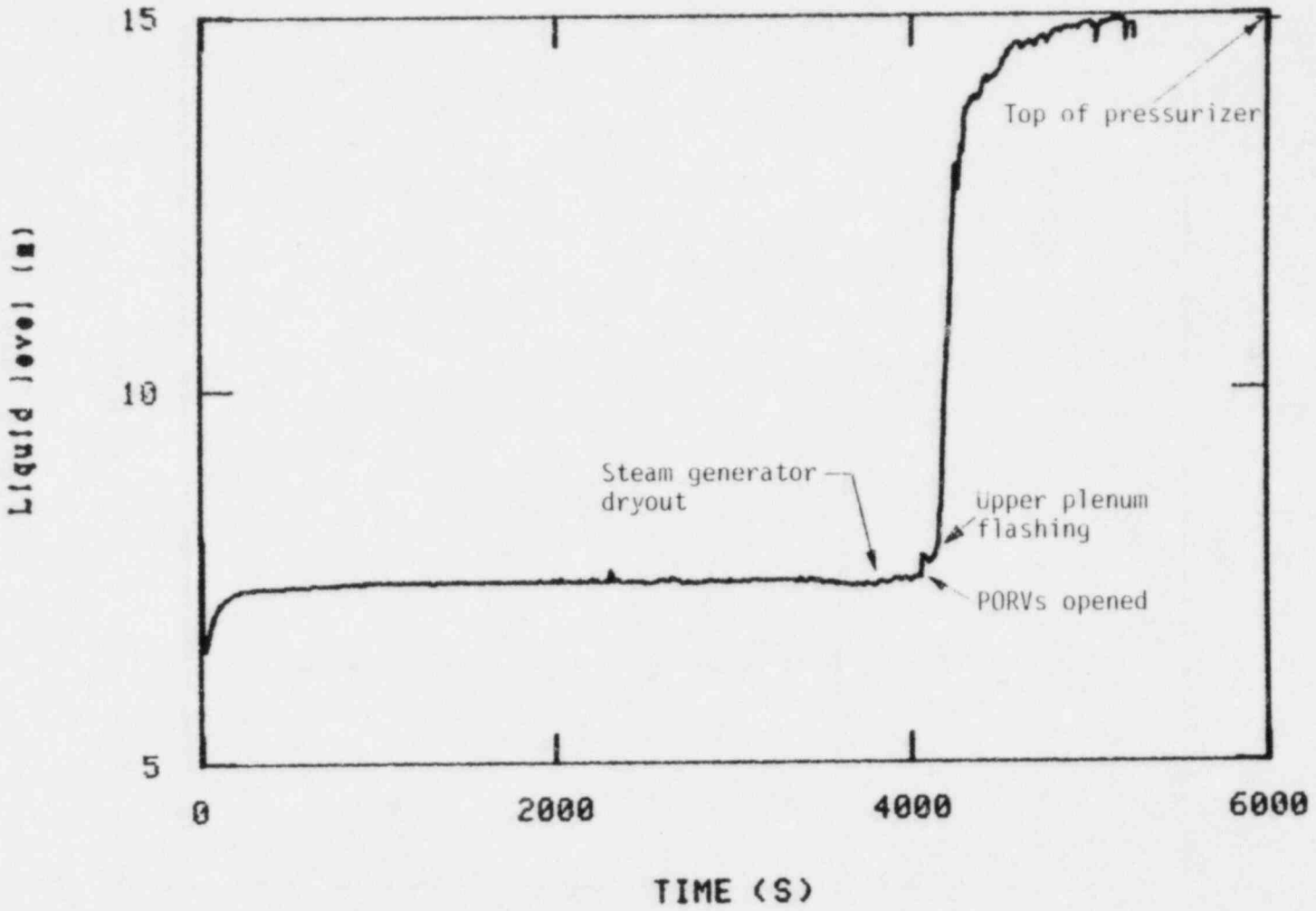

Figure 54. Calculated pressurizer liquid level for RESAR feed and bleed.

A comparison of the calculated PORV mass flow rate and the total ECC flow rate is shown in Figure 55. The total ECC flow rate represents the output of two charging and two HPIS pumps. The PORV mass flow rapidly increased to values representative of choked steam flow after the PORVs were latched open. The PORV mass flow rate decreased with pressurizer pressure until 4150 s when the pressurizer liquid level increased (see Figure 54) and liquid was entrained out the PORVs. The mass flow rate then increased irregularly as the fluid quality upstream of the PORVs decreased. The quality in the uppermost control volume in the pressurizer, which was the donor cell for the PORVs, decreased to 2% at 4550 s. The quality remained less than 2% for the remainder of the calculation with mostly liquid exiting the PORVs.

Charging flow was initiated simultaneously with the opening of the PORVs. The primary coolant pressure dropped below HPIS shutoff head at 4100 s allowing the initiation of HPIS flow. The combined charging and HPIS flow was greater than the PORV flow after 4100 s, which resulted in an increasing primary coolant liquid inventory. After 4300 s, the feed and bleed operation was removing about 25% more energy from the primary coolant system than was being generated by core decay heat. Consequently, the feed and bleed operation cooled the primary coolant system. Subcooling was re-established in the hot legs at 4500 s. The calculation was terminated at 5260 s with the primary coolant liquid inventory and system subcooling increasing. At the end of the calculation, the primary coolant system was liquid solid except for a small amount of steam in the pressurizer and steam pockets in the single loop steam generator, the upper head, and the uppermost control volume in the upper plenum.

Results from the RELAP5 calculation described above indicate that an operator-initiated feed and bleed operation in a RESAR plant with full charging and HPIS capacity could successfully mitigate the consequences of a simultaneous loss-of-offsite power and loss of auxiliary feedwater. RELAP5 predicted that the feed and bleed operation could remove core decay power and maintain sufficient liquid inventory to keep the core covered and cooled. Only minor (less than 30%) voiding was calculated in the hot legs.

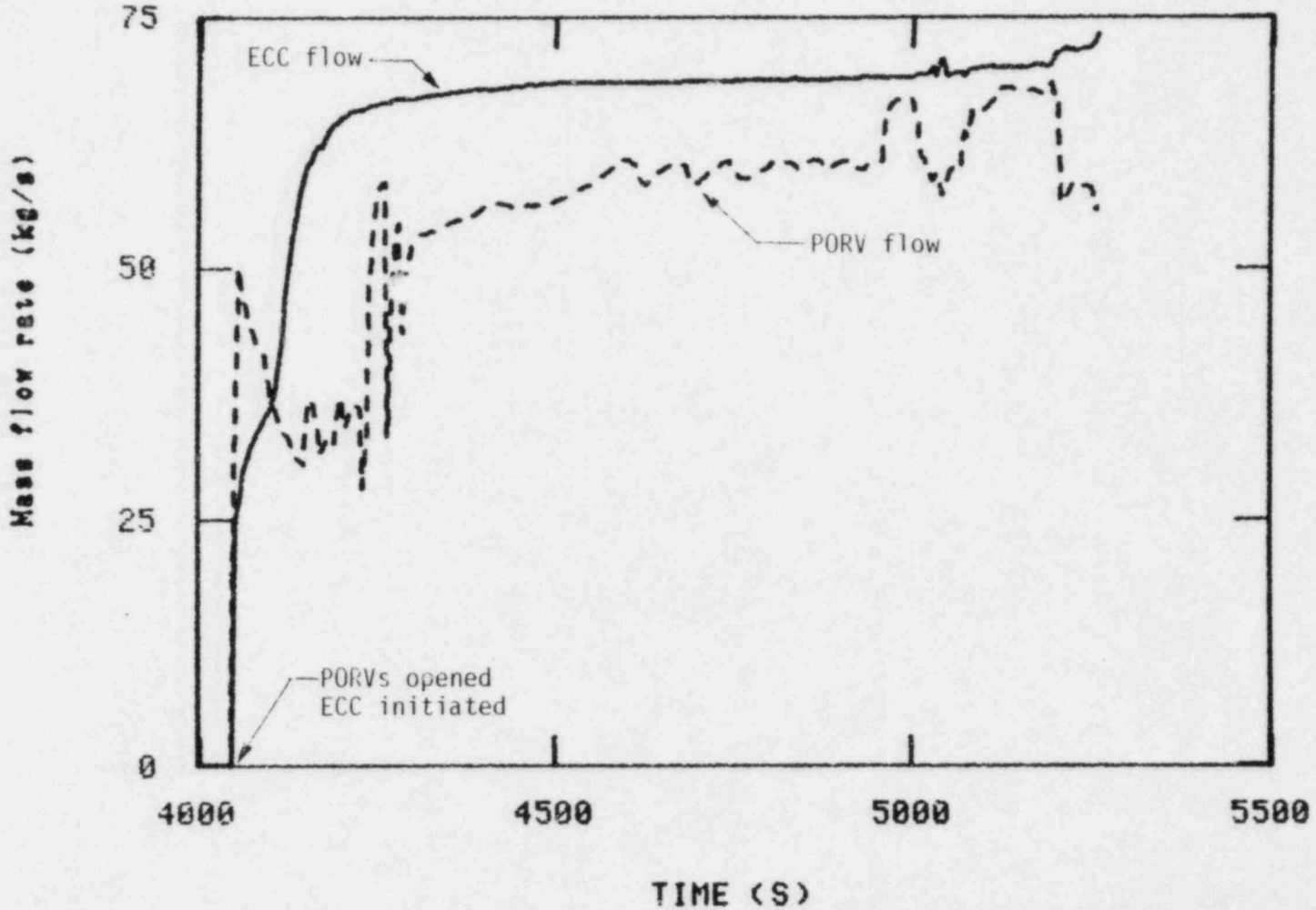

Figure 55. A comparison of PORV and ECC flow rates during RESAR feed and bleed.

6.3 Loss of Secondary Heat Sink With No ECC

Best-estimate RELAP5 calculations indicated that a feed and bleed operation in a RESAR plant would not result in core uncovery. A sensitivity calculation was performed to help determine the typicality of the Semiscale results relative to a large PWR for similar transients which do result in core uncovery. The sensitivity calculation was restarted at 4052 s from the base case calculation described previously. The sensitivity calculation was identical to the base case except that charging and HPIS injection were not used.

The sequence of significant events is presented in Table 8. The calculated thermal-hydraulic response of the system is illustrated by Figures 56 through 59. The effect of ECC on pressurizer pressure is shown in Figure 56 which compares the results of the base case calculation (with ECC) and the sensitivity calculation (without ECC). The pressure was similar in the two calculations until 4150 s when the upper plenum began flashing. In the base case, the cooling associated with ECC injection helped stablize the pressure shortly after flashing began in the upper plenum. In the sensitivity calculation, the cooling mechanism of ECC injection was not present. Consequently, boiling occurred in the core resulting in fluid expansion. The PORVs were incapable of relieving the fluid expansion after liquid reached the PORVs and reduced their volumetric flow. Consequently, the pressure increased in the sensitivity calculation until 5300 s when the pressurizer had voided sufficiently to allow enough steam out the PORVs to stop the pressure rise. The pressure remained at about 14.5 MPa for the remainder of the calculation.

The effect of ECC on pressurizer level is shown in Figure 57. The ECC added into the primary coolant system in the base case caused a slight level increase between the time the PORVs were latched open (4052 s) and the time of upper plenum flashing (4150 s). The level decreased during the same period in the sensitivity calculation because ECC was not added to the system. Upper plenum flashing at 4150 s resulted in a rapid filling of the pressurizer in both calculations. In the base case, the ECC flow generally exceeded the PORV flow (see Figure 55), thus, maintaining the liquid level

TABLE 8. SEQUENCE OF EVENTS IN THE RESAR CALCULATION WITHOUT ECC

Time (s)	Event
4052	Both PORVs latched open, ECC failed
4150	Flashing in upper plenum; primary system begins to repressurize
4300	Pressurizer nearly full
4500	Pressurizer level decreasing
5300	Primary system repressurization halted
5900	Core uncovery
6025	Calculation terminated

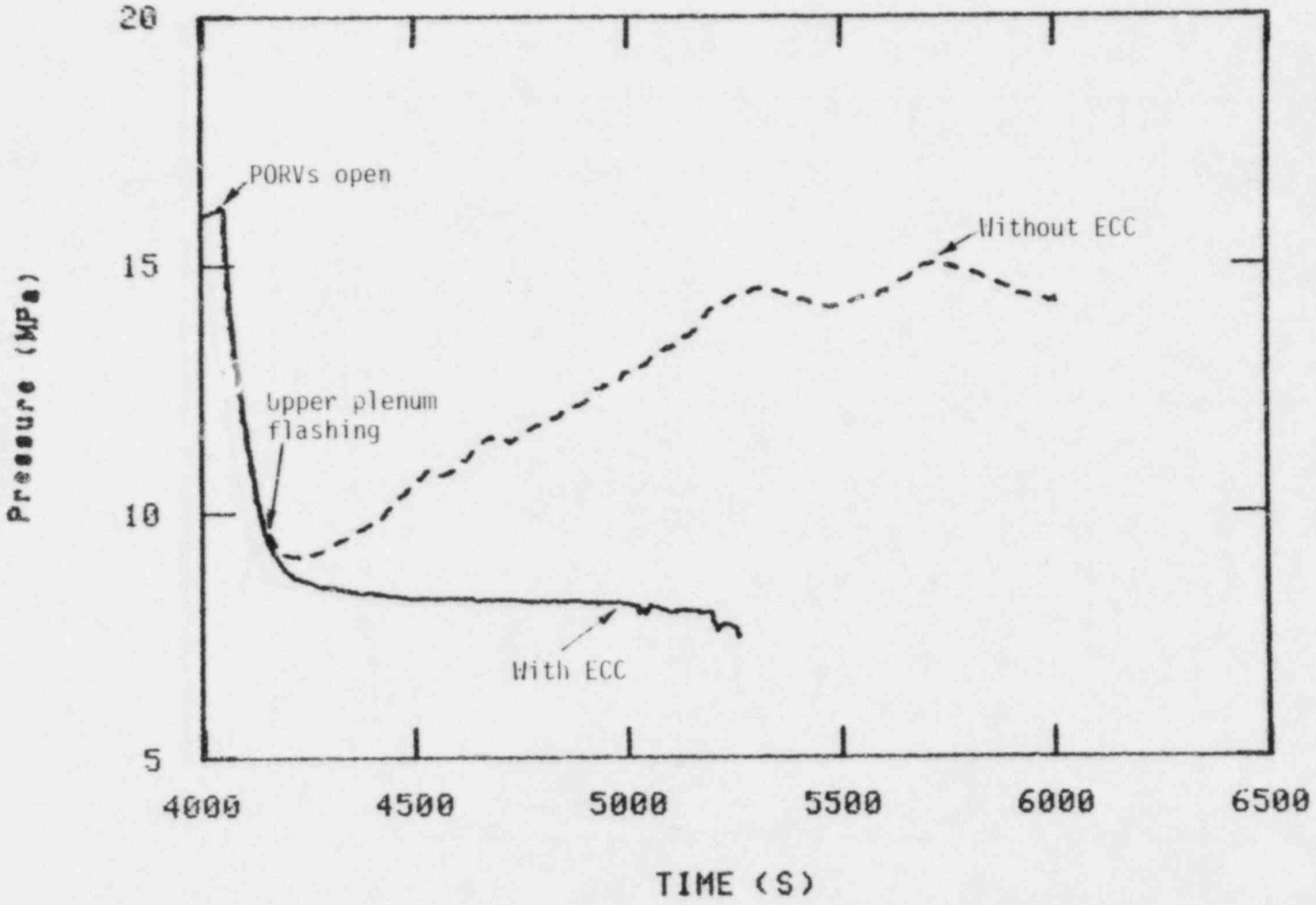

Figure 56. The effect of ECC on pressurizer pressure (RESAR).

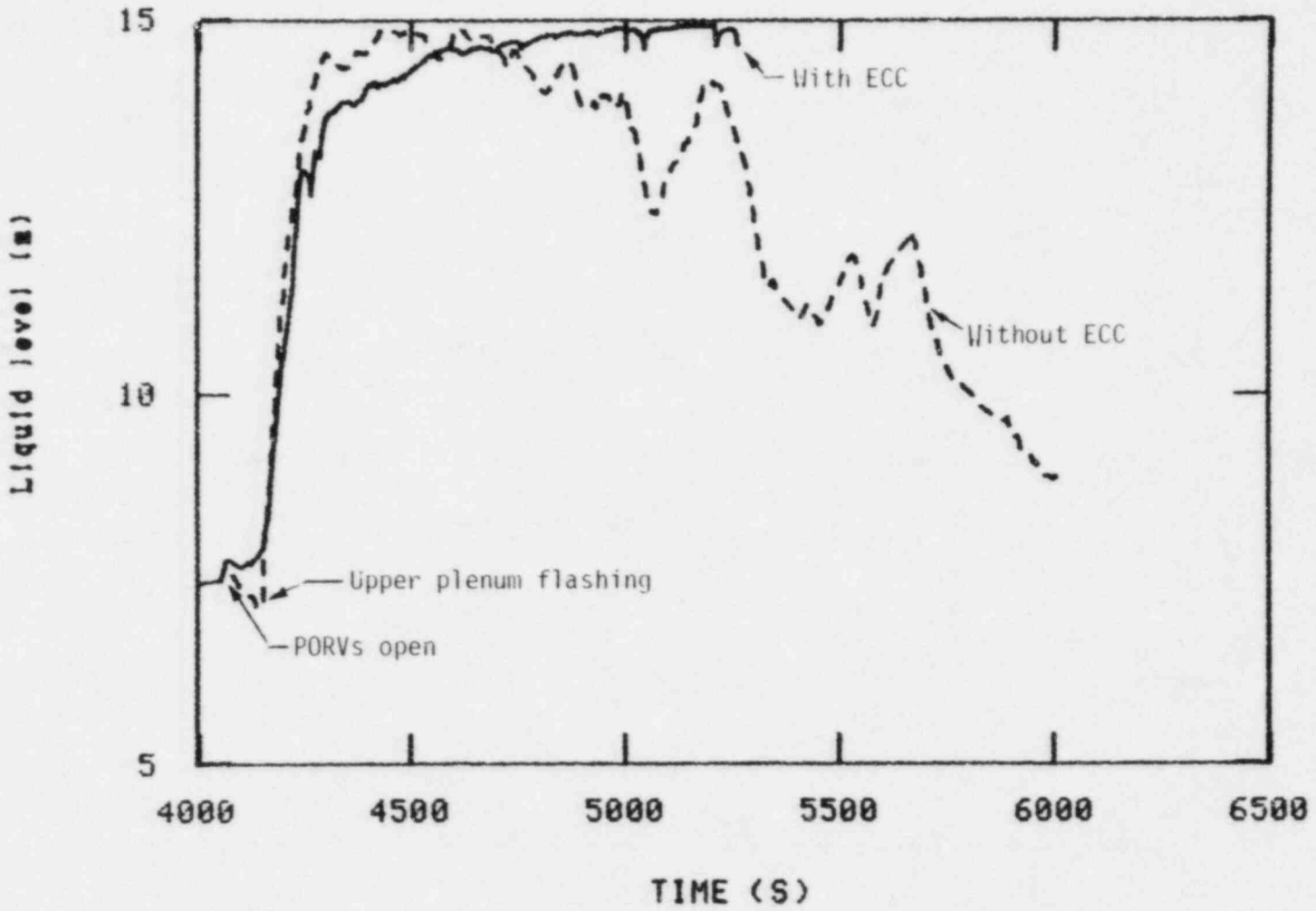

Figure 57. The effect of ECC on pressurizer level (RESAR).

near the top of the pressurizer. In the calculation without ECC, the level generally decreased along with the primary coolant inventory after 4500 s. The pressurizer level decreased because of liquid lost out the PORVs rather than because of draining through the surge line to the hot leg. The collapsed liquid level continued to decrease even after the level dropped several meters below the top of the pressurizer because mixture level swell due to steam bubbles was sufficient to allow some liquid to exit the PORVs. The level stopped decreasing at 6000 s when the hot leg had essentially voided. Steam then flowed from the hot leg through the surge line to the pressurizer where it bubbled through the liquid and out the PORVs.

The effect of ECC on PORV mass flow rate is shown in Figure 58. The PORV flow rates were similar until 4300 s after which the calculation without ECC had a substantially higher flow rate. The higher mass flow rate without ECC was due to the higher pressurizer pressure shown in Figure 56. The higher pressurizer pressure increased the PORV flow rate partially because critical mass flux increases with stagnation pressure. The higher pressure also subcooled the pressurizer liquid which then condensed steam bubbles resulting in a lower quality fluid, or a more highly subcooled fluid, at the top of the pressurizer which further increased the critical mass flux. The influence of hot leg fluid density on the PORV flow in the calculation without ECC is shown in Figure 59. The density of the fluid at the top of the pressurizer, was significantly different than the density in the hot leg, due to storage within the pressurizer, until 5500 s after which the two densities were similar. At the end of the calculation, the top of the pressurizer and the hot leg contained nearly pure steam (void fractions 99% or above). Consequently, the PORV mass flow dropped to values representative of choked steam flow at the end of the calculation.

Core uncovery began at 5900 s in the calculation without ECC. The distribution of primary coolant mass at the time of core uncovery was as follows: 50% in the vessel, 27% in the loops, and 23% in the pressurizer. The loop seals were nearly full of liquid while the rest of the loops were voided. The sensitivity calculation was terminated at 6025 s.

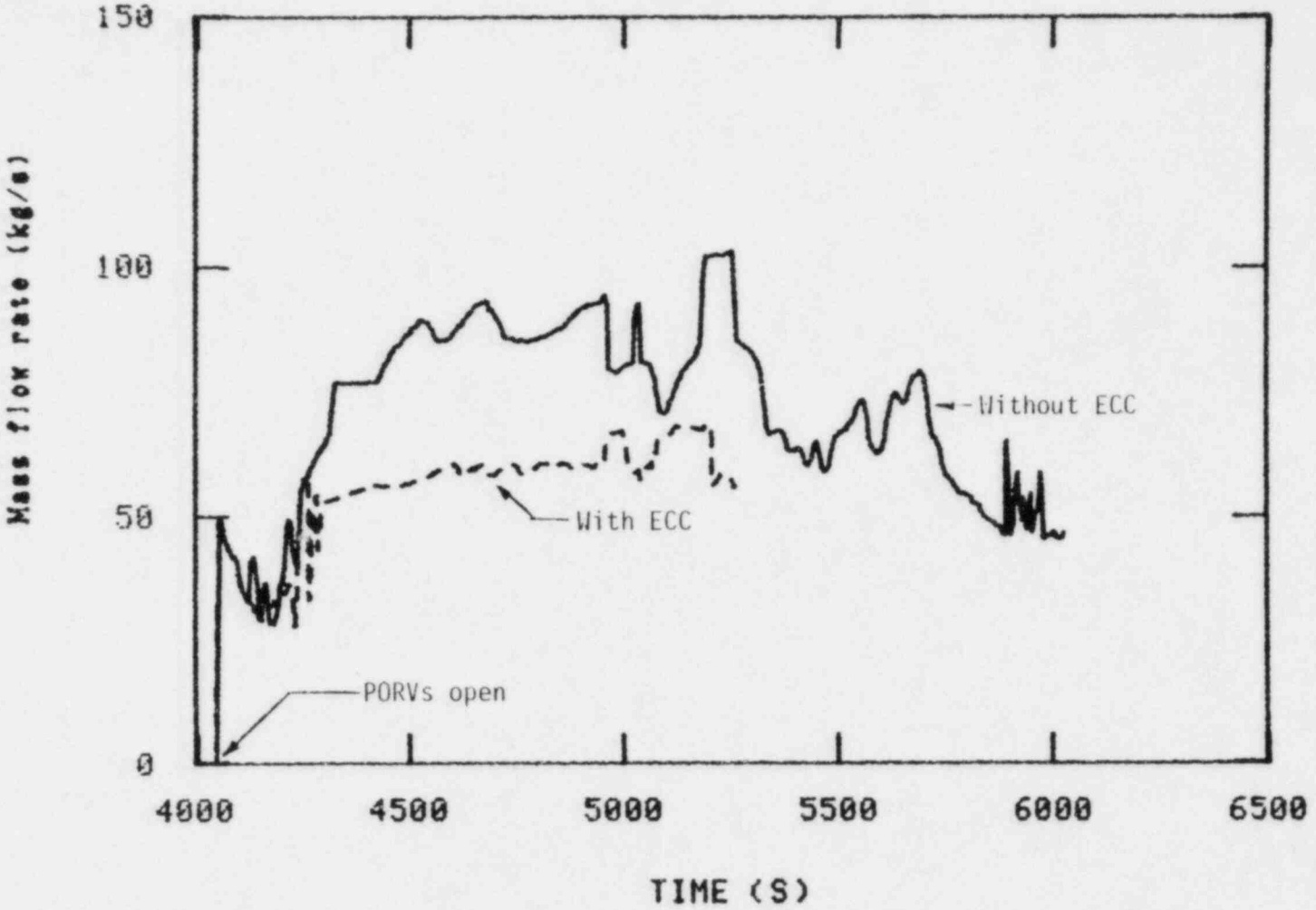

Figure 58. The effect of ECC on PORV mass flow rate (RESAR).

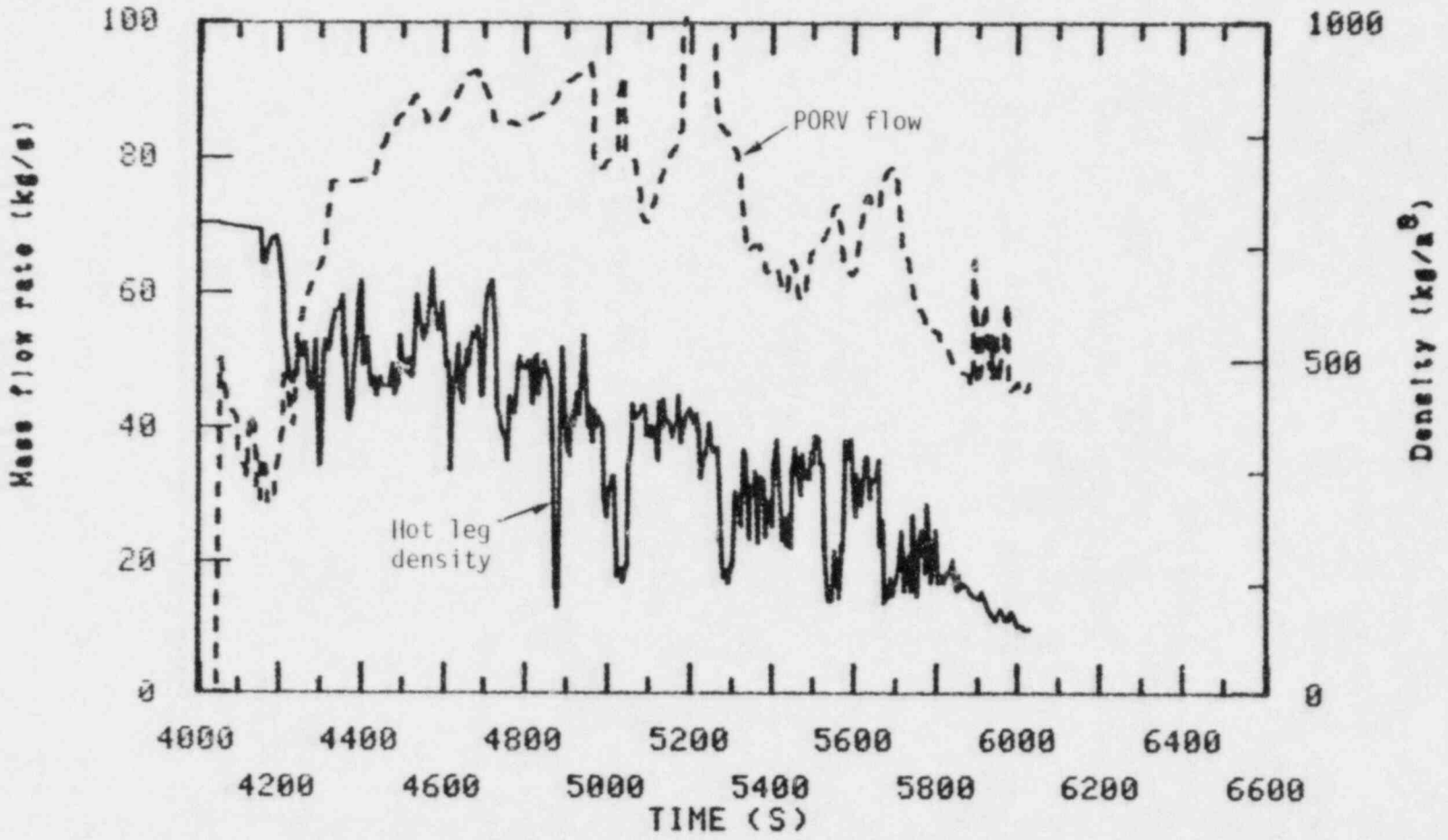

Figure 59. PORV flow rate and hot leg density for the RESAR calculation without ECC.

7. CONCLUSIONS

Primary feed and bleed cooling in a pressurized water reactor system with no secondary heat sink has been analyzed through a study of the basic parameters that govern feed and bleed, the interpretation of experimental data, and finally by verification of computer codes and extrapolation of the identified phenomena to full-scale plants. An orderly examination of the results draws the following conclusions:

Ultimately, the capability for maintaining steady-state feed and bleed cooling is a function of the decay heat level, and the plant specific PORV characteristics and pumped injection capacity. These parameters may be used to perform energy and mass balances which define (or show the non-existence of) a steady-state operating band bounded by a minimum and maximum system pressure.

The greatest uncertainty in the governing parameters lies in the pressurizer PORV mass and energy discharge rates which are strong functions of upstream quality. Semiscale experiments have highlighted the fact that the PORV upstream conditions are strongly influenced by the hot leg fluid conditions at the surge line connection. Until sufficient primary coolant inventory is lost such that the hot leg is highly voided, the low quality PORV flow rate can greatly exceed the HPIS capacity and allow continuous coolant depletion. However, results also showed that cycling the PORV promotes phase separation and thus reduces the dependency of PORV flow rate on hot leg coolant conditions.

Dryout of the core was eventually observed during the Semiscale experiments. Due to the rather narrow steady-state operating range defined by the boundary conditions used, the energy and mass balances were highly subject to experimental uncertainties. A small reduction in core power, PORV mass flow, or an increase in HPIS injection rate would probably have resulted in steady-state cooling after the hot leg had voided.

Code calculations with RELAP5 were successful in predicting the Semiscale experimental results. The phenomena observed in the experiments

that governed pressurizer conditions and PORV flow were reproduced with very good quantitative agreement. This provided verification of the basic ability of the code to calculate a feed and bleed transient prior to performing full-scale plant predictions.

A RELAP5 best-estimate calculation of a loss of feedwater transient in a full-scale PWR that led to a primary feed and bleed operation, showed that for the case of nondegraded HPIS and charging capacity, steady-state cooling and eventual return to system subcooling was predicted. This is consistent with the low decay heat levels and high charging rates (relative to the Semiscale experiment) at which the feed and bleed operation was calculated. For both the best estimate calculation and an additional calculation with no ECC injection, the phenomena governing pressurizer liquid level behavior, PORV flow and system mass distribution were in agreement with the general behavior observed in the Semiscale experiments. It is clear that there exists a minimum injection capacity below which feed and bleed is not viable, assuming saturated steam flow out the PORV. It should be noted, however, that the Zion operating map (for 1.5% decay heat) indicates that feed and bleed could be successfully used even without the charging pumps. A similar result is obtained for the RESAR plant.

No notable distortions were identified as to the typicality of phenomena observed in the Semiscale Mod-2A experiments. Analysis of Semiscale and LOFT data, and examination of code calculations, indicates that the orientation of the surge line connection to the hot leg influences phase separation and therefore the coolant inventory at which feed and bleed cooling becomes viable.

In summary, primary feed and bleed appears to be a feasible means of maintaining the primary coolant system in a safe condition in the absence of secondary heat removal, but its viability depends on plant-specific characteristics and postulated scenarios. The present analysis indicates that the Westinghouse RESAR plant design (and likewise the Zion plant) can be successfully recovered from a complete loss of secondary heat sink. While analysis of other plant designs (i.e., Combustion Engineering and Babcock and Wilcox) was outside the scope of the present analysis, it is

clear that such analysis should be undertaken. A simplified approach, consisting of constructing the "operating map" as illustrated in this report, for each design would be a significant step in this direction.

Finally, it should be pointed out that no attempt was made in the present study to examine implications of the results presented herein relative to existing emergency operator guidelines. This is an area that needs to be explored to determine if these guidelines appear adequate and are reflective of an understanding of the limits and dynamics of primary feed and bleed.

8. REFERENCES

1. W. Tauche, Loss of Feedwater Induced Loss of Coolant Accident Analysis Report, WCAP-9744, Westinghouse Electric Corp., May 1980.

2. N. S. DeMuth, D. Dobranich, R. J. Henninger, Loss-of-Feedwater Transients for the Zion-1 Pressurized Water Reactor, NUREG/CR-2656, May 1982.

3. "Zion Station Final Safety Analysis Report", Commonwealth Edison Co., 1973

4. G. W. Johnson, Personnal communication regarding information from the BE/EM study, Idaho National Engineering Laboratory

5. System Design Description for Mod-2A Semiscale System, Addendum I, "Mod-2A Phase I Addendum to Mod-3 Sytem Design Description," EG&G Idaho, Inc., December 1980.

6. G. R. Berglund, "Experiment Operating Specification for Semiscale Mod-2A Primary Feed and Bleed Experiment S-SR-1," EG&G Idaho Inc., June 1982.

7. G. R. Berglund and D. J. Shimeck, "Experiment Operating Specification for Semiscale Mod-2A Primary Feed and Bleed Experiment S-SR-2," EG&G Idaho Inc., July 1982.

8. D. J. Shimeck, M. T. Leonard, Results from Semicale Mod-2A Upper Head Injection Test Series, Transactions of American Nuclear Society 1981 Winter Meeting., Volume 39, November-December 1981.

9. H. J. Richter, "Flooding in Tubes and Annuli", Int. Journal of Multiphase Flow, Volume 7, No. 6, pp 647-658, 1981

10. T. K. Larson, G. G. Loomis, R. W. Shumway, Simulation of Three Mile Island Transient in Semiscale, SEMI-TR-010, EG&G Idaho Inc., July 1979.

11. G. G. Loomis, K. Soda, C. P. Fineman, Quick Look Report for Semiscale Mod-2A Test S-NC-2, EGG-SEMI-5507, EG&G Idaho Inc., July 1981.

12. N. Zuber, Problems in Modeling of Small Break LOCA, NUREG-0724, October 1980.

13. Y. Taitel, A. E. Dukler, "A Model for Predicting Flow Regime Transitions in Horizontal and Near Horizontal Gas-Liquid Flow," AIChE Journal, (Vol. 22, No. 1), January 1976.

14. James P. Adams, Quick-Look Report on LOFT Nuclear Experiment L9-1/L3-3, EGG-LOFT-5430, April 1981.

15. Mary L. McCormick-Barger and Janice M. Divine, Experiment Data Report for LOFT Anticipated Transient with Multiple Failures Experiment L9-1 and Small Break Experiment L3-3ç, NUREG/CR-2119, EFF-2101, June 1981.

16. "Alternate Heat Removal Capability Demonstrated in the LOFT PWR", LOFT Highlights, EGG-LOFT-5664, No. 3, January 1982.

17. Douglas L. Reeder, LOFT System and Test Description (5.5 ft Nuclear Core 1 LOCES), NUREG/CR-0247, TREE-1208, July 1978.

18. Larry J. Ybarrondo, et al. "Examination of LOFT Scaling", ASME 74-WA/HT-53, Winter Annual Meeting of the ASME, New York, N.Y., November 17-22, 1974.

19. Douglas G. Hall and Linda S. Czapary, Tables of Homogeneous Equilbrium Critical Flow Parameters for Water in SI Units, EGG-2056, September 1980.

20. V. H. Ransom, et al., RELAP5/Mod 1 Code Manual, Volumes 1 and 2, NUREG/CR-1826, November, 1980.

21. M. T. Leonard, RELAP5 Standard Model Description for the Semiscale Mod-2A System, EGG-SEMI-5692, December 1981

22. G. G. Loomis, Summary Report Semiscale Mod-2A Heat Loss Characterization Test Series, EGG-SEMI-5448, May 1981

23. J. E. Blakely, J. M. Cozzuol, E. T. Laats, RELAP5 RESAR-3S Small Break Calculation, EG&G Idaho, Inc. Interim Report, to be published September 1982.

24. American Nuclear Society Proposed Standard, "Decay Energy Release Rates Following Shutdown of Uranium-Fueled Thermal Reactors", Approved by Subcommittee ANS 5.1, ANS Standards Committee, October 1971, Revised October 1973.